1-1-2010

Spectral Methods For The Hamiltonian Systems

Nairat Kanyamee
Wayne State University

SPECTRAL METHODS FOR THE HAMILTONIAN SYSTEMS

by

NAIRAT KANYAMEE

DISSERTATION

Submitted to the Graduate School

of Wayne State University,

Detroit, Michigan

in partial fulfillment of the requirements

for the degree of

DOCTOR OF PHILOSOPHY

2010

MAJOR: MATHEMATICS

Approved by:

_____

Advisor Date

_____

_____

_____

_____

DEDICATION

To My Parents

To My Teachers

ACKNOWLEDGEMENTS

I would like to express my sincere gratitude and deep appreciation to Professor Zhimin Zhang for his guidance, invaluable advice, supervision and encouragement throughout this research which enabled me to complete this thesis successfully. I am very honored to have him as my advisor while I took on this difficult academic endeavor. He was patient and was never lacking in showing his concerns and support. Professor Zhang's vast knowledge and understanding of the subject have been fundamental in shaping my thesis and my mathematical career. I am also taking this opportunity to thank Professors Boris Mordukhovich, George Yin, Guozhen Lu, and Weisong Shi for serving as my committee members.

I wish to thank the staff of the Department of Mathematics at Wayne State University for their co-operation and generous assistance which allowed me to finish my dissertation at this time.

Finally, I am grateful to my parents, family and friends for their encouragement, understanding and help.

TABLE OF CONTENTS

1 Introduction

1.1 Hamiltonian Systems

The Hamiltonian dynamical systems have been of much interest in many research areas. They are the systems that can be expressed as Hamiltonian equations. The equations are formulated by the Hamiltonian mechanics, an alternative and equivalent formalism of Newtonian and Lagrangian which have become one of the most useful tools in the mathematical theory of physical and engineering sciences. Hamiltonian mechanics were first introduced by William Rowan Hamilton in 1833. Since then, many famous scientists, such as Poincaré, Jacobi, Birkhoff, Weyl, Kolmogorov, and Arnold, have studied the subject [1]. A system is governed by the total energy or the "Hamiltonian": H. The Hamiltonian generally, for a closed system, comprises the kinetic and the potential energy.

Hamiltonian systems typically arise as models of conservative physical systems and have many applications in classical mechanics, molecular dynamics, hydrodynamics, electrodynamics, plasma physics, relativity, astronomy, and other scientific fields [41, 42]. Almost all real physical processes with negligible dissipation can be described in some way or another by Hamiltonian formalism [1].

The formulation of a Hamiltonian system with a given Hamitonian function $H(p_1, \ldots, p_n; q_1, \ldots, q_n)$ is given by

$$\frac{dp_i}{dt} = -\frac{\partial H}{\partial q_i}, \quad \frac{dq_i}{dt} = \frac{\partial H}{\partial p_i}; \qquad i = 1, 2, \ldots, n \tag{1}$$

This system can be represented in a matrix form as

$$\frac{\partial z}{\partial t} = J^{-1}\frac{\partial H}{\partial z}, \quad z = (\mathbf{p}, \mathbf{q})^{\mathbf{T}}.$$

where $J = \begin{pmatrix} 0 & I_n \\ -I_n & 0 \end{pmatrix}$.

In particular, a canonical linear Hamiltonian system is defined by a quadratic Hamiltonian

$$H = \frac{1}{2} z^T L z$$

where L is a $2d \times 2d$, d is degree of freedoms, symmetric matrix and $z = [\mathbf{p}, \mathbf{q}]^T$.

1.2 Conservation properties of the Hamiltonian Systems

In addition to its elegance and symmetry, a Hamiltonian system has some remarkable qualitative properties; Geometrical structure, Conservation laws, Symmetries, and Asymtotic behaviors would be some examples. Most important among those properties are its symplectic structure, discussed in section 1.3, and the optimality for energy preservation. Any good numerical scheme should be able to replicate as many of these physical properties as possible. The symplectic structure is, in nature, volume-preserving. Traditional ODE solvers such as Runge-Kutta or multi-step methods usually do not preserve the symplectic structure and energy. As a consequence, numerical trajectories tend to gradually drift away from the true solution trajectories in a phenomenon called phase shift.

One of the reasons why it is important to preserve qualitative structure is that those properties can be found in a system that occurs naturally ,e.g. stellar dynam-

ics or molecular dynamics, mechanical system evolving under rotational constraints. Those systems can be described by Hamiltonian systems with many conservative laws [6].

Theoretical study shows that the solution of a Hamiltonian system can be described by an evolution semigroup which is a symplectic mapping for any fixed t. Furthermore, the Hamiltonian is conserved along trajectories,

$$H(p_N(t_N), q_N(t_N)) = H(p_N(t_0), q_N(t_0)) = H(p_0, q_0),$$

i.e., a spectral method preserves the energy up to numerical integration error. In many practical problems, due to the analytic nature of $H(p, q)$ and the spectral accuracy, we are able to control the numerical quadrature error to the machine epsilon, i.e., 10^{-15} with a reasonable N, say, $N \leq 20$. In this case, the spectral methods that we are introducing preserve the energy in practice.

For another important feature or property of the Hamiltonian system or the symplectic structure (discussed further in section 1.3.1), namely, the Jacobi matrix of the transformation

$$\left(\frac{\partial \boldsymbol{z}_N}{\partial \boldsymbol{z}_0}\right), \qquad \boldsymbol{z} = \begin{pmatrix} \boldsymbol{p} \\ \boldsymbol{q} \end{pmatrix}$$

satisfies

$$\left(\frac{\partial \boldsymbol{z}_N}{\partial \boldsymbol{z}_0}\right) J \left(\frac{\partial \boldsymbol{z}_N}{\partial \boldsymbol{z}_0}\right)^T = J, \qquad J = \begin{pmatrix} 0 & I_N \\ -I_N & 0 \end{pmatrix}.$$

Note that with the above notation, the Hamiltonian system can be written as

$$\boldsymbol{z}_t = J^{-1} H_z.$$

Based on the high accuracy of the spectral Galerkin and the spectral collocation methods, it is reasonable to expect that

$$\left(\frac{\partial \boldsymbol{z}_N}{\partial \boldsymbol{z}_0}\right)^T J \left(\frac{\partial \boldsymbol{z}_N}{\partial \boldsymbol{z}_0}\right) = J + O(e^{-\sigma N}).$$

This has a significant meaning in practice. When the error reaches the machine epsilon which is about 10^{-15}, the scheme is, in practice, volume-preserving (i.e., preserves the symplectic structure)! The reader is referred to [50] for more conservation properties of numerical methods.

1.3 Numerical Methods for the Hamiltonian Systems

The numerical study for the ordinary differential equations has attracted a lot of interests from many research areas. It has continued to be a lively area of numerical analysis for more than a century [16]. There are useful and well known theoretical studies and results shown in e.g., Hairer [35], Butcher [7, 8]. However, the theory of numerical methods for ordinary differential equations has reached a certain level of maturity in the last few decades [35]. Many ordinary numerical approximations of the systems , e.g. most of the Runge- Kutta methods, finite element method, finite difference method, are not structurally stable for the long-term behavior of the numerical solution. The motivation for developing structure-preserving algorithms for special classes of problems came independently from different areas of research such as astronomy, molecular dynamics, mechanics, theoretical physics, and numerical analysis as well as from other areas of both applied and pure mathematics. It turns out that

the preservation of geometric properties of the flow not only produces an improved qualitative behavior, but also allows for a more accurate long-time integration when compared with the general-purpose methods.

1.3.1 Symplectic Algorithms

The numerical solution of a Hamiltonian system is one of the significant topics in geometric numerical integration [16]. The implementation of the numerical approximation as the exact solution of an ordinary differential equation should be insight with the long-time behavior.

The idea of developing numerical methods that maintain the symplectic structure was first studied in a general setting by Feng in the 1980s [19]. This was followed by a successful systematic study of designing so-called symplectic algorithms [20, 21, 22, 23, 24, 25, 26, 35, 47]. But, none of these symplectic algorithms is energy-preserving in general. Indeed, it was proved that there exists no energy-preserving symplectic algorithm for the general nonlinear Hamiltonian systems [28, 18]. On the other hand, Galerkin-type methods such as finite element methods are well-known to preserve energy. Now we face a dilemma having to choose between preserving energy and preserving symplectic structure. Some argue that for highly oscillatory problems, preserving energy may be more important than the symplectic structure [13, 14, 46, 10, 27, 6].

Let ψ be a $\mathcal{C}^1$ transformation in a domain Ω given by [46]

$$(\boldsymbol{p}^*, \boldsymbol{q}^*) = \psi(\boldsymbol{p}, \boldsymbol{q}).$$

This transformation ψ is area preserving if and only if the Jacobian determinant is 1 ($|\psi'| = 1$);

$$
\begin{aligned}
|\psi'(\boldsymbol{p},\boldsymbol{q})| &= \begin{vmatrix} \frac{\partial \boldsymbol{p}^*}{\partial \boldsymbol{p}} & \frac{\partial \boldsymbol{p}^*}{\partial \boldsymbol{q}} \\ \frac{\partial \boldsymbol{q}^*}{\partial \boldsymbol{p}} & \frac{\partial \boldsymbol{q}^*}{\partial \boldsymbol{q}} \end{vmatrix} = \frac{\partial \boldsymbol{p}^*}{\partial \boldsymbol{p}}\frac{\partial \boldsymbol{q}^*}{\partial \boldsymbol{q}} - \frac{\partial \boldsymbol{p}^*}{\partial \boldsymbol{q}}\frac{\partial \boldsymbol{q}^*}{\partial \boldsymbol{p}} = 1 \\
&= \begin{pmatrix} \frac{\partial \boldsymbol{p}^*}{\partial \boldsymbol{p}} & \frac{\partial \boldsymbol{q}^*}{\partial \boldsymbol{p}} \\ \frac{\partial \boldsymbol{p}^*}{\partial \boldsymbol{q}} & \frac{\partial \boldsymbol{q}^*}{\partial \boldsymbol{q}} \end{pmatrix} \begin{pmatrix} 0 & I_N \\ -I_N & 0 \end{pmatrix} \begin{pmatrix} \frac{\partial \boldsymbol{p}^*}{\partial \boldsymbol{p}} & \frac{\partial \boldsymbol{p}^*}{\partial \boldsymbol{q}} \\ \frac{\partial \boldsymbol{q}^*}{\partial \boldsymbol{p}} & \frac{\partial \boldsymbol{q}^*}{\partial \boldsymbol{q}} \end{pmatrix} \\
&= \psi'^T J \psi' \quad \text{where} \quad J = \begin{pmatrix} 0 & I_N \\ -I_N & 0 \end{pmatrix}
\end{aligned}
$$

Therefore, in order to check symplecticness, the transformation must satisfies

$$
\left(\frac{\partial \boldsymbol{z}_N}{\partial \boldsymbol{z}_0}\right)^T J \left(\frac{\partial \boldsymbol{z}_N}{\partial \boldsymbol{z}_0}\right) = J, \qquad J = \begin{pmatrix} 0 & I_N \\ -I_N & 0 \end{pmatrix}.
$$

Some examples of symplectic algorithms are shown in the Appendix(B).

1.3.2 Spectral Methods

Spectral methods were originally introduced in 1944 by Blinova and were first implemented in 1954 by Silberman. It was virtually abandoned in the mid 1960s but resurrected in 1969−70 by Orszag and by Eliason, Machenhauer and Rasmussen. Then it was developed for specialized applications in the 1970s, endowed with the first mathematical foundations by the seminal work of Gottlieb and Orszag in 1977. The extension of the methods and their analysis to a broader class of problems was

proposed in the 1980s, and entered the mainstream of scientific computation in the 1990s [12].

Spectral methods are a class of spatial discretizations for differential equations. The key components for their formulation are the trial functions (also called the expansion or approximating functions) and the test functions (also known as weight functions). The trial functions, which are linear combinations of suitable trial basis functions, are used to provide the approximate representation of the solution. The test functions are used to ensure that the differential equation and perhaps some boundary conditions are satisfied as closely as possible by the truncated series expansion. The spectral method and finite element method are closely related and built on the same concepts. The main difference is that the spectral method approximates the solution as a linear combination of continuous functions over the domain (global smooth functions), while the FEM approximates the solution as a linear combination of piecewise functions on a small subdomain(local smooth functions).

There are three classifications of spectral methods according to the test functions and the residual. Consider the problem [37]

$$\begin{aligned} \frac{\partial u(x,t)}{\partial t} &= \mathcal{L}u(x,t) \quad , \quad x \in [a,b], t \geq 0 \\ \mathcal{B}_L u = 0 \quad &, \quad \mathcal{B}_R u = 0 \quad t \geq 0 \\ u(x,0) &= f(x) \end{aligned}$$

where $\mathcal{B}_{L,R}$ are the boundary operators at $x = a \ , \ x = b$.

The residual of the numerical solution $u_N(x,t)$ is defined by

$$R_N(x,t) = \frac{\partial u_N(x,t)}{\partial t} - \mathcal{L}u_N(x,t).$$

1. Spectral Galerkin Method

In this method, we seek solutions, $u_N(x,t) \in B_N$ of the form

$$u_N(x,t) = \sum_{j=0}^{N} a_j(t)\phi_j(x)$$

where $\phi_j(x)$ is a polynomial taken from space

$$B_N = \text{span}\{\phi_j(x) \in \text{span}\{x^k\}_{k=0}^{N} \mid \ \mathcal{B}_L u = 0 \ \ , \ \ \mathcal{B}_R u = 0\}_{j=0}^{N}.$$

This method requires the residual R_N to be orthogonal to the test functions from the space B_N.

2. Spectral Tau Method

In this method, we seek solutions $u_N(x,t) \in B_N$. However, we do not project the residual onto the space B_N but rather onto the polynomial space $P_{N-k} = \text{span}\{x^n\}_{n=0}^{N-k}$ where k is the number of boundary conditions i.e. the test functions are not required to satisfy the boundary conditions. However, the boundary conditions are enforced by an additional set of k equations.

3. Spectral Collocation Method

This method does not require the projection of the residual onto some polynomial space to be zero. The method is obtained by seeking $u_N(x,t) \in B_N$ and requiring the residual to vanish at a certain set of grid points, normally some set of Gaussian-type points

$$\frac{\partial u_N(x,t)}{\partial t}|_{x_j} - \mathcal{L}u_N(x,t)|_{x_j}$$

where $\{x_j\}$'s are Gaussian-type points.

For more references regarding spectral and spectral collocation methods, the reader is referred to [4, 5, 11, 12, 29, 30, 38, 45, 48, 51] and references therein.

There have been some recent attempts in using the spectral method [49] and the spectral collocation method, derived from a recursive relation of the Legendre polynomials [31], to solve the ODEs. We introduce an algorithm based on spectral collocation and Tau method to preserve both energy and volume (symplectic structure) up to numerically negligible error terms. If the error term is so small that it reaches the machine epsilon, the computer round-off error, then the algorithm is practically energy and volume preserving. We shall use a series of numerical benchmark problems to demonstrate that our methods are effective and much more accurate than the symplectic methods with a similar computational cost.

This work carries on a systematic comparison between the proposed spectral collocation method and the symplectic methods. It gives a comparison of numerical results of both linear and nonlinear Hamiltonian systems by using the spectral methods and the symplectic methods. The collocation methods demonstrate an evidence of a better approximation on linear and nonlinear Hamiltonian systems.

2 Methods

In this section, we will discuss the methods to obtain the optimum results for a given Hamiltonian system. As mentioned in the first chapter, a good numerical method should preserve the structure of the solution in a long-term period. There are several spectral methods that will be considered in this chapter. We also compare the result with the symplectic methods.

For simplicity, we use the case $n = 1$ in (1) to illustrate the idea. We can apply this simple model to a larger system, with $n > 1$, in a similar way. Consider the nonlinear Hamiltonian system

$$p' = -\frac{\partial H}{\partial q} = F(p,q), \quad q' = \frac{\partial H}{\partial p} = G(p,q), \qquad p(0) = p_0, \quad q(0) = q_0,$$

where F and G are nonlinear functions. We solve the system on $[0, T]$ first, then use the obtained values $(p(T), q(T))$ as an initial condition to repeat the process on $[T, 2T]$, and so on. Here T could be large; but a convenient choice is $T = 2$. However, the best T is within $[0.75, 2]$.

2.1 Spectral Collocation Method with the Differentiation Matrices

We use either the Chebyshev-Gauss-Lobatto or the Legendre-Gauss-Lobatto collocation methods to solve it. Let $t_0 < t_1 < \cdots t_N$ be collocation points where $t_0 = 0$ and $t_N = T$.

2.1.1 Spectral Collocation Method with the Chebyshev Differentiation Matrix

We are seeking numerical approximations (interpolations of p and q) $p^N, q^N \in \mathcal{P}_N[0,T]$, $p^N(0) = p_0$ and $q^N(0) = q_0$ of the form

$$p^N(t) = \sum_{j=0}^{N} a_j T_j(t) = \sum_{j=0}^{N} p_N(t_j) l_j(t)$$

$$q^N(t) = \sum_{j=0}^{N} b_j T_j(t) = \sum_{j=0}^{N} q_N(t_j) l_j(t)$$

such that

$$\begin{aligned} \frac{dp^N}{dt}(t_k) &= F(p^N(t_k), q^N(t_k)) \quad , \quad 0 \le k \le N, \\ \frac{dq^N}{dt}(t_k) &= G(p^N(t_k), q^N(t_k)) \quad , \quad 0 \le k \le N, \end{aligned}$$

where $t_0, t_1, ..., t_N$ are the transformed Chebyshev-Gauss-Lobatto quadrature points, i.e. $t_j = \frac{T(x_j+1)}{2}$ where $x_j = -cos(\frac{\pi}{N}j)$, $j = 0, 1, ..., N$ and $T_j's$ are the Chebyshev polynomials on $[0,T]$.

Note that $l_j(x_i) = \delta_{ij}$ where , for Chebyshev-Gauss-Lobatto,

$$l_j(x) = \frac{(-1)^{N+j}(1-x^2)T_N'(x)}{c_j N^2 (x - x_j)}$$

$c_0 = c_N = 2$ and $c_j = 1$ otherwise [37, 12].

The system can then be written as

$$\sum_{j=0}^{N} d_{ji} p^N(t_j) = F(p^N(t_i), q^N(t_i))$$

$$\sum_{j=0}^{N} d_{ji} q^N(t_j) = G(p^N(t_i), q^N(t_i))$$

for each $i = 0, 1, ..., N$.

In the literature of the spectral method, the explicit form of the differentiation matrix $D = (d_{ij})_{i,j=0}^{N}$ is known [4, 5, 37, 11, 12, 30, 48] where

$$d_{ij} = \ell_j'(t_i) \quad = \quad \begin{cases} -\frac{2N^2+1}{6}, i = j = 0 \\ \frac{c_i}{c_j}\frac{(-1)^{i+j}}{x_i - x_j}, i \neq j \\ -\frac{x_i}{2(1-x_i^2)}, i = j \in 1, ..., N-1 \\ \frac{2N^2+1}{6}, i = j = N \end{cases}.$$

With the scaling of $\frac{2}{T}$, this differentiation matrix can be transformed to the interval $[0, T]$.

Note that the rank of the $(N+1) \times (N+1)$ matrix D is N. Therefore, we may solve the system

$$\begin{aligned} d_{11}p_1 + d_{12}p_2 + \cdots d_{1N}p_N &= f(p_1, q_1) - d_{10}p_0 \\ &\vdots \\ d_{N1}p_1 + d_{N2}p_2 + \cdots d_{NN}p_N &= F(p^N, q^N) - d_{N0}p_0 \\ d_{11}q_1 + d_{12}q_2 + \cdots d_{1N}q_N &= g(p_1, q_1) - d_{10}q_0 \\ &\vdots \\ d_{N1}q_1 + d_{N2}q_2 + \cdots d_{NN}q_N &= G(p^N, q^N) - d_{N0}q_0 \end{aligned}$$

to obtain $\boldsymbol{p} = (p_1, p_2, \ldots, p_N)^T$ and $\boldsymbol{q} = (q_1, q_2, \ldots, q_N)^T$, where here we denote $p^N(t_k) = p_k, q^N(t_k) = q_k$, and use the rest two equations

$$d_{01}p_1 + d_{02}p_2 + \cdots d_{0N}p_N = F(p_0, q_0) - d_{00}p_0,$$

$$d_{01}q_1 + d_{02}q_2 + \cdots d_{0N}q_N = G(p_0, q_0) - d_{00}q_0$$

to estimate the error.

If we denote,

$$\boldsymbol{F}(\boldsymbol{p},\boldsymbol{q}) = \begin{pmatrix} F(p_1,q_1) - d_{10}p_0 \\ F(p_2,q_2) - d_{20}p_0 \\ \vdots \\ F(p^N,q^N) - d_{N0}p_0 \end{pmatrix}, \text{ and } \quad \boldsymbol{G}(\boldsymbol{p},\boldsymbol{q}) = \begin{pmatrix} G(p_1,q_1) - d_{10}q_0 \\ G(p_2,q_2) - d_{20}q_0 \\ \vdots \\ G(p^N,q^N) - d_{N0}q_0 \end{pmatrix}$$

then we design a numerical iteration in the matrix form

$$\begin{pmatrix} \tilde{D} & 0 \\ 0 & \tilde{D} \end{pmatrix} \begin{pmatrix} \boldsymbol{p}^{new} \\ \boldsymbol{q}^{new} \end{pmatrix} = \begin{pmatrix} \boldsymbol{F}(\boldsymbol{p}^{old},\boldsymbol{q}^{old}) \\ \boldsymbol{G}(\boldsymbol{p}^{old},\boldsymbol{q}^{old}) \end{pmatrix},$$

where $\tilde{D}$ is a $N \times N$ matrix by eliminating the first row and the first column of D. This format is valid for any N. In the process, we may use Gauss-Seidal-type iteration to update the information as soon as possible.

The initial guesses to start the spectral collocation are $(N \times 1)$ vectors $(p_0, ..., p_0)^T$ and $(q_0, ..., q_0)^T$ where p_0, q_0 are the initial values.

2.1.2 Spectral Collocation Method with the Legendre Differentiation Matrix

We are seeking numerical approximations $(p^N(t_j), q^N(t_j))$, denoted as (p_j^N, q_j^N), where interpolation of p and q are of the form

$$p^N(t) = \sum_{j=0}^{N} a_j L_j(t) = \sum_{j=0}^{N} p^N(x_j) l_j(t)$$

$$q^N(t) = \sum_{j=0}^{N} b_j L_j(t) = \sum_{j=0}^{N} q^N(x_j) l_j(t)$$

where $t_0, t_1, ..., t_N$ are the transformed Legendre-Gauss-Lobatto quadrature points, i.e. $t_j = \frac{T(x_j+1)}{2}$ where x_j , $j = 0, 1, ..., N$ are zeros of $(1-x^2)\frac{d}{dx}L_N(x)$ and $L_j's$ are the Legendre polynomials on $[0, T]$ [37, 12].

Note that $l_j(x_i) = \delta_{ij}$ where , for Legendre-Gauss-Lobatto,

$$l_j(x) = \frac{-(1-x^2)L'_N(x)}{N(N+1)(x-x_j)L_N(x_j)}.$$

The system can then be written as

$$\sum_{j=0}^{N} d_{ji} p_N(t_j) = F(p_N(t_i), q_N(t_i))$$

$$\sum_{j=0}^{N} d_{ji} q_N(t_j) = G(p_N(t_i), q_N(t_i))$$

for each $i = 0, 1, ..., N$.

The explicit form of the Legendre differentiation matrix $D = (d_{ij})_{i,j=0}^{N}$ can be found in a similar way with $d_{ij} = \ell'_j(t_i)$ where

$$d_{ij} = \ell'_j(t_i) \quad = \quad \begin{cases} -\frac{N(N+1)}{4}, i = j = 0 \\ \frac{L_N(x_i)}{L_N(x_j)} \frac{1}{x_i - x_j}, i \neq j \\ 0, i = j \in 1, ..., N-1 \\ \frac{N(N+1)}{4}, i = j = N \end{cases} .$$

With the scaling of $\frac{2}{T}$, this differentiation matrix can be transformed to the interval $[0, T]$.

2.2 Spectral Tau Methods

2.2.1 Spectral Tau Method with Legendre-Phi

To establish the method in the following section, we introduce a set of trial functions

$$\varphi_0(t) = \frac{T-t}{T} \quad , \quad \varphi_1(t) = \frac{t}{T} \quad , \quad \varphi_j(t) = \int_0^t L_{j-1}(s)ds \quad , \quad j = 2, ..., N.$$

The recursive relation of Legendre polynomials provides

$$\varphi_j(t) = \frac{T}{2j+1}(L_j(t) - L_{j-2}(t)).$$

These trial functions have the value at the boundary that $\varphi_0(0) = 1$, $\varphi_0(T) = 0$, $\varphi_1(0) = 0$, $\varphi_1(T) = 1$ and $\varphi_i(0) = 0 = \varphi_i(T)$, for $i = 2, ..., N$.

The inner product of Legendre polynomial on $[0, T]$ is given by [31]

$$(L_i, L_j)_T = \int_0^T L_i(s)L_j(s)ds = \begin{cases} \frac{T}{2j+1} \text{ , for } i = j \\ 0 \qquad \text{otherwise} \end{cases}$$

With this method, we find the solution

$p - p_0, q - q_0 \in H^1_{(0}[0, T] = \{v \in H^1[0, r] : v(0) = 0\}$ such that

$$\begin{aligned} (\frac{dp}{dt}, v) &= (-H_q, v) \quad , \quad v \in H^1[0, T] \\ (\frac{dq}{dt}, v) &= (\ H_p, v) \end{aligned}$$

For the weak form, we seek solutions $p^N, q^N \in \mathcal{P}_N[0, T]$, $p^N(0) = p_0$ and $q^N(0) = q_0$ of the form

$$p^N(t) = p_0\varphi_0(t) + p_N\varphi_1(t) + \sum_{j=2}^{N} p_{j-1}\varphi_j(t) \quad , \quad q^N(t) = q_0\varphi_0(t) + q_N\varphi_1(t) + \sum_{j=2}^{N} q_{j-1}\varphi_j(t)$$

such that

$$\begin{aligned}(\frac{dp^N}{dt}, L_i) &= (-H_q(p^N, q^N), L_i) \quad , \quad i = 0, ..., N-1 \\ (\frac{dq^N}{dt}, L_i) &= (\ H_p(p^N, q^N), L_i) \end{aligned} \tag{2.2.1}$$

With the derivative of the expansion

$$\frac{dp^N(t)}{dt} = \frac{(p_N - p_0)}{T} + \sum_{j=1}^{N-1} p_j L_j(t) \quad , \quad \frac{dq^N(t)}{dt} = \frac{(q_N - q_0)}{T} + \sum_{j=1}^{N-1} q_j L_j(t),$$

the system (2.2.1) can be written as a matrix equation

$$A\mathbf{z}(t) = \mathbf{F(z(t))}$$

where

$$A = \begin{pmatrix} D & 0 \\ 0 & D \end{pmatrix} \quad , \quad D = \begin{pmatrix} 1 & 0 & \dots & 0 \\ 0 & \frac{T}{3} & \dots & 0 \\ \vdots & \vdots & \ddots & \vdots \\ 0 & 0 & \dots & \frac{T}{2N-1} \end{pmatrix}$$

$$\mathbf{z} = \begin{pmatrix} \mathbf{p} \\ \mathbf{q} \end{pmatrix} = \begin{pmatrix} p_N - p_0 \\ p_1 \\ \vdots \\ p_{N-1} \\ q_N - q_0 \\ q_1 \\ \vdots \\ q_{N-1} \end{pmatrix} \quad , \quad \mathbf{F(z)} = \begin{pmatrix} (-H_q(p^N, q^N), L_0) \\ (-H_q(p^N, q^N), L_1) \\ \vdots \\ (-H_q(p^N, q^N), L_{N-1}) \\ (H_p(p^N, q^N), L_0) \\ (H_p(p^N, q^N), L_1) \\ \vdots \\ (H_p(p^N, q^N), L_{N-1}) \end{pmatrix}.$$

We solve the system by using an iterative method.

$$A\mathbf{z}^{new} = \mathbf{F}(\mathbf{z}^{old})$$

The benefit of this expansion is that the numerical values at the right endpoint of each interval, for example $p^N(T), q^N(T)$, are just the coefficients of $\varphi_1(t)$.

$$p^N(T) = p_N \quad , \quad q^N(T) = q_N$$

The initial guesses to start the iterative method are $(N \times 1)$ vectors $(p_0, ..., p_0)^T$ and $(q_0, ..., q_0)^T$ where p_0 and q_0 are the initial values. Then evaluate p^N and q^N at $t = T$ which is the same thing as using the coefficients p_N and q_N as the new initial conditions to the next interval.

2.2.2 Spectral Tau Method with Chebyshev-Phi

In this method, we introduce a set of trial functions which are similar to those in section 2.2.1

$$\varphi_0(t) = \frac{T-t}{T} \quad , \quad \varphi_1(t) = \frac{t}{T} \qquad , \qquad \varphi_j(t) = \int_0^t T_{j-1}(s)ds \quad , \quad j = 2, ..., N$$

For the Chebyshev polynomials, the recursive relation for the integral on $[-1, 1]$ is given by

$$\int \hat{T}_n(x)dx \quad = \quad \begin{cases} \frac{1}{2}\left[\frac{\hat{T}_{n+1}(x)}{n+1} - \frac{\hat{T}_{|n-1|}(x)}{n-1}\right] & , \ n \neq 1 \\ \frac{1}{4}\hat{T}_2(x) & , \quad n = 1 \end{cases}$$

Therefore, for $t \in [0,T]$,

$$\begin{aligned}
\varphi_2(t) &= \frac{T}{2}\Big(\frac{1}{4}T_2(t) - \frac{1}{4}T_2(0)\Big) = \frac{T}{8}T_2(t) - \frac{T}{8} \\
\varphi_j(t) &= \frac{T}{2}\Big\{\frac{1}{2}\Big[\frac{T_j(t)}{j} - \frac{T_{j-2}(t)}{j-2}\Big] + \frac{(-1)^j}{2}\Big[\frac{1}{j-2} - \frac{1}{j}\Big]\Big\} \quad , \quad j = 3,4,...
\end{aligned}$$

At this point, we shall make an observation that

$$\varphi_0(0) = 1 \ ; \ \varphi_0(T) = 0 \ ; \ \varphi_1(0) = 0 \ ; \ \varphi_1(T) = 1 \ ;$$

and , for $j \geq 2$,

$$\begin{aligned}
\varphi_j(0) = 0 \ ; \ \varphi_j(T) &= \frac{T}{4}\Big[\frac{1}{j}(1-(-1)^j) - \frac{1}{j-2}(1-(-1)^j)\Big] \\
&= \begin{cases} \frac{T}{2}\Big[\frac{1}{j} - \frac{1}{j-2}\Big] \ , \ j \text{ is odd} \\ 0 \ , \qquad j \text{ is even} \end{cases}
\end{aligned}$$

The inner product of Chebyshev polynomials on $[0,T]$ is given by

$$(T_i, T_j)_T = \int_0^T T_i(s)T_j(s)ds = \begin{cases} \frac{1}{4}T\pi \ , \quad i = j = 1,2,... \\ \frac{T}{2}\pi \ , \quad i = j = 0 \\ 0 \quad \text{otherwise} \end{cases}$$

In this method, we find the solution

$p - p_0, q - q_0 \in H^1_{(0}[0,T] = \{v \in H^1[0,r] : v(0) = 0\}$ such that

$$\begin{aligned}
(\frac{dp}{dt}, v) &= (-H_q, v) \quad , \quad v \in H^1[0,T] \\
(\frac{dq}{dt}, v) &= (\ H_p, v)
\end{aligned}$$

For the weak form, we seek solutions $p^N, q^N \in \mathcal{P}_N[0,T]$, $p^N(0) = p_0$ and $q^N(0) = q_0$ of the form

$$p^N(t) = p_0\varphi_0(t) + p_N\varphi_1(t) + \sum_{j=2}^{N} p_{j-1}\varphi_j(t) \quad , \quad q^N(t) = q_0\varphi_0(t) + q_N\varphi_1(t) + \sum_{j=2}^{N} q_{j-1}\varphi_j(t)$$

such that

$$\begin{aligned} (\frac{dp^N}{dt}, T_i) &= (-H_q(p^N, q^N), T_i) \quad , \quad i = 0, ..., N-1 \\ (\frac{dq^N}{dt}, T_i) &= (\ H_p(p^N, q^N), T_i) \end{aligned} \tag{2.2.2}$$

With the derivative of the expansion

$$\frac{dp^N(t)}{dt} = \frac{(p_N - p_0)}{T} + \sum_{j=1}^{N-1} p_j T_j(t) \quad , \quad \frac{dq^N(t)}{dt} = \frac{(q_N - q_0)}{T} + \sum_{j=1}^{N-1} q_j T_j(t),$$

the system (2.2.2) can be written as a matrix equation

$$A\mathbf{z}(t) = \mathbf{F(z(t))}$$

where

$$A = \frac{T}{2}\begin{pmatrix} D & 0 \\ 0 & D \end{pmatrix} \quad , \quad D = \begin{pmatrix} \pi & 0 & \dots & 0 \\ 0 & \frac{\pi}{2} & \dots & 0 \\ \vdots & \vdots & \ddots & \vdots \\ 0 & 0 & \dots & \frac{\pi}{2} \end{pmatrix}$$

$$\mathbf{z} = \begin{pmatrix} \mathbf{p} \\ \mathbf{q} \end{pmatrix} = \begin{pmatrix} \frac{p_N - p_0}{T} \\ p_1 \\ \vdots \\ p_{N-1} \\ \frac{q_N - q_0}{T} \\ q_1 \\ \vdots \\ q_{N-1} \end{pmatrix}, \quad \mathbf{F(z)} = \begin{pmatrix} (-H_q(p^N, q^N), T_0) \\ (-H_q(p^N, q^N), T_1) \\ \vdots \\ (-H_q(p^N, q^N), T_{N-1}) \\ (H_p(p^N, q^N), T_0) \\ (H_p(p^N, q^N), T_1) \\ \vdots \\ (H_p(p^N, q^N), T_{N-1}) \end{pmatrix}$$

or

$$\mathbf{z}(t) = \frac{4}{\pi T}\mathbf{F(z(t))}$$

where

$$\mathbf{z} = \begin{pmatrix} \mathbf{p} \\ \mathbf{q} \end{pmatrix} = \begin{pmatrix} \frac{2}{T}(p_N - p_0) \\ p_1 \\ \vdots \\ p_{N-1} \\ \frac{2}{T}(q_N - q_0) \\ q_1 \\ \vdots \\ q_{N-1} \end{pmatrix}, \quad \mathbf{F(z)} = \begin{pmatrix} (-H_q(p^N, q^N), T_0) \\ (-H_q(p^N, q^N), T_1) \\ \vdots \\ (-H_q(p^N, q^N), T_{N-1}) \\ (H_p(p^N, q^N), T_0) \\ (H_p(p^N, q^N), T_1) \\ \vdots \\ (H_p(p^N, q^N), T_{N-1}) \end{pmatrix}.$$

We solve the system by using an iterative method

$$\mathbf{z}^{new} = \frac{4}{\pi T}\mathbf{F}(\mathbf{z}^{old}).$$

We keep the same concept on the initial guesses. The initial guesses to start the iterative method are $(N \times 1)$ vectors $(p_0, ..., p_0)^T$ and $(q_0, ..., q_0)^T$ where p_0 and q_0 are the initial values. However, the values at the terminal point of each interval need to be evaluated differently from the previous two methods with Legendre-Phi. In this method, we need to compute the end value by using the original expansions.

$$\begin{aligned} p^N(T) &= p_N + \sum_{\text{odd j};j=2}^{N} p_{j-1} \frac{T}{2}\Big[\frac{1}{j} - \frac{1}{j-2}\Big] \\ q^N(T) &= q_N + \sum_{\text{odd j};j=2}^{N} q_{j-1} \frac{T}{2}\Big[\frac{1}{j} - \frac{1}{j-2}\Big] \end{aligned}$$

2.3 Spectral Collocation Methods

2.3.1 Spectral Collocation Method with Legendre-Phi

In this method, we use the same set of trial functions that we have introduced in the previous section

$$\varphi_0(t) = \frac{T-t}{T} \quad , \quad \varphi_1(t) = \frac{t}{T} \quad , \quad \varphi_j(t) = \int_0^t L_{j-1}(s)ds \quad , \quad j = 2, ..., N$$

The recursive relation of Legendre polynomials provides

$$\varphi_j(t) = \frac{T}{2j+1}(L_j(t) - L_{j-2}(t)).$$

We seek for the solutions $p^N, q^N \in \mathcal{P}_N[0,T]$, $p^N(0) = p_0$ and $q^N(0) = q_0$

$$\begin{aligned} p^N(t) &= p_0\varphi_0(t) + p_N\varphi_1(t) + \sum_{j=2}^{N} p_{j-1}\varphi_j(t) \\ q^N(t) &= q_0\varphi_0(t) + q_N\varphi_1(t) + \sum_{j=2}^{N} q_{j-1}\varphi_j(t) \end{aligned}$$

such that

$$\begin{aligned}\frac{dp^N}{dt}(t_k) &= F(p^N(t_k), q^N(t_k)) \quad , \quad 1 \leq k \leq N, \\ \frac{dq^N}{dt}(t_k) &= G(p^N(t_k), q^N(t_k)) \quad , \quad 1 \leq k \leq N,\end{aligned}$$

where $t_1, ..., t_N$ are the transformed Legendre-Gauss quadrature points, i.e. $t_j = \frac{T(x_j + 1)}{2}$ where $x_j' s \quad , \ j = 1, ..., N$ are zeros of L_N(i.e. $\hat{L}_N(x_j) = 0$) and $L_j' s$ are Legendre polynomials on $[0, T]$. It follows that for $k = 1, ..., N$

$$\begin{aligned}\frac{(p_N - p_0)}{T} + \sum_{j=1}^{N-1} p_j L_j(t_k) &= F(p^N(t_k), q^N(t_k)) \\ \frac{(q_N - q_0)}{T} + \sum_{j=1}^{N-1} q_j L_j(t_k) &= G(p^N(t_k), q^N(t_k)),\end{aligned}$$

the system can be written as a matrix equation

$$A\mathbf{z}(t) = \mathbf{F(z(t))}$$

where

$$A = \begin{pmatrix} \boldsymbol{L} & 0 \\ 0 & \boldsymbol{L} \end{pmatrix} \quad , \quad \boldsymbol{L} = \begin{pmatrix} 1 & L_1(t_1) & L_2(t_1) & \dots & L_{N-1}(t_1) \\ 1 & L_1(t_2) & L_2(t_2) & \dots & L_{N-1}(t_2) \\ \vdots & \vdots & \vdots & \ddots & \vdots \\ 1 & L_1(t_N) & L_2(t_N) & \dots & L_{N-1}(t_N) \end{pmatrix}$$

$$\mathbf{z} = \begin{pmatrix} \mathbf{p} \\ \mathbf{q} \end{pmatrix} = \begin{pmatrix} \frac{p_N - p_0}{T} \\ p_1 \\ \vdots \\ p_{N-1} \\ \frac{q_N - q_0}{T} \\ q_1 \\ \vdots \\ q_{N-1} \end{pmatrix} \quad , \quad \mathbf{F(z)} = \begin{pmatrix} -H_q(p^N(t_1), q^N(t_1)) \\ -H_q(p^N(t_2), q^N(t_2)) \\ \vdots \\ -H_q(p^N(t_N), q^N(t_N)) \\ H_p(p^N(t_1), q^N(t_1)) \\ H_p(p^N(t_2), q^N(t_2)) \\ \vdots \\ H_p(p^N(t_N), q^N(t_N)) \end{pmatrix}.$$

We solve the system by using an iterative method

$$A\mathbf{z}^{new} = \mathbf{F}(\mathbf{z}^{old}).$$

The initial guess and the values at the end point of each interval are evaluated in the same way as the spectral Tau method with Legendre-Phi.

2.3.2 Spectral Collocation Method with Chebyshev-Phi

In this method, we use a set of trial functions as in section 2.2.2.

$$\varphi_0(t) = \frac{T-t}{T} \quad , \quad \varphi_1(t) = \frac{t}{T} \quad , \quad \varphi_j(t) = \int_0^t T_{j-1}(s)ds \quad , \quad j = 2, ..., N$$

We seek for the solutions $p^N, q^N \in \mathcal{P}_N[0,T]$, $p^N(0) = p_0$ and $q^N(0) = q_0$

$$\begin{aligned} p^N(t) &= p_0\varphi_0(t) + p_N\varphi_1(t) + \sum_{j=2}^{N} p_{j-1}\varphi_j(t) \\ q^N(t) &= q_0\varphi_0(t) + q_N\varphi_1(t) + \sum_{j=2}^{N} q_{j-1}\varphi_j(t) \end{aligned}$$

such that

$$\begin{aligned}\frac{dp^N}{dt}(t_k) &= F(p^N(t_k), q^N(t_k)) \quad , \quad 1 \leq k \leq N, \\ \frac{dq^N}{dt}(t_k) &= G(p^N(t_k), q^N(t_k)) \quad , \quad 1 \leq k \leq N,\end{aligned}$$

where $t_1, ..., t_N$ are the transformed Chebyshev-Gauss quadrature points, i.e. $t_j = \frac{T(x_j + 1)}{2}$ where $x_j' s \quad , \ j = 1, ..., N$ are zeros of T_N(i.e. $T_N(x_j) = 0$) and $T_j' s$ are the Chebyshev polynomials on $[0, T]$. It follows that for $k = 1, ..., N$

$$\begin{aligned}\frac{(p_N - p_0)}{T} + \sum_{j=1}^{N-1} p_j T_j(t_k) &= F(p^N(t_k), q^N(t_k)) \\ \frac{(q_N - q_0)}{T} + \sum_{j=1}^{N-1} q_j T_j(t_k) &= G(p^N(t_k), q^N(t_k)),\end{aligned}$$

the system can be written as a matrix equation

$$A\mathbf{z}(t) = \mathbf{F(z(t))}$$

where

$$A = \begin{pmatrix} C & 0 \\ 0 & C \end{pmatrix} \quad , \quad C = \begin{pmatrix} 1 & T_1(t_1) & T_2(t_1) & \dots & T_{N-1}(t_1) \\ 1 & T_1(t_2) & T_2(t_2) & \dots & T_{N-1}(t_2) \\ \vdots & \vdots & \vdots & \ddots & \vdots \\ 1 & T_1(t_N) & T_2(t_N) & \dots & T_{N-1}(t_N) \end{pmatrix}$$

$$\mathbf{z} = \begin{pmatrix} \mathbf{p} \\ \mathbf{q} \end{pmatrix} = \begin{pmatrix} \frac{p_N - p_0}{T} \\ p_1 \\ \vdots \\ p_{N-1} \\ \frac{q_N - q_0}{T} \\ q_1 \\ \vdots \\ q_{N-1} \end{pmatrix}, \quad \mathbf{F(z)} = \begin{pmatrix} -H_q(p^N(t_1), q^N(t_1)) \\ -H_q(p^N(t_2), q^N(t_2)) \\ \vdots \\ -H_q(p^N(t_N), q^N(t_N)) \\ H_p(p^N(t_1), q^N(t_1)) \\ H_p(p^N(t_2), q^N(t_2)) \\ \vdots \\ H_p(p^N(t_N), q^N(t_N)) \end{pmatrix}.$$

We solve the system by using an iterative method

$$A\mathbf{z}^{new} = \mathbf{F}(\mathbf{z}^{old}).$$

We keep the same concept on the initial guesses. However,the values at the end-point of each interval need to be evaluated differently from the previous two methods with Chebyshev-Phi. In this method, we need to compute the end value by using the original expansion.

$$\begin{aligned} p^N(T) &= p_N + \sum_{\text{odd j};j=2}^{N} p_{j-1} \frac{T}{2} \Big[\frac{1}{j} - \frac{1}{j-2} \Big] \\ q^N(T) &= q_N + \sum_{\text{odd j};j=2}^{N} q_{j-1} \frac{T}{2} \Big[\frac{1}{j} - \frac{1}{j-2} \Big]. \end{aligned}$$

If we further consider the system

$$A\mathbf{z}(t) = \mathbf{F(z(t))}$$

we discussed above , we could avoid the inverse of the matrix A by multiplying both

sides by the transpose of C and the Gaussian weights.

$$C^T W C = \begin{pmatrix} 1 & 1 & \dots & 1 \\ T_1(t_1) & T_1(t_2) & \dots & T_1(t_N) \\ \vdots & \vdots & \ddots & \vdots \\ T_{N-1}(t_1) & T_{N-1}(t_2) & \dots & T_{N-1}(t_N) \end{pmatrix} \begin{pmatrix} w_1 & 0 & \cdots & 0 \\ 0 & w_2 & \cdots & 0 \\ \vdots & \vdots & \ddots & \vdots \\ 0 & 0 & \cdots & w_N \end{pmatrix} \begin{pmatrix} 1 & T_1(t_1) & \dots & T_{N-1}(t_1) \\ 1 & T_1(t_2) & \dots & T_{N-1}(t_2) \\ \vdots & \vdots & \ddots & \vdots \\ 1 & T_1(t_N) & \dots & T_{N-1}(t_N) \end{pmatrix}.$$

Using the orthogonality of Chebyshev polynomials together with the Gaussian quadrature, the matrix can be considered as

$$\tilde{C} = C^T W C = [\tilde{c}]_{ij}$$

where

$$\begin{aligned} c_{11} &= \sum_{k=1}^{N} w_k \quad = \quad (T_0, T_0)_T = \frac{T}{2}\pi \\ c_{ii} &= \sum_{k=1}^{N} w_k T_i^2(t_k) \quad = \quad (T_i, T_i)_T = \frac{T}{2}\frac{\pi}{2} \quad = \frac{T\pi}{4} \quad , \quad i = 2, ..., N-1 \\ c_{ij} &= \sum_{k=1}^{N} w_k T_i(t_k) T_j(t_k) = \ (T_i, T_j)_T = 0 \ , \ i \neq j. \end{aligned}$$

We obtain the result by the property of Guassian quadrature. For N Gaussian points $t_1, .., t_N$, the integral is exact for all polynomials whose degree is at most $(2N-1)$ [37]. It follows that

$$\tilde{C} = \frac{T}{2} \begin{pmatrix} \pi & 0 & \cdots & 0 \\ 0 & \frac{\pi}{2} & \cdots & 0 \\ \vdots & \vdots & \ddots & \vdots \\ 0 & 0 & \cdots & \frac{\pi}{2} \end{pmatrix} = \frac{T\pi}{4} \begin{pmatrix} 2 & 0 & \cdots & 0 \\ 0 & 1 & \cdots & 0 \\ \vdots & \vdots & \ddots & \vdots \\ 0 & 0 & \cdots & 1 \end{pmatrix}.$$

The system becomes

$$\tilde{\mathbf{z}}(t) = \frac{4}{T\pi}\tilde{\mathbf{F}}(\mathbf{z}(t))$$

where

$$\tilde{\mathbf{z}}(t) = \begin{pmatrix} \mathbf{p} \\ \mathbf{q} \end{pmatrix} = \begin{pmatrix} \frac{2(p_N - p_0)}{T} \\ p_1 \\ \vdots \\ p_{N-1} \\ \frac{2(q_N - q_0)}{T} \\ q_1 \\ \vdots \\ q_{N-1} \end{pmatrix} \quad , \quad \tilde{\mathbf{F}}(\mathbf{z}) = \begin{pmatrix} C^T W & 0 \\ 0 & C^T W \end{pmatrix} \begin{pmatrix} -H_q(p^N(t_1), q^N(t_1)) \\ -H_q(p^N(t_2), q^N(t_2)) \\ \vdots \\ -H_q(p^N(t_N), q^N(t_N)) \\ H_p(p^N(t_1), q^N(t_1)) \\ H_p(p^N(t_2), q^N(t_2)) \\ \vdots \\ H_p(p^N(t_N), q^N(t_N)) \end{pmatrix} .$$

2.4 Spectral Collocation Methods with Scaling

2.4.1 Spectral Collocation Method with Scaling Legendre-Phi

This method is similar to the spectral collocation method with Legendre-Phi in section 2.3.1 except the trial functions are those in section 2.3.1 but with the scaling.

$$\varphi_0(t) = \frac{T-t}{T} \quad , \quad \varphi_1(t) = \frac{t}{T} \quad , \quad \tilde{\varphi}_j(t) = \int_0^t \tilde{L}_{j-1}(s)ds \quad , \quad j = 2, ..., N$$

$$\text{where} \quad \tilde{L}_j(t) = \sqrt{\frac{2j+1}{T}} L_j(t) \qquad \text{so} \quad \tilde{\varphi}_j{}'(t) = \tilde{L}_j(t)$$

The advantage of these trial functions is that

$$(\tilde{L}_i, \tilde{L}_j)_T = \int_0^T \tilde{L}_i(s)\tilde{L}_j(s)ds = \begin{cases} 1 \ , & i = j \\ 0 \ , & \text{otherwise} \end{cases}$$

We seek for the solutions $p^N, q^N \in \mathcal{P}_N[0,T]$, $p^N(0) = p_0$ and $q^N(0) = q_0$

$$\begin{aligned} p^N(t) &= p_0\varphi_0(t) + p_N\varphi_1(t) + \sum_{j=2}^{N} p_{j-1}\tilde{\varphi}_j(t) \\ q^N(t) &= q_0\varphi_0(t) + q_N\varphi_1(t) + \sum_{j=2}^{N} q_{j-1}\tilde{\varphi}_j(t) \end{aligned}$$

such that

$$\begin{aligned} \frac{dp^N}{dt}(t_k) &= F(p^N(t_k), q^N(t_k)) \quad , \quad 1 \le k \le N, \\ \frac{dq^N}{dt}(t_k) &= G(p^N(t_k), q^N(t_k)) \quad , \quad 1 \le k \le N, \end{aligned}$$

where $t_1, ..., t_N$ are the transformed Legendre-Gauss quadrature points, i.e. $t_j = \frac{T(x_j+1)}{2}$ where $x_j's$, $j = 1, ..., N$ are zeros of L_N(i.e. $L_N(x_j) = 0$) and $L_j's$ are the Legendre polynomials on $[0,T]$. It follows that for $k = 1, ..., N$

$$\begin{aligned} \frac{(p_N - p_0)}{T} + \sum_{j=1}^{N-1} p_j\tilde{L}_j(t_k) &= F(p^N(t_k), q^N(t_k)) \\ \frac{(q_N - q_0)}{T} + \sum_{j=1}^{N-1} q_j\tilde{L}_j(t_k) &= G(p^N(t_k), q^N(t_k)), \end{aligned}$$

the system can be written as a matrix equation

$$A\mathbf{z}(t) = \mathbf{F(z(t))}$$

where

$$A = \begin{pmatrix} \tilde{\boldsymbol{L}} & 0 \\ 0 & \tilde{\boldsymbol{L}} \end{pmatrix} \quad , \quad \tilde{\boldsymbol{L}} = \begin{pmatrix} 1 & \tilde{L}_1(t_1) & \tilde{L}_2(t_1) & \dots & \tilde{L}_{N-1}(t_1) \\ 1 & \tilde{L}_1(t_2) & \tilde{L}_2(t_2) & \dots & \tilde{L}_{N-1}(t_2) \\ \vdots & \vdots & \vdots & \ddots & \vdots \\ 1 & \tilde{L}_1(t_N) & \tilde{L}_2(t_N) & \dots & \tilde{L}_{N-1}(t_N) \end{pmatrix}$$

$$\mathbf{z} = \begin{pmatrix} \mathbf{p} \\ \mathbf{q} \end{pmatrix} = \begin{pmatrix} \frac{p_N - p_0}{T} \\ p_1 \\ \vdots \\ p_{N-1} \\ \frac{q_N - q_0}{T} \\ q_1 \\ \vdots \\ q_{N-1} \end{pmatrix} \quad , \quad \mathbf{F(z)} = \begin{pmatrix} -H_q(p^N(t_1), q^N(t_1)) \\ -H_q(p^N(t_2), q^N(t_2)) \\ \vdots \\ -H_q(p^N(t_N), q^N(t_N)) \\ H_p(p^N(t_1), q^N(t_1)) \\ H_p(p^N(t_2), q^N(t_2)) \\ \vdots \\ H_p(p^N(t_N), q^N(t_N)) \end{pmatrix}.$$

We multiply $\tilde{\boldsymbol{L}}$ by the transpose of $\tilde{\boldsymbol{L}}$ and Gaussian weights,

$$\tilde{\boldsymbol{L}}^T W \tilde{\boldsymbol{L}} = \begin{pmatrix} 1 & 1 & \dots & 1 \\ \tilde{L}_1(t_1)1 & \tilde{L}_1(t_2) & \dots & \tilde{L}_1(t_N) \\ \vdots & \vdots & \ddots & \vdots \\ \tilde{L}_{N-1}(t_1) & \tilde{L}_{N-1}(t_2) & \dots & \tilde{L}_{N-1}(t_N) \end{pmatrix} \begin{pmatrix} w_1 & 0 & \cdots & 0 \\ 0 & w_2 & \cdots & 0 \\ \vdots & \vdots & \ddots & \vdots \\ 0 & 0 & \cdots & w_N \end{pmatrix} \begin{pmatrix} 1 & \tilde{L}_1(t_1) & \dots & \tilde{L}_{N-1}(t_1) \\ 1 & \tilde{L}_1(t_2) & \dots & \tilde{L}_{N-1}(t_2) \\ \vdots & \vdots & \ddots & \vdots \\ 1 & \tilde{L}_1(t_N) & \dots & \tilde{L}_{N-1}(t_N) \end{pmatrix}.$$

Using the orthogonality of Legendre polynomials together with the Gaussian quadrature, and with N Gaussian points, $t_1, ..., t_N$, the integral is exact for all polynomials whose degree is at most $(2N-1)$ [37]. The matrix can be considered as

$$\tilde{\boldsymbol{L}}^T W \tilde{\boldsymbol{L}} = [\tilde{l}]_{ij}$$

where

$$\begin{aligned} l_{11} &= \sum_{k=1}^{N} w_k \quad = \quad (L_0, L_0)_T = T \\ l_{ii} &= \sum_{k=1}^{N} w_k \tilde{L}_i^2(t_k) \quad = \quad (\tilde{L}_i, \tilde{L}_i)_T = 1 \quad , \quad i = 2, ..., N-1 \\ l_{ij} &= \sum_{k=1}^{N} w_k \tilde{L}_i(t_k)\tilde{L}_j(t_k) = \ (\tilde{L}_i, \tilde{L}_j)_T = 0 \ , \ i \neq j. \end{aligned}$$

We obtain the result by the property of Guassian quadrature. It follows that

$$\tilde{\boldsymbol{L}}^T W \tilde{\boldsymbol{L}} = \begin{pmatrix} T & 0 & \cdots & 0 \\ 0 & 1 & \cdots & 0 \\ \vdots & \vdots & \ddots & \vdots \\ 0 & 0 & \cdots & 1 \end{pmatrix}$$

The system becomes

$$\tilde{\mathbf{z}}(t) = \tilde{\mathbf{F}}(\mathbf{z}(t))$$

where

$$\tilde{\mathbf{z}}(t) = \begin{pmatrix} \mathbf{p} \\ \mathbf{q} \end{pmatrix} = \begin{pmatrix} p_N - p_0 \\ p_1 \\ \vdots \\ p_{N-1} \\ q_N - q_0 \\ q_1 \\ \vdots \\ q_{N-1} \end{pmatrix} \quad , \quad \tilde{\mathbf{F}}(\mathbf{z}) = \begin{pmatrix} \tilde{\boldsymbol{L}}^T W & 0 \\ 0 & \tilde{\boldsymbol{L}}^T W \end{pmatrix} \begin{pmatrix} -H_q(p^N(t_1), q^N(t_1)) \\ -H_q(p^N(t_2), q^N(t_2)) \\ \vdots \\ -H_q(p^N(t_N), q^N(t_N)) \\ H_p(p^N(t_1), q^N(t_1)) \\ H_p(p^N(t_2), q^N(t_2)) \\ \vdots \\ H_p(p^N(t_N), q^N(t_N)) \end{pmatrix}.$$

We solve the system by using an iterative method

$$\mathbf{z}^{\tilde{new}}(t) = \tilde{\mathbf{F}}(\mathbf{z}^{old}(t)).$$

The initial guess and the values at the end point of each interval are evaluated in the same way as the spectral Tau method with Legendre-Phi.

2.5 Spectral Tau with Legendre-Phi using Newton Iteration

Let $\vec{p} = (p_N, p_1, ..., p_{N-1})^T$, and $\vec{q} = (q_N, q_1, ..., q_{N-1})^T$. These $\vec{p}$ and $\vec{q}$ are coefficient vectors of a solution p^N and q^N. With Newton iteration, we will consider the iteration of $\vec{p}, \vec{q}$. This means the Jacobian matrix is with respect to the coefficients p_i, q_i, where $i = 1, ..., N$, of $\vec{p}, \vec{q}$. The system can be written as

$$\mathbf{F} = \begin{pmatrix} D & 0 \\ 0 & D \end{pmatrix} \begin{pmatrix} \vec{p} \\ \vec{q} \end{pmatrix} - \begin{pmatrix} \vec{p_0} \\ \vec{q_0} \end{pmatrix} - \begin{pmatrix} (-H_q(\vec{p}, \vec{q}), \mathbf{L}) \\ (H_p(\vec{p}, \vec{q}), \mathbf{L}) \end{pmatrix} = 0$$

where

$$D = \begin{pmatrix} 1 & 0 & \cdots & 0 \\ 0 & \frac{T}{3} & & 0 \\ \vdots & & \ddots & \vdots \\ 0 & & \cdots & \frac{T}{2N-1} \end{pmatrix}, \quad \vec{p_0} = \begin{pmatrix} p_0 \\ 0 \\ \vdots \\ 0 \end{pmatrix}, \quad \vec{q_0} = \begin{pmatrix} q_0 \\ 0 \\ \vdots \\ 0 \end{pmatrix}, \quad \mathbf{L} = \begin{pmatrix} L_0 \\ L_1 \\ \vdots \\ L_{N-1} \end{pmatrix}$$

The iteration is

$$\begin{pmatrix} \vec{p} \\ \vec{q} \end{pmatrix}^{(k+1)} = \begin{pmatrix} \vec{p} \\ \vec{q} \end{pmatrix}^{(k)} - [\nabla \mathbf{F}(\vec{p}^{(k)}, \vec{q}^{(k)})]^{-1} \mathbf{F}(\vec{p}^{(k)}, \vec{q}^{(k)})$$

NOTE: Here we need to find $\nabla\mathbf{F}$ with respect to the coefficients p_i's and q_i's.

$$\nabla\mathbf{F}(\vec{p},\vec{q}) = \begin{pmatrix} D & 0 \\ 0 & D \end{pmatrix} - \begin{pmatrix} H_1 & H_2 \\ H_3 & H_4 \end{pmatrix}$$

where

$$H_1 = \begin{pmatrix} (-H_{qp_N}(\vec{p},\vec{q}), L_0) & (-H_{qp_1}(\vec{p},\vec{q}), L_0) & \cdots & (-H_{qp_{N-1}}(\vec{p},\vec{q}), L_0) \\ (-H_{qp_N}(\vec{p},\vec{q}), L_1) & (-H_{qp_1}(\vec{p},\vec{q}), L_1) & \cdots & (-H_{qp_{N-1}}(\vec{p},\vec{q}), L_1) \\ \vdots & \vdots & \ddots & \vdots \\ (-H_{qp_N}(\vec{p},\vec{q}), L_{N-1}) & (-H_{qp_1}(\vec{p},\vec{q}), L_{N-1})) & \cdots & (-H_{qp_{N-1}}(\vec{p},\vec{q}), L_{N-1})) \end{pmatrix}$$

$$H_1 = \begin{pmatrix} (-H_{qp}(p^N,q^N)\varphi_1, L_0) & (-H_{qp}(p^N,q^N)\varphi_2, L_0) & \cdots & (-H_{qp}(p^N,q^N)\varphi_N, L_0) \\ (-H_{qp}(p^N,q^N)\varphi_1, L_1) & (-H_{qp}(p^N,q^N)\varphi_2, L_1) & \cdots & (-H_{qp}(p^N,q^N)\varphi_N, L_1) \\ \vdots & \vdots & \ddots & \vdots \\ (-H_{qp}(p^N,q^N)\varphi_1, L_{N-1}) & (-H_{qp}(p^N,q^N)\varphi_2, L_{N-1}) & \cdots & (-H_{qp}(p^N,q^N)\varphi_N, L_{N-1}) \end{pmatrix}$$

$$H_2 = \begin{pmatrix} (-H_{qq_N}(\vec{p},\vec{q}), L_0) & (-H_{qq_1}(\vec{p},\vec{q}), L_0) & \cdots & (-H_{qq_{N-1}}(\vec{p},\vec{q}), L_0) \\ (-H_{qq_N}(\vec{p},\vec{q}), L_1) & (-H_{qq_1}(\vec{p},\vec{q}), L_1) & \cdots & (-H_{qq_{N-1}}(\vec{p},\vec{q}), L_1) \\ \vdots & \vdots & \ddots & \vdots \\ (-H_{qq_N}(\vec{p},\vec{q}), L_{N-1}) & (-H_{qq_1}(\vec{p},\vec{q}), L_{N-1})) & \cdots & (-H_{qq_{N-1}}(\vec{p},\vec{q}), L_{N-1})) \end{pmatrix}$$

$$H_2 = \begin{pmatrix} (-H_{qq}(p^N,q^N)\varphi_1, L_0) & (-H_{qq}(p^N,q^N)\varphi_2, L_0) & \cdots & (-H_{qq}(p^N,q^N)\varphi_N, L_0) \\ (-H_{qq}(p^N,q^N)\varphi_1, L_1) & (-H_{qq}(p^N,q^N)\varphi_2, L_1) & \cdots & (-H_{qq}(p^N,q^N)\varphi_N, L_1) \\ \vdots & \vdots & \ddots & \vdots \\ (-H_{qq}(p^N,q^N)\varphi_1, L_{N-1}) & (-H_{qq}(p^N,q^N)\varphi_2, L_{N-1}) & \cdots & (-H_{qq}(p^N,q^N)\varphi_N, L_{N-1}) \end{pmatrix}$$

$$H_3 = \begin{pmatrix} (H_{pp_N}(\vec{p},\vec{q}), L_0) & (H_{pp_1}(\vec{p},\vec{q}), L_0) & \cdots & (H_{pp_{N-1}}(\vec{p},\vec{q}), L_0) \\ (H_{pp_N}(\vec{p},\vec{q}), L_1) & (H_{pp_1}(\vec{p},\vec{q}), L_1) & \cdots & (H_{pp_{N-1}}(\vec{p},\vec{q}), L_1) \\ \vdots & \vdots & \ddots & \vdots \\ (H_{pp_N}(\vec{p},\vec{q}), L_{N-1}) & (H_{pp_1}(\vec{p},\vec{q}), L_{N-1})) & \cdots & (H_{pp_{N-1}}(\vec{p},\vec{q}), L_{N-1})) \end{pmatrix}$$

$$H_3 = \begin{pmatrix} (H_{pp}(p^N,q^N)\varphi_1, L_0) & (H_{pp}(p^N,q^N)\varphi_2, L_0) & \cdots & (H_{pp}(p^N,q^N)\varphi_N, L_0) \\ (H_{pp}(p^N,q^N)\varphi_1, L_1) & (H_{pp}(p^N,q^N)\varphi_2, L_1) & \cdots & (H_{pp}(p^N,q^N)\varphi_N, L_1) \\ \vdots & \vdots & \ddots & \vdots \\ (H_{pp}(p^N,q^N)\varphi_1, L_{N-1}) & (H_{pp}(p^N,q^N)\varphi_2, L_{N-1}) & \cdots & (H_{pp}(p^N,q^N)\varphi_N, L_{N-1}) \end{pmatrix}$$

$$H_3 = \begin{pmatrix} (H_{pq_N}(\vec{p},\vec{q}), L_0) & (H_{pq_1}(\vec{p},\vec{q}), L_0) & \cdots & (H_{pq_{N-1}}(\vec{p},\vec{q}), L_0) \\ (H_{pq_N}(\vec{p},\vec{q}), L_1) & (H_{pq_1}(\vec{p},\vec{q}), L_1) & \cdots & (H_{pq_{N-1}}(\vec{p},\vec{q}), L_1) \\ \vdots & \vdots & \ddots & \vdots \\ (H_{pqq_N}(\vec{p},\vec{q}), L_{N-1}) & (H_{pq_1}(\vec{p},\vec{q}), L_{N-1})) & \cdots & (H_{pq_{N-1}}(\vec{p},\vec{q}), L_{N-1})) \end{pmatrix}$$

$$H_3 = \begin{pmatrix} (H_{pq}(p^N,q^N)\varphi_1, L_0) & (H_{pq}(p^N,q^N)\varphi_2, L_0) & \cdots & (H_{pq}(p^N,q^N)\varphi_N, L_0) \\ (H_{pq}(p^N,q^N)\varphi_1, L_1) & (H_{pq}(p^N,q^N)\varphi_2, L_1) & \cdots & (H_{pq}(p^N,q^N)\varphi_N, L_1) \\ \vdots & \vdots & \ddots & \vdots \\ (H_{pq}(p^N,q^N)\varphi_1, L_{N-1}) & (H_{pq}(p^N,q^N)\varphi_2, L_{N-1}) & \cdots & (H_{pq}(p^N,q^N)\varphi_N, L_{N-1}) \end{pmatrix}$$

Notes:

1) For a linear Hamiltonian system, we could solve the system explicitly.

2) There are several iterative methods that could be applied. We chose a simple iterative method and the Newton iteration for our systems.

3 Error Analysis

Consider a canonical linear Hamiltonian system defined by a quadratic Hamiltonian

$$H = \frac{1}{2} z^T L z$$

where L is a $2d \times 2d$, d is degree of freedoms, symmetric matrix and $z = [\mathbf{p}, \mathbf{q}]^T$.

If we consider H as energy, H then needs to be positive which implies L is a positive definite matrix. The corresponding equation of motion is given by

$$\frac{dz}{dt} = J^{-1} L z$$

where $J = \begin{pmatrix} 0 & I_d \\ I_d & 0 \end{pmatrix}$ and $J^{-1} = -J$.

For simplicity, we will consider the case $d = 1$, i.e. $z = [p, q]^T$, $L = \begin{pmatrix} d & a \\ a & b \end{pmatrix}$.

L is positive definite. It follows automatically that $d > 0, b > 0, bd > a^2$. WLOG, we take $a \geq 0$. The analysis is similar for the case that $a < 0$. Here

$$H = \frac{1}{2} [p \quad q] \begin{bmatrix} d & a \\ a & b \end{bmatrix} \begin{bmatrix} p \\ q \end{bmatrix} = \frac{1}{2} dp^2 + \frac{1}{2} bq^2 + apq.$$

The Hamiltonian system becomes

$$\frac{dp}{dt} = -H_q = -ap - bq$$

$$\frac{dq}{dt} = H_p = dp + aq.$$

Consider a linear Hamiltonian system with $p(0) = p_0$ and $q(0) = q_0$,

$$\begin{aligned} \frac{dp}{dt} &= -ap - bq \\ \frac{dq}{dt} &= dp + aq \end{aligned} \qquad (3.1)$$

Here $a, b, d > 0$ from the previous section.

3.1 Spectral Tau Method with Gauss-Lobatto points and Chebyshev Polynomials

Weak Form: Find $p - p_0, q - q_0 \in H^1_{(0}[0,T] = \{u \in H^1[0,T] : u(0) = 0\}$ such that

$$\begin{aligned} (p', v) &= -a(p, v) - b(q, v) \quad , \forall v, w H^1_{(0}[0,T] \\ (q', w) &= d(p, w) + a(q, w) \quad , \end{aligned} \qquad (3.2)$$

Variational Form : Find $p_N, q_N \in \mathcal{P}_N[0,T]$, $p_N(0) = p_0$ and $q_N(0) = q_0$ such that

$$\begin{aligned} (p'_N, v) &= -a(p_N, v) - b(q_N, v) \quad , \forall v \in \mathcal{P}_N[0,T], v(0) = 0 \\ (q'_N, w) &= d(p_N, w) + a(q_N, w) \quad , \forall w \in \mathcal{P}_N[0,T], w(0) = 0 \end{aligned} \qquad (3.3)$$

3.1.1 Error Analysis for a Linear System

Subtract (3.3) from (3.2)

$$\begin{aligned} (p' - p'_N, v) &= -a(p - p_N, v) - b(q - q_N, v) \\ (q' - q'_N, w) &= d(p - p_N, w) + a(q - q_N, w) \end{aligned} \qquad (3.4)$$

Choose the interpolation that $\mathcal{I}_N p(0) = p_0$ so $\mathcal{I}_N p(0) - p_N(0) = 0$ and similarly for space of w.

Take $v = \mathcal{I}_N p - p_N$, $w = \mathcal{I}_N q - q_N$ so $v(0) = 0 = w(0)$.

$$\begin{aligned}(p' - p'_N, \mathcal{I}_N p - p_N) &= -a(p - p_N, \mathcal{I}_N p - p_N) - b(q - q_N, \mathcal{I}_N p - p_N) \\ (q' - q'_N, \mathcal{I}_N q - q_N) &= d(p - p_N, \mathcal{I}_N q - q_N) + a(q - q_N, \mathcal{I}_N q - q_N) \quad (3.5)\end{aligned}$$

L_2-projection property:

$$\begin{aligned}(p - \Pi_N p, v) &= 0 \quad , \forall v \in \mathcal{P}_N \\ \text{Similarly} \quad (p' - \Pi_N p', v) &= 0 \quad , \forall v \in \mathcal{P}_N \\ \Rightarrow (p, v) = (\Pi_N p, v) \quad &\text{and similarly} \qquad (p', v) = (\Pi_N p', v).\end{aligned}$$

$$\text{Then} \qquad (p' - p'_N, v) = (\Pi_N p' - p'_N, v), \forall v \in \mathcal{P}_N.$$

Then (3.5) becomes

$$\begin{aligned}(\Pi_N p' - p'_N, \mathcal{I}_N p - p_N) &= -a(p - p_N, \mathcal{I}_N p - p_N) - b(q - q_N, \mathcal{I}_N p - p_N) \\ (\Pi_N q' - q'_N, \mathcal{I}_N q - q_N) &= d(p - p_N, \mathcal{I}_N q - q_N) + a(q - q_N, \mathcal{I}_N q - q_N) \quad (3.6)\end{aligned}$$

Multiply the first equation by d and the second by b.

$$\begin{aligned}d(\Pi_N p' - p'_N, \mathcal{I}_N p - p_N) &= -ad(p - \mathcal{I}_N p + \mathcal{I}_N p - p_N, \mathcal{I}_N p - p_N) \\ &\quad -bd(q - \mathcal{I}_N q + \mathcal{I}_N q - q_N, \mathcal{I}_N p - p_N) \\ b(\Pi_N q' - q'_N, \mathcal{I}_N q - q_N) &= bd(p - \mathcal{I}_N p + \mathcal{I}_N p - p_N, \mathcal{I}_N q - q_N) \\ &\quad +ab(q - \mathcal{I}_N q + \mathcal{I}_N q - q_N, \mathcal{I}_N q - q_N) \quad (3.7)\end{aligned}$$

Add the two equation with a cancelation.

$$d(\Pi_N p' - p'_N, \mathcal{I}_N p - p_N) + b(\Pi_N q' - q'_N, \mathcal{I}_N q - q_N) = -ad(p = \mathcal{I}_N p, \mathcal{I}_N p - p_N) - ad\|\mathcal{I}_N p - p_N\|^2$$

$$-bd(q-\mathcal{I}_N q, \mathcal{I}_N p - p_N) + bd(p-\mathcal{I}_N p, \mathcal{I}_N q - q_N)$$

$$+ab(q-\mathcal{I}_N q, \mathcal{I}_N q - q_N) + ab\|\mathcal{I}_N q - q_N\|^2 \qquad (3.8)$$

Let $E_N^p = \mathcal{I}_N p - p_N$ and $E_N^q = \mathcal{I}_N q - q_N$.The right hand side becomes

$$\begin{aligned} R.H.S &= -ad(p-\mathcal{I}_N p, E_N^p) - ad\|E_N^p\|^2 - bd(q-\mathcal{I}_N q, E_N^p) + bd(p-\mathcal{I}_N p, E_N^q) \\ &\quad +ab(q-\mathcal{I}_N q, E_N^q) + ab\|E_N^q\|^2 \end{aligned}$$

By Hölder's Inequality,

$$\begin{aligned} R.H.S &\leq ad\|\mathcal{I}_N p - p\|\|E_N^p\| - ad\|E_N^p\|^2 + bd\|\mathcal{I}_N q - q\|\|E_N^p\|^2 + bd\|\mathcal{I}_N p - p\|\|E_N^q\|^2 \\ &\quad +ab\|\mathcal{I}_N q - q\|\|E_N^q\|^2 + ab\|E_N^q\|^2 \end{aligned}$$

By Young's Inequality,

$$\begin{aligned} R.H.S &\leq (\frac{ad}{2}+\frac{bd}{2})\|\mathcal{I}_N p - p\|^2 + (\frac{bd}{2}+\frac{ab}{2})\|\mathcal{I}_N q - q\|^2 + +(\frac{ad}{2}+ad+\frac{bd}{2})\|E_N^p\|^2 \\ &\quad +(\frac{bd}{2}+\frac{ab}{2}+ab)\|E_N^q\|^2 \\ &= (\frac{ad+bd}{2})\|\mathcal{I}_N p - p\|^2 + (\frac{ab+bd}{2})\|\mathcal{I}_N q - q\|^2 + (\frac{3ad}{2}+\frac{bd}{2})\|E_N^p\|^2 + (\frac{3ab}{2}+\frac{bd}{2})\|E_N^q\|^2 \end{aligned}$$

$$\begin{aligned} L.H.S. &= d(\Pi_N p' - p_N', E_N^p) + b(\Pi_N q' - q_N', E_N^q) \\ &= d(\Pi_N p' - (\mathcal{I}_N p)' + (\mathcal{I}_N p - p_N)', E_N^p) + b(\Pi_N q' - (\mathcal{I}_N q)' + (\mathcal{I}_N q - q_N)', E_N^q) \\ &= d(\Pi_N p' - (\mathcal{I}_N p)', E_N^p) + d(\frac{d}{dt}E_N^p, E_N^p) + b(\Pi_N q' - (\mathcal{I}_N q)', E_N^q) + b(\frac{d}{dt}E_N^q, E_N^q) \end{aligned}$$

All together with Hölder's and Young's Inequality,

$$\begin{aligned} d(\frac{d}{dt}E_N^p, E_N^p) + b(\frac{d}{dt}E_N^q, E_N^q) &\leq \frac{d}{2}\|\Pi_N p' - (\mathcal{I}_N p)'\|^2 + \frac{d}{2}\|E_N^p\|^2 + \frac{b}{2}\|\Pi_N q' - (\mathcal{I}_N q)'\|^2 + \frac{b}{2}\|E_N^q\|^2 \\ &\quad +(\frac{ad+bd}{2})\|\mathcal{I}_N p - p\|^2 + (\frac{ad+bd}{2})\|\mathcal{I}_N q - q\|^2 \\ &\quad +(\frac{3ad}{2} + \frac{bd}{2})\|E_N^p\|^2 + (\frac{3ab}{2} + \frac{bd}{2})\|E_N^q\|^2 \\ &= \frac{d}{2}\|\Pi_N p' - (\mathcal{I}_N p)'\|^2 + \frac{b}{2}\|\Pi_N q' - (\mathcal{I}_N q)'\|^2 \\ &\quad +(\frac{ad+bd}{2})\|\mathcal{I}_N p - p\|^2 + (\frac{ad+bd}{2})\|\mathcal{I}_N q - q\|^2 \\ &\quad +\frac{d}{2}(1+3a+b))\|E_N^p\|^2 + \frac{b}{2}(1+3a+d))\|E_N^q\|^2 \end{aligned}$$

Let $D = max\{b, d\}$.

$$\begin{aligned} d(\frac{d}{dt}E_N^p, E_N^p) + b(\frac{d}{dt}E_N^q, E_N^q) &\leq \frac{d}{2}\|\Pi_N p' - (\mathcal{I}_N p)'\|^2 + \frac{b}{2}\|\Pi_N q' - (I_N q)'\|^2 \\ &\quad +(\frac{ad+bd}{2})\|\mathcal{I}_N p - p\|^2 + (\frac{ad+bd}{2})\|\mathcal{I}_N q - q\|^2 \\ &\quad +(\frac{1+3a+D}{2})[d\|E_N^p\|^2 + b\|E_N^q\|^2] \end{aligned}$$

Use Fundamental Theorem of Calculus**(A1)** for L.H.S with $E_N^p(0) = 0$ and $E_N^q(0) = 0$.

$$\begin{aligned} dE_N^p(T) + bE_N^q(T) &\leq d\|\Pi_N p' - (\mathcal{I}_N p)'\|^2 + b\|\Pi_N q' - (\mathcal{I}_N q)'\|^2 \\ &\quad +(ad+bd)\|\mathcal{I}_N p - p\|^2 + (ad+bd)\|\mathcal{I}_N q - q\|^2 \\ &\quad +(1+3a+D)[d\|E_N^p\|^2 + b\|E_N^q\|^2] \end{aligned}$$

We then apply the Gronswall's inequality **A2** on [0,T] with $\varphi(t) = d[E_N^p(t)]^2 + b[E_N^q(t)]^2$,

$r_0 = d\|\Pi_N p' - (\mathcal{I}_N p)'\|^2 + b\|\Pi_N q' - (\mathcal{I}_N q)'\|^2 + (ad+bd)\|\mathcal{I}_N p - p\|^2 + (ad+bd)\|\mathcal{I}_N q -$

$q\|^2$ and $k = 1 + 3a + D$ so

$$d\|E_N^p\|^2 + b\|E_N^q\|^2 = \int_0^T d[E_N^p(s)]^2 + b[E_N^q(s)]^2 ds = \int_0^T \varphi(s) ds.$$

The upper bound becomes

$$\begin{aligned} dE_N^p(T) + bE_N^q(T) \leq & \Big[d\|\Pi_N p' - (\mathcal{I}_N p)'\|^2 + b\|\Pi_N q' - (\mathcal{I}_N q)'\|^2 \\ & + (ad + bd)\|\mathcal{I}_N p - p\|^2 + (ad + bd)\|\mathcal{I}_N q - q\|^2 \Big] e^{(1+3a+D)T} \end{aligned}$$

From **A7**, we have

$$dE_N^p(T) + bE_N^q(T) \leq C\Big(\frac{TAe}{8(N+1)}\Big)^{2N} e^{(1+3a+D)T} \quad (3.9)$$

Next we estimate the end-point error $d|(p - p_N)(T)|^2 + b|(q - q_N)(T)|^2$.

$$\begin{aligned} d|(p - p_N)(T)|^2 + b|(q - q_N)(T)|^2 \leq & \; d[|(p - \mathcal{I}_N p)(T)| + |(\mathcal{I}_N p - p_N)(T)|]^2 \\ & + b[|(q - \mathcal{I}_N q)(T)| + |(\mathcal{I}_N q - q_N)(T)|]^2 \end{aligned}$$

With Young's inequality,

$$\begin{aligned} d|(p - p_N)(T)|^2 + b|(q - q_N)(T)|^2 \leq & \; 2d|(\mathcal{I}_N p - p)(T)|^2 + 2b|(\mathcal{I}_N q - q)(T)|^2 \\ & + 2d|(\mathcal{I}_N p - p_N)(T)|^2 + 2b|(\mathcal{I}_N q - q_N)(T)|^2. \quad (3.10) \end{aligned}$$

We approximate the last two terms with (3.9). For the first two term on the right side, we use the property **A3, A5.1, A5.2,A6.1** and a regularity assumption [54, 55, 56] $|p^k(t)| \leq cM^k, |q^k(t)| \leq cR^k$ provided that p and q satisfying condition

(M) or (R).

$$\begin{aligned} |(\mathcal{I}_N p - p)(T)| &\leq max_{t\in[0,T]}|\mathcal{I}_N p(t) - p(t)| \\ &\leq C(\|\mathcal{I}_N p - p\|_T + \|\frac{d}{dt}(\mathcal{I}_N p - p)\|_T) \\ &\leq C\Big[C_1\Big(\frac{TMe}{4(N+1)}\Big)^{N+1} + C_2\Big(\frac{TMe}{8(N+1)}\Big)^{N}\Big] \\ |(\mathcal{I}_N p - p)(T)| &\leq C\Big(\frac{TMe}{4(N+1)}\Big)^{N} \end{aligned} \tag{3.11}$$

$$\text{Similarly, } |(\mathcal{I}_N q - q)(T)| \leq C\Big(\frac{TRe}{4(N+1)}\Big)^{N}. \tag{3.12}$$

With (3.9), (3.11) and (3.12), the inequality (3.10) becomes

$$\begin{aligned} d|(p-p_N)(T)|^2 + b|(q-q_N)(T)|^2 &\leq C\Big(\frac{TAe}{8(N+1)}\Big)^{2N} + e^{(1+3a+D)T}\Big(\frac{TAe}{8(N+1)}\Big)^{2N} \\ d|(p-p_N)(T)|^2 + b|(q-q_N)(T)|^2 &\leq Ce^{(1+3a+D)T}\Big(\frac{TAe}{8(N+1)}\Big)^{2N} \end{aligned} \tag{3.13}$$

3.1.2 Error Analysis for a Nonlinear System

For nonlinear system, we need to establish some condition of the right hand side of equation in order to achieve the upper bound.

$$\begin{aligned} p'(t) &= -\frac{\partial H}{\partial q} = F(p,q) \\ q'(t) &= \frac{\partial H}{\partial p} = G(p,q) \end{aligned} \tag{3.14}$$

Variational Form : Find $p_N, q_N \in \mathcal{P}_N[0,T]$, $p_N(0) = p_0$ and $q_N(0) = q_0$ such that

$$\begin{aligned} (p'_N, v) &= (F(p_N, q_N), v), \forall v \in \mathcal{P}_N[0,T], v(0) = p_0 \\ (q'_N, w) &= (G(p_N, q_N), w) \quad , \forall w \in \mathcal{P}_N[0,T], w(0) = q_0 \end{aligned} \tag{3.15}$$

(3.14)-(3.15);

$$\begin{aligned}(p' - p'_N, v) &= (F(p,q) - F(p_N, q_N), v) \\ (q' - q'_N, w) &= (G(p,q) - G(p_N, q_N), w) \end{aligned} \tag{3.16}$$

Choose the interpolation that $\mathcal{I}_N p(0) = p_0$ so $\mathcal{I}_N p(0) - p_N(0) = 0$ and similarly for space of w.

Take $v = \mathcal{I}_N p - p_N$, $w = \mathcal{I}_N q - q_N$.

$$\begin{aligned}(p' - p'_N, \mathcal{I}_N p - p_N) &= (F(p,q) - F(p_N, q_N), \mathcal{I}_N p - p_N) \\ (q' - q'_N, \mathcal{I}_N q - q_N) &= (G(p,q) - G(p_N, q_N), \mathcal{I}_N q - q_N) \end{aligned} \tag{3.17}$$

Use L_2 projection property,

$$\begin{aligned}(\Pi_N p' - p'_N, \mathcal{I}_N p - p_N) &= (F(p,q) - F(p_N, q_N), \mathcal{I}_N p - p_N) \\ (\Pi_N q' - q'_N, \mathcal{I}_N q - q_N) &= (G(p,q) - G(p_N, q_N), \mathcal{I}_N q - q_N) \end{aligned}$$

$$\begin{aligned}(\Pi_N p' - (\mathcal{I}_N p)' + (\mathcal{I}_N p)' - p'_N, \mathcal{I}_N p - p_N) &= (F(p,q) - F(\mathcal{I}_N p, \mathcal{I}_N q) + F(\mathcal{I}_N p, \mathcal{I}_N q) - F(p_N, q_N), \mathcal{I}_N p - p_N) \\ (\Pi_N q' - (\mathcal{I}_N q)' + (\mathcal{I}_N q)' - q'_N, \mathcal{I}_N q - q_N) &= (G(p,q) - G(\mathcal{I}_N p, \mathcal{I}_N q) + G(\mathcal{I}_N p, \mathcal{I}_N q) - G(p_N, q_N), \mathcal{I}_N q - q_N) \end{aligned}$$

$$\begin{aligned}(\mathcal{I}_N p)' - p'_N, \mathcal{I}_N p - p_N) &= (F(p,q) - F(\mathcal{I}_N p, \mathcal{I}_N q), \mathcal{I}_N p - p_N) + (F(\mathcal{I}_N p, \mathcal{I}_N q) - F(p_N, q_N), \mathcal{I}_N p - p_N) \\ &\quad -(\Pi_N p' - (\mathcal{I}_N p)', \mathcal{I}_N p - p_N) \\ (\mathcal{I}_N q)' - q'_N, \mathcal{I}_N q - q_N) &= (G(p,q) - G(\mathcal{I}_N p, \mathcal{I}_N q), \mathcal{I}_N q - q_N) + (G(\mathcal{I}_N p, \mathcal{I}_N q) - G(p_N, q_N), \mathcal{I}_N q - q_N) \\ &\quad -(\Pi_N q' - (\mathcal{I}_N q)', \mathcal{I}_N q - q_N) \end{aligned} \tag{3.19}$$

Let $E_N^p = \mathcal{I}_N p - p_N$ and $E_N^q = \mathcal{I}_N q - q_N$. With $E_N^p(0) = 0$ and $E_N^q(0) = 0$.

On the left hand side,

$(\mathcal{I}_N p)' - p'_N, \mathcal{I}_N p - p_N) = \frac{1}{2}(E_N^p(T))^2$ and $(\mathcal{I}_N q)' - q'_N, \mathcal{I}_N q - q_N) = \frac{1}{2}(E_N^q(T))^2$

Add the two equations and apply Hölder and Young's inequalities

$$\begin{aligned}
\frac{1}{2}(E_N^p(T))^2 + \frac{1}{2}(E_N^q(T))^2 &\leq \frac{1}{2}\|F(p,q) - F(\mathcal{I}_N p, \mathcal{I}_N q)\|^2 + \frac{1}{2}\|F(\mathcal{I}_N p, \mathcal{I}_N q) - F(p_N, q_N)\|^2 \\
&\quad + \frac{3}{2}\|E_N^p\|^2 + \frac{1}{2}\|\Pi_N p' - (\mathcal{I}_N p)'\|^2 + \frac{1}{2}\|G(p,q) + G(\mathcal{I}_N p, \mathcal{I}_N q)\|^2 \\
&\quad + \frac{1}{2}\|G(\mathcal{I}_N p, \mathcal{I}_N q) - G(p_N, q_N)\|^2 + \frac{3}{2}\|E_N^q\|^2 + \frac{1}{2}\|\Pi_N q' - (\mathcal{I}_N q)'\|^2 \\
(E_N^p(T))^2 + (E_N^q(T))^2 &\leq \|F(p,q) - F(\mathcal{I}_N p, \mathcal{I}_N q)\|^2 + \|G(p,q) - G(\mathcal{I}_N p, \mathcal{I}_N q)\|^2 \\
&\quad + \|F(\mathcal{I}_N p, \mathcal{I}_N q) - F(p_N, q_N)\|^2 + \|G(\mathcal{I}_N p, \mathcal{I}_N q) - G(p_N, q_N)\|^2 \\
&\quad + 3(\|E_N^p\|^2 + \|E_N^q\|^2) + \|\Pi_N p' - (\mathcal{I}_N p)'\|^2 + \|\Pi_N q' - (\mathcal{I}_N q)'\|^2
\end{aligned}$$

We consider the first four terms in two cases. We use Euclidean norm for the following cases.

Case 1: In this case, $\vec{f} = (F, G)^T$ satisfies the condition that for any $\vec{\mathbf{z}}_1 = (p_1, q_1)^T$ and $\vec{\mathbf{z}}_2 = (p_2, q_2)^T$,

$$\|\vec{f}(\vec{\mathbf{z}}_1, t) - \vec{f}(\vec{\mathbf{z}}_2, t)\|_2 \leq \alpha\|\vec{\mathbf{z}}_1 - \vec{\mathbf{z}}_2\|_2 \quad , \quad \alpha > 0$$

i.e.

$$\sqrt{(F(p_1,q_1,t) - F(p_2,q_2,t))^2 + (G(p_1,q_1,t) - G(p_2,q_2,t))^2} \leq \alpha\sqrt{(p_1-p_2)^2 + (q_1-q_2)^2}$$

It follows that

$$\begin{aligned}
(E_N^p(T))^2 + (E_N^q(T))^2 &\leq \int_0^T (F(p,q) - F(\mathcal{I}_N p, \mathcal{I}_N q))^2 + (G(p,q) - G(\mathcal{I}_N p, \mathcal{I}_N q))^2 dt \\
&\quad \int_0^T (F(\mathcal{I}_N p, \mathcal{I}_N q) - F(p_N, q_N))^2 + +(G(\mathcal{I}_N p, \mathcal{I}_N q) - G(p_N, q_N))^2 dt \\
&\quad + 3(\|E_N^p\|^2 + \|E_N^q\|^2) + \|\Pi_N p' - (\mathcal{I}_N p)'\|^2 + \|\Pi_N q' - (\mathcal{I}_N q)'\|^2
\end{aligned}$$

If F and G satisfy the given condition, we have

$$\begin{aligned}(E_N^p(T))^2 + (E_N^q(T))^2 &\leq \alpha^2(\|\mathcal{I}_N p - p)\|^2 + \|\mathcal{I}_N q - q)\|^2) + \alpha^2(\|E_N^p\|^2 + \|E_N^q\|^2) \\ &\quad +3(\|E_N^p\|^2 + \|E_N^q\|^2) + \|\Pi_N p' - (\mathcal{I}_N p)'\|^2 + \|\Pi_N q' - (\mathcal{I}_N q)'\|^2 \\ &= \alpha^2(\|\mathcal{I}_N p - p)\|^2 + \|\mathcal{I}_N q - q)\|^2) + \|\Pi_N p' - (\mathcal{I}_N p)'\|^2 \\ &\quad +\|\Pi_N q' - (\mathcal{I}_N q)'\|^2 + (\alpha^2+3)(\|E_N^p\|^2 + \|E_N^q\|^2)\end{aligned}$$

By using Gronswall's Theorem **A.2** and **A6.1,A7**

$$\begin{aligned}(E_N^p(T))^2 + (E_N^q(T))^2 &\leq [\alpha^2(\|\mathcal{I}_N p - p)\|^2 + \|\mathcal{I}_N q - q)\|^2) + \|\Pi_N p' - (\mathcal{I}_N p)'\|^2 \\ &\quad +\|\Pi_N q' - (\mathcal{I}_N q)'\|^2] e^{(\alpha^2+3)T} \\ &\leq C\Big(\frac{TAe}{8(N+1)}\Big)^N\end{aligned}$$

Case 2: In this case, $\vec{f} = (F, G)^T$ satisfies the condition that for any $\vec{\mathbf{z}}_1 = (p_1, q_1)^T$ and $\vec{\mathbf{z}}_2 = (p_2, q_2)^T$,

$$(\vec{f}(\vec{\mathbf{z}}_1, t) - \vec{f}(\vec{\mathbf{z}}_2, t)) \cdot (\vec{\mathbf{z}}_1 - \vec{\mathbf{z}}_2) \leq -\alpha\|\vec{\mathbf{z}}_1 - \vec{\mathbf{z}}_2\|_2 \quad , \quad \alpha > 0$$

We also have error estimate which is similar to case 1.

4 Numerical Results

In this numerical study, we are interested in a long-time behavior of the Hamiltonian system, which many science and engineering problems need to predict, see, e.g., [32, 33, 34, 27]. Traditional finite difference, finite element, and the Runge-Kutta methods fail when time runs sufficiently large; even for the symplectic structure-preserving algorithms. Our numerical tests on Hamiltonian systems demonstrate that the spectral methods preserve both energy and volume very well even for a large value of t. The numerical solution follows the trajectory nicely without a phase shift.

For the numerical examples below, we use $T = 1$ for the spectral collocation. The reasonable values for T are within the interval $[0.75, 2]$. However, the convenient value is $T = 2$ (without any translation). In each updating process, we compare the maximum pointwise errors,

$$\max_{1\le j\le N}(\|(\boldsymbol{p}^{new} - \boldsymbol{p}^{old})(t_j)\|_{L^\infty}, \|(\boldsymbol{q}^{new} - \boldsymbol{q}^{old})(t_j)\|_{L^\infty})$$

and set the tolerance as 10^{-15} together with maximum iteration numbers, 1000, to terminate the iterative process. The initial guesses to start the spectral methods are $(N \times 1)$ vectors $(p_0, ..., p_0)^T$ and $(q_0, ..., q_0)^T$ where p_0, q_0 are the initial values.

We compare the numerical results from different spectral methods in Chapter 2 with the collocation method from Guo-Wang using Legendre's recursive relation [31]. We also compare the spectral collocation method (with the differentiation matrix) with the results from symplectic methods provided in the Appendix. In a linear case, we compare the exact solution with the numerical solution by using the maximum

pointwise norm,

$$\|(\boldsymbol{p}-\boldsymbol{p}_N)(t_j)\|_{L^\infty}, \|(\boldsymbol{q}-\boldsymbol{q}_N)(t_j)\|_{L^\infty}, \|\boldsymbol{H}(t_j)-\boldsymbol{H}_0\|_{L^\infty}$$

on the terminal interval. However, for a nonlinear system, we compare only the energy $H(p(t), q(t))$ to the initial energy $H_0 = H(p(0), q(0))$ by using the maximum pointwise norm

$$\|\boldsymbol{H}(t_j)-\boldsymbol{H}_0\|_{L^\infty}$$

as well.

Symplectic schemes 1, 2, 3 and 4 are second order schemes where scheme 1 is a second order midpoint Euler scheme and scheme 3 and 4 are specially designed for the threefold symmetry and Henon-Heiles systems, respectively. The comparison of the CPU times (after the graphic outputs) used from collocation with Chebyshev differentiation matrix and symplectic methods is considered by using Lenovo X61, Core 2 Duo 1.8GHz, RAM 3GB, Window Vista; and for the other spectral methods is by using Lenovo X61, Core 2 Duo 1.8GHz, RAM 3GB, Window 7.

In coding, for the spectral collocation with differentiation matrix, we store $\tilde{D}^{-1}$ since it will be used repeatedly, in some cases, billions of times. It is well known that the condition number of $\tilde{D}$ is $O(N^2)$. For relatively large values of N, it would be ideal to develop an explicit formula for $\tilde{D}^{-1}$ instead of inverting the explicit form of $\tilde{D}$. Similarly, we store the matrix $\boldsymbol{L}$ for Legendre polynomials and $\boldsymbol{\Phi}$. The condition numbers of $\boldsymbol{L}$ and $\boldsymbol{\Phi}$ are discussed in Chapter 5.

4.1 Linear Hamiltonian System

Example 1: Consider a linear system of ordinary differential equations

$$\begin{aligned} p'(t) &= -4q(t) \\ q'(t) &= p(t) \end{aligned}$$

with initial condition $p(0) = 0,\ q(0) = 0.6$.

The Hamiltonian for this system is given by $H(p,q) = \frac{1}{2}p^2 + 2q^2$. The exact solutions are $p(t) = -1.2\sin(2t)$ and $q(t) = 0.6\cos(2t)$. The initial energy $H(p_0, q_0) = H_0 = 0.72$.

The numerical methods for a linear system can be practically solved explicitly without using an iterative method. We achieve a much better result by solving the system explicitly. We first compare the collocation method with Chebyshev differentiation matrix D, symplectic schemes 1 and 2 then we compare the results among the spectral methods. Figure 1 represents the end behavior of each method. From the graphs, we can barely see the difference between the exact and numerical solutions from the spectral collocation ($t = 10^6$) while the phase shift is visible for the symplectic methods at $t = 2000$.

Figures below shows the error propagations of three different methods. The errors oscillate evenly through out the interval and within the range of 10^{-11}. The two collocation methods, collocation with Legendre-Phi and Guo-Wang, have a similar pattern while the error from the Tau method with Legendre-Phi propagates in a pattern that is dense in the middle. This means the error is very small throughout

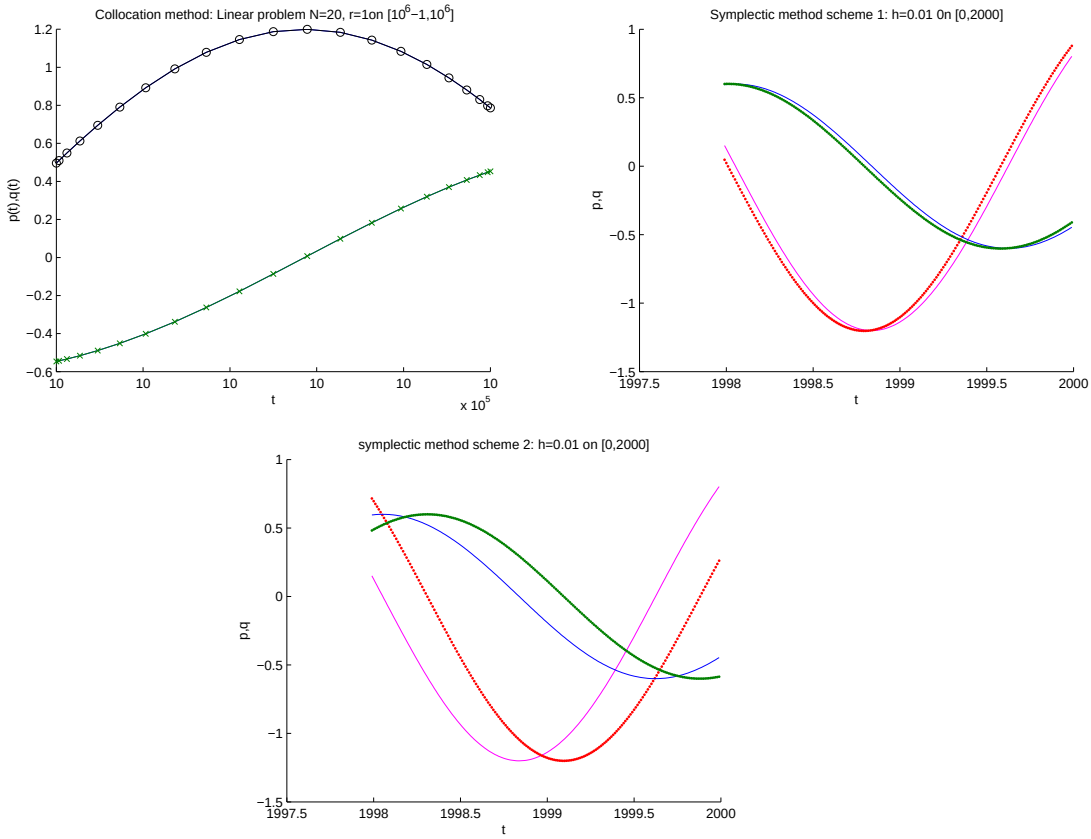

Figure 1: Graphs of solution p, q versus t by (a) spectral collocation with Chebyshev differentiation matrix when $N = 20$ on $[10^6 - 1, 10^6]$ (p:-o-,q:-x-); (b) symplectic 1, h=0.01 on [1998,2000] (p:dash,q:dot); (c) symplectic 2, h=0.01 on [1998,2000]

the interval.

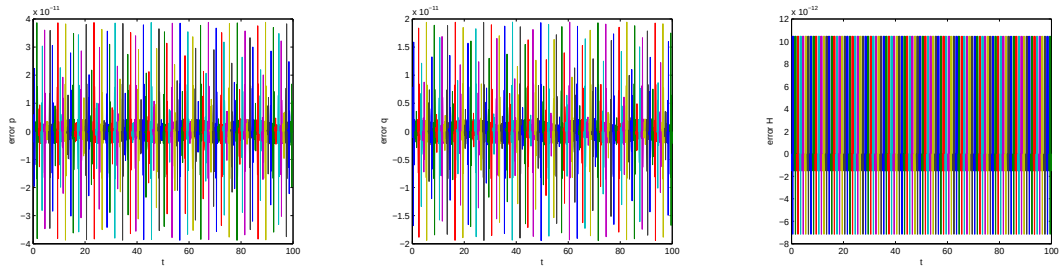

Figure 2: Error propagations by Tau method with Legendre-Phi when when $N = 15$ (a) $(p^N(t_i) - p(t_i))$ versus t (b) $(q^N(t_i) - q(t_i))$ versus t (c) $(H_N(t_i) - H_0)$ versus t.

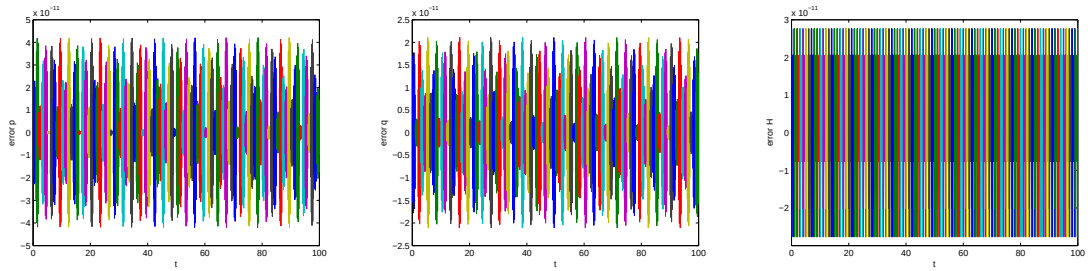

Figure 3: Patterns of errors by collocation method with Legendre-Phi when $N = 15$ (a) $(p^N(t_i) - p(t_i))$ versus t (b) $(q^N(t_i) - q(t_i))$ versus t (c) $(H_N(t_i) - H_0)$ versus t.

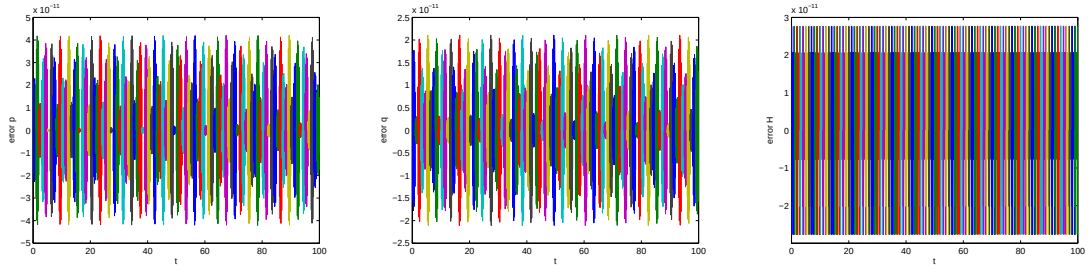

Figure 4: Patterns of errors by Guo-Wang method when $N = 15$ (a) $(p^N(t_i) - p(t_i))$ versus t (b) $(q^N(t_i) - q(t_i))$ versus t (c) $(H_N(t_i) - H_0)$ versus t.

Figure 5 shows the rates of convergence of the numerical error for p from both methods. The spectral collocation method with Chebyshev differentiation matrix D gives a super-exponential rate [54, 55]. The convergence rate is of order $(\frac{1}{N})^{(0.75N)}$ for the spectral collocation and h^2 for the symplectic scheme 1 (second order scheme).

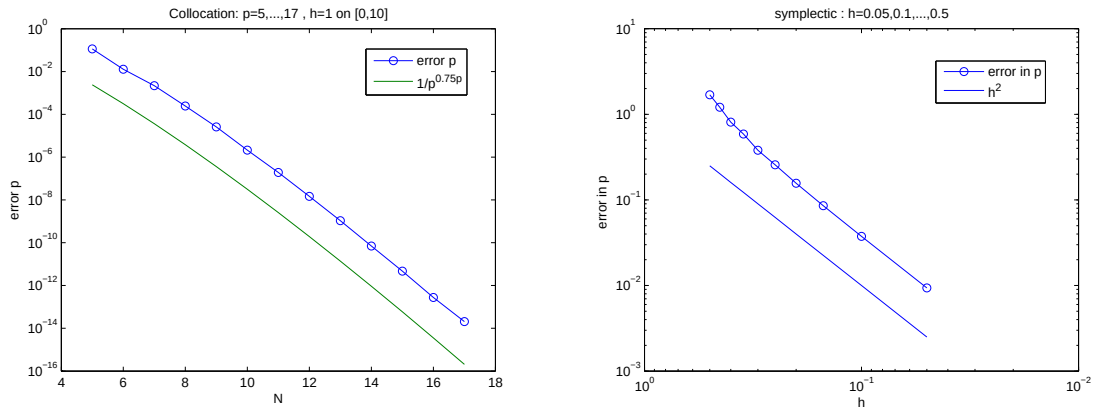

Figure 5: (a) Collocation method, N=5,6,...,17 on [0,10]; (b) symplectic 1,h=0.05,0.1,...,0.5 on [0,10].

In the next Figures, we compare the spectral methods discussed in Chapter 2. The results can be compared with the symplectic methods by using the result of the collocation method with differentiation matrix as a reference graph.

Figure 6 shows the convergence rates of the endpoint error of five different methods; Guo-Wang, Tau with Legendre-Phi , collocation with Legendre-Phi, collocation with Legendre-Phi-Scaling and collocation with Chebyshev differentiation matrix on [0,10] and [0,100] consecutively. Spectral Tau with Legendre-Phi gives the best convergence rate among all the methods. It shows a stable error trend when the error approaches the machine epsilon (10^{-14}) or when $N \geq 9$ while the error from Guo-

Wang method gives an oscillate tale. The collocation method with Legendre-Phi as basis functions is better than the collocation method with differentiation matrix but still loses to Spectral Tau with Legendre-Phi. Figure 6 (b) represents the convergence rate, when the endpoint t is larger, $t \in [0, 100]$. The results are almost the same at the beginning then they start to shift when $N = 5$.

The convergence rate, $\sqrt{(p(T) - p_N(T))^2 + 4(q(T) - q_N(T))^2}$, versus N of Tau method with Legendre-Phi is shown in Figure 8. From the theoretical result, it is of the order $e^{(1+3a+D)T}\left(\frac{TAe}{4(N+1)}\right)^{2N}$ where $a = 0, D = 4, A = 2, T = 1$, i.e.

$$\sqrt{(p(T) - p_N(T))^2 + 4(q(T) - q_N(T))^2} \leq e^5\left(\frac{2e}{4(N+1)}\right)^{2N}.$$

However, the result shown in Figure 7 is of the order $2N + 0.75$ which is better than the theoretical result.

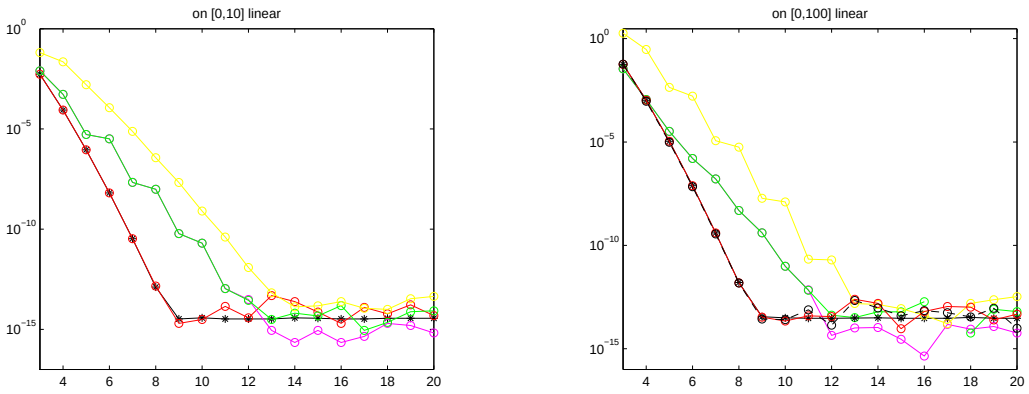

Figure 6: Errors of $|p(T) - p_N(T)|$ with respect to N (a) on [0,10] (b) on [0,100] by using 1) Guo-Wang(red-o) 2) Tau(black-*) with Phi 3) collocation with Phi(pink-o) 4) collocation with Phi-Scaling(green-o) 5) collocation with differentiation matrix(yellow-o).

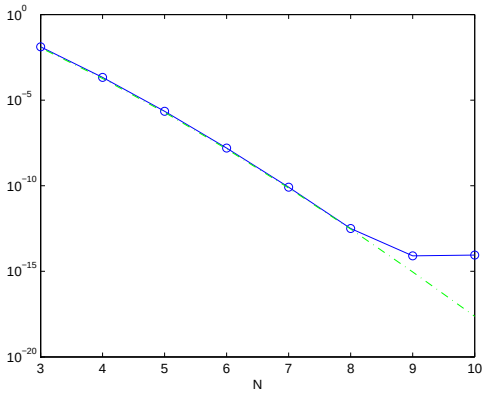

Figure 7: Errors of $\sqrt{(p(T)-p_N(T))^2+4(q(T)-q_N(T))^2}$ (blue-o) and $5e^5(\frac{2e}{8(N+1)})^{(1.6N)}$ (green) with respect to N on [0,100] by using Tau method with Legendre-Phi.

We next make a further comparison by considering the CPU times used by each method. Tables 1 and 2 provide the maximum errors of energy H, $p(t)$, $q(t)$, and the CPU times used on the end interval. The spectral collocation method provides more nodal data with similar CPU times, or can go further in term of time t than a simple symplectic method as shown in Table 1. This means the spectral collocation method with Chebyshev differentiation matrix is less expensive in a long run compared with a simple symplectic method. Table 2 shows the CPU times used when the end point is fixed as $t = 100$. With a low number of collocation points N and small step size h (symplectic), the errors are almost the same from both methods. However, the CPU times used for the symplectic method are much longer than those from the spectral method.

Table 3 shows the comparison of the CPU times, number of iterations on the last interval and terminal errors among the spectral methods when $N = 10$ on $[0, 100]$.

The Tau method gives the same order of errors as the method from Guo-Wang [31]. However, for a linear case, the system can be solved explicitly using the Tau method. As a result, the CPU times for the Tau method are better than Guo-Wang. The other three collocation methods, though better than the symplectic 1 or 2, still lose to the Tau method.

	time(secs)	Error in Energy	Error in $p(t)$	Error in $q(t)$
Colloc. N=20,$[0, 10^5]$	621	2.294946×10^{-10}	2.228963×10^{-10}	9.142997×10^{-10}
Symp 1,h=0.01 [0,2000]	484	2.884887×10^{-3}	7.999879×10^{-2}	6.323009×10^{-1}
Symp 1,h=0.01,[0,2350]	642	3.391444×10^{-3}	9.409463×10^{-2}	4.703431×10^{-2}
Symp 1,h=0.01,$[0, 10^5]$	$>$ 6hrs			
Symp 2,h=0.01,[0,2000]	445	7.200007×10^{-7}	4.001598×10^{-2}	3.160331×10^{-1}
Symp 2,h=0.01,[0,2250]	603	7.200007×10^{-7}	7.090428×10^{-1}	3.543846×10^{-1}
Symp 2,h=0.01,$[0, 10^5]$	$>$ 5hrs			

Table 1: Comparison of the CPU times between the three methods.

	time(secs)	Error in Energy	Error in $p(t)$	Error in $q(t)$
Colloc.,N=8,[0,100]	0.35	6.185243×10^{-6}	5.631718×10^{-6}	2.062186×10^{-7}
Symp 1,h=0.001,[0,100]	78.29	7.188678×10^{-7}	3.958494×10^{-5}	1.994939×10^{-5}
Symp 1,h=0.0008,[0,100]	191.98	4.600998×10^{-7}	2.533450×10^{-5}	1.276760×10^{-5}
Symp 1,h=0.0001,[0,100]	591.45	1.796755×10^{-7}	9.896375×10^{-6}	4.987343×10^{-6}

Table 2: Comparison of the CPU times between the two methods with the same order of errors.

Spectral Methods	time(secs)	Error in Energy	Error in $p(t)$	Error in $q(t)$
Colloc. with D matrix	0.46	1.364651×10^{-8}	1.258733×10^{-8}	2.786321×10^{-10}
Tau with Legendre-Phi	0.099	2.442490×10^{-15}	3.130828×10^{-14}	3.014255×10^{-14}
Colloc. with Legendre-Phi	0.063	2.025812×10^{-11}	9.823919×10^{-12}	$8.8107854 \times 10^{-12}$
Colloc. with L-Phi scaling	1.86	2.026090×10^{-11}	9.810818×10^{-12}	8.825662×10^{-12}
Guo-Wang	0.54	5.317968×10^{-14}	2.198241×10^{-14}	2.575717×10^{-14}

Table 3: Comparisons of the CPU times, number of iterations on the last interval and the terminal errors among the spectral methods when $N = 10$ on $[0, 100]$.

Spectral Methods	time(secs)	Error in Energy	Error in $p(t)$	Error in $q(t)$
Colloc. with D matrix	2913	1.629202×10^{-10}	5.394734×10^{-11}	6.998968×10^{-11}
Tau with Legendre-Phi	1718	3.571365×10^{-12}	3.606229×10^{-11}	2.002842×10^{-13}
Colloc. with Legendre-Phi	2549	1.168842×10^{-12}	9.823919×10^{-12}	9.026113×10^{-12}
Guo-Wang	0.54	5.317968×10^{-14}	2.198241×10^{-14}	2.575717×10^{-14}

Table 4: Comparisons of the CPU times, number of iterations on the last interval and the terminal errors among the spectral methods when $N = 15$ on $[0, 100000]$.

4.2 Nonlinear Hamiltonian Systems

Example 2: Consider a system with a Hamiltonian $H(p,q) = p^2 - q^2 + q^4$ [21].

The corresponding system of nonlinear ODEs is

$$\begin{aligned} p'(t) &= -\frac{\partial H}{\partial q} = 2q - 4q^3 \\ q'(t) &= \frac{\partial H}{\partial p} = 2p \end{aligned}$$

with initial condition $p(0) = p_0,\ q(0) = q_0$.

There are three equilibrium points for this system: $E_1 = (\bar{p}, \bar{q}) = \mathbf{0}$, $E_2 = (0, \frac{1}{\sqrt{2}})$ and $E_3 = (0, -\frac{1}{\sqrt{2}})$. The zero equilibrium point is a saddle point and the other two are centers. As a result, we have to be careful when we choose initial values for our system in order to avoid the neighborhood of $(0,0)$. The iterative method will not converge otherwise.

For the spectral collocation with Chebyshev differentiation matrix, the range of the initial condition for q that can be used in order for the numerical solution to converge is approximately from 0.625 to 0.88. For the oscillatory behavior, we choose q_0 within 0.625-0.7 and 0.715-0.88. If we choose a number close to the equilibrium $(0, 0.7071067811865475)$, we will get almost a straight line. The initial values were chosen as $p_0 = 0$, $q_0 = 0.73$. This gives $H(p_0, q_0) = H_0 = -0.24891758$.

We begin with the comparison of a sixth-order symplectic method and collocation with the differentiation matrix. Figure 9 represents phase plots of p and q. We can see that with symplectic 1, the loop is thicker (there is a phase shift) and with the spectral collocation method, the loop is thinner and sharper. The other spectral

methods give a similar result to Figure 8 (a) and (c).

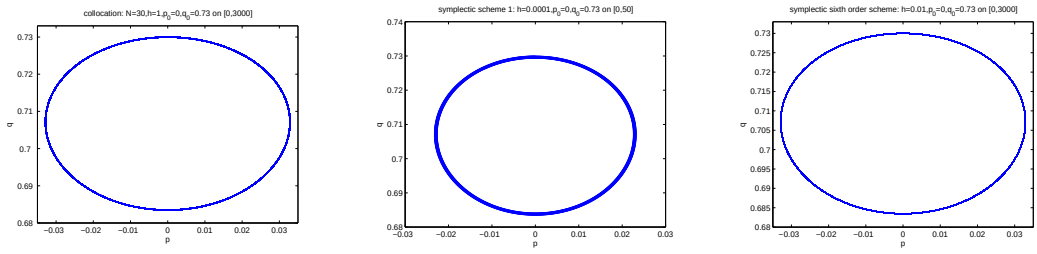

Figure 8: Phase plots q versus p by (a) spectral collocation when $N = 30$ on $[0, 3000]$; (b) symplectic 1 h=0.0001 on [0,50]; (c) symplectic sixth order h=0.01 on [0,3000].

Figures 9, 10 and 11 show the propagations of errors in energy at the nodal points $|H(t_i) - H_0|$ of different methods. From the Figures, we observe that the errors from the spectral collocation method with Chebyshev-Differentiation matrix and Guo-wang method increase as t increases whereas the errors of the collocation and Tau methods with Legendre-Phi keep the same pattern all the way to the end point ($t = 10000$). From this observation, we compare the maximum pointwise errors in energy rather than the errors at the terminal point.

Figures 12 shows the difference of the errors at the terminal point(a) the maximum pointwise errors in energy(b). The errors of the collocation methods and Tau methods with Legendre-Phi depend on the terminal point chosen.

The convergence rates of the energy H for both methods are shown in Figure 13. The rate is $(\frac{1}{N})^{(0.6N)}$ for the spectral collocation, $O(h^2)$ for the symplectic scheme 2, and $O(h^6)$ for the sixth order symplectic scheme. Figure 14 represents the convergence rate of Tau method with Legendre-Phi. The rate is of the order $0.25e^{0.5}(\frac{e}{4(N+1)})^{(\sqrt[4]{N^3})}$ approximately.

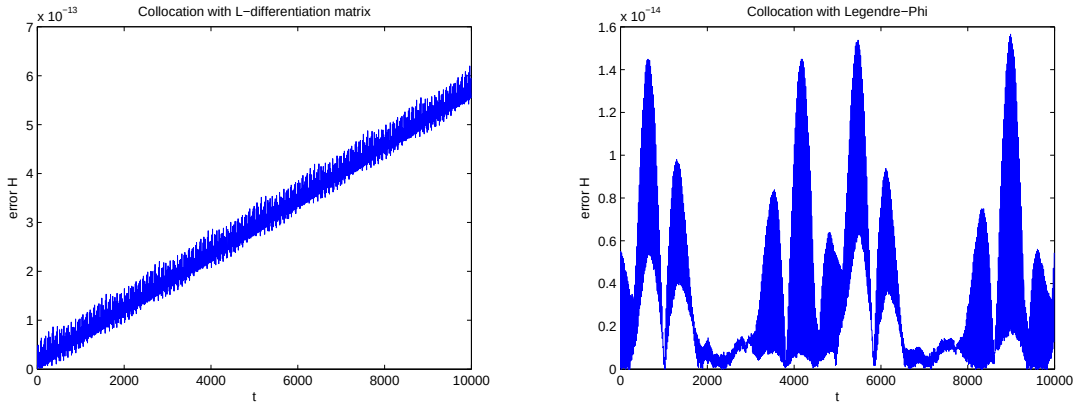

Figure 9: Patterns of errors $|H(t_i) - H_0|$ versus t on [0,10000] when $N = 15$ by (a) collocation method with Chebyshev-Differentiation matrix (b) collocation method with Legendre-Phi.

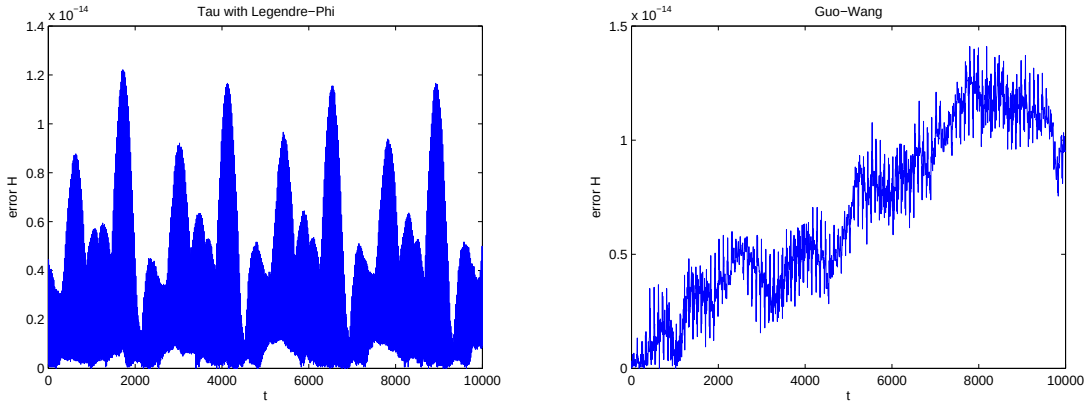

Figure 10: Patterns of errors $|H(t_i) - H_0|$ versus t on [0,10000] when $N = 15$ by (a) Tau method with Legendre-Phi (b) Guo-Wang.

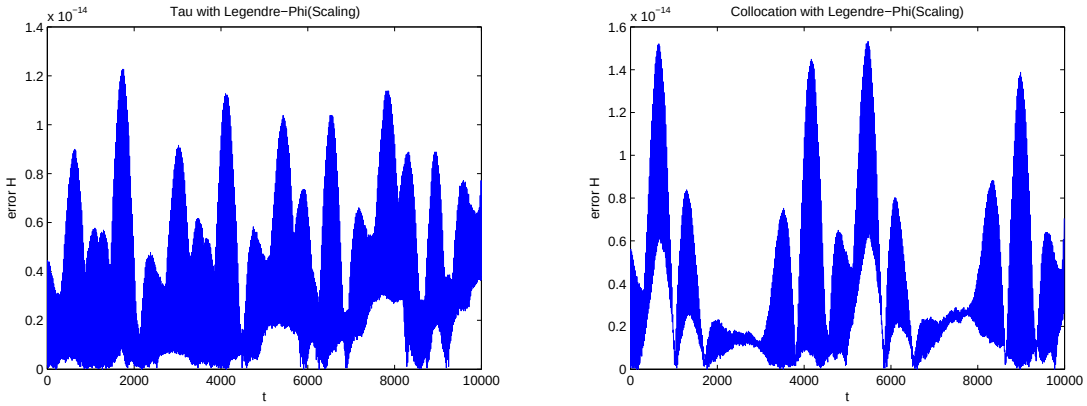

Figure 11: Patterns of errors $|H(t_i) - H_0|$ versus t on [0,10000] when $N = 15$ by (a) Tau method with Legendre-Phi(Scaling) (b) collocation method with Legendre-Phi(Scaling).

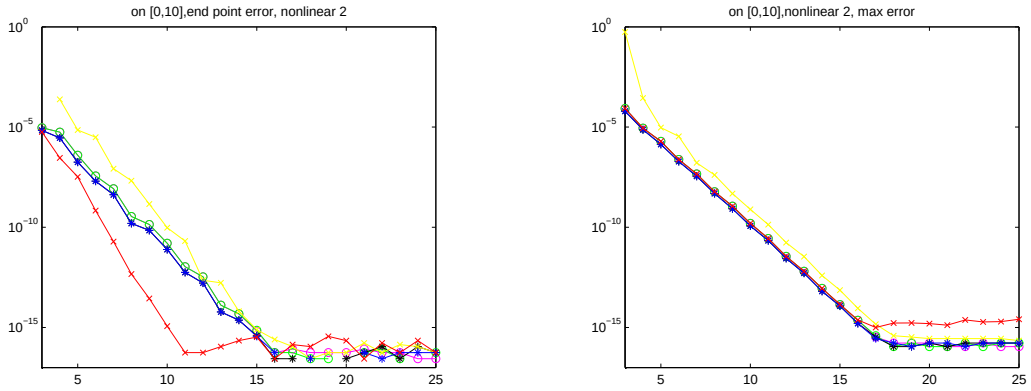

Figure 12: (a)Errors of $|H_0 - H_N(T)|$ and (b) $\|\boldsymbol{H}(t_j) - \boldsymbol{H}_0\|_{L^\infty}$ with respect to N on [0,10] by using 1) Guo-Wang(red-o) 2) Tau(black-*) with Phi 3) Tau(black-*) with Phi-Newton 4) collocation with Phi(x)(pink-o) 5) collocation with Phi(x)-Scaling(green-o) 6) collocation with differentiation matrix(yellow-o) matrix.

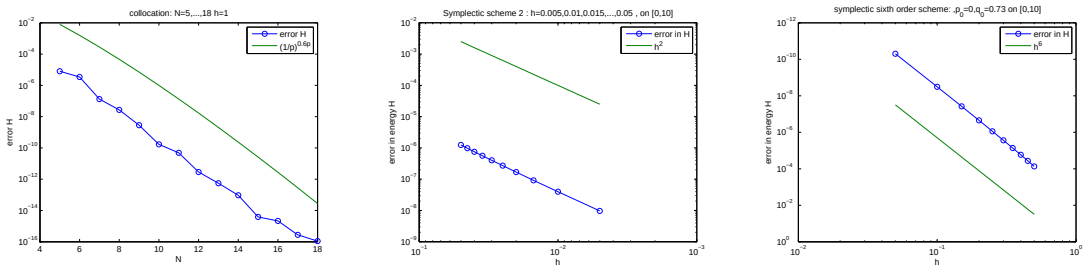

Figure 13: (a)Error in H and $(\frac{1}{N})^{(0.6N)}$ versus $N = 5, 6, ..., 16$ by spectral collocation on $[0, 10]$(b) Error in H by symplectic 2 with h=0.005,0.01,0.015,...,0.05, on [0,10]; (c) Error in H by the sixth order symplectic scheme.

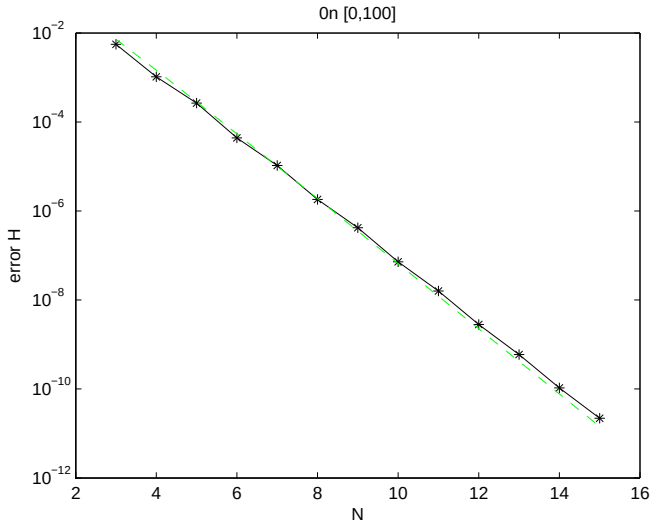

Figure 14: $\|\boldsymbol{H}(t_j) - \boldsymbol{H}_0\|_{L^\infty}$ (blue-o) and $0.25e^{0.5}(\frac{e}{4(N+1)})^{(\sqrt[4]{N^3})}$ (green) with respect to N on [0,100] by using Tau with Phi

The CPU times for each method are shown in Table 5. We use $h = 0.001$ for the symplectic schemes 1, 2 and $h = 0.01$ for a sixth order symplectic method [53]. Similar to the linear case, the spectral collocation is more effective in the long run. It takes less CPU times than all three symplectic methods.

Table 6 compares the CPU times used on the same interval [0,10000] for the spectral methods when $N = 15$. We can see that the errors are about the same but collocation method with Legendre-Phi(Scaling) takes much longer time. The collocation method with Chebyshev-Differentiation matrix takes less time but the error is one order less than the others.

	time(secs)	Error in Energy
Collocation, N=50 on [0,10000]	2898	$5.2735593669 \times 10^{-15}$
Collocation, N=30 on [0,5000]	668	$7.6605388699 \times 10^{-15}$
Symplectic 1 on [0,450]	2849	$9.9279222845 \times 10^{-4}$
Symplectic 1 on [0,500]	3585	$1.0088809618 \times 10^{-3}$
Symplectic 1 on [0,1000]	$>$ 2 hrs	
Symplectic 2 on [0,460]	3010	$3.8086767073 \times 10^{-10}$
Symplectic 2 on [0,1000]	$>$ 2 hrs	
Symplectic 6th order on [0,4200]	2602	$5.4956039718 \times 10^{-15}$
Symplectic 6th order on [0,5000]	9833	$7.6327832942 \times 10^{-15}$
Symplectic 6th order on [0,10000]	>3hrs	

Table 5: Comparison of the CPU times between the collocation with Chebyshev differentiation matrix and symplectic methods.

Spectral Methods	time(secs)	Error in Energy
Colloc. with D matrix	59	$6.481482017761664 \times 10^{-13}$
Tau with Legendre-Phi	112	$1.260103132949553 \times 10^{-14}$
Tau with Legendre-Phi(Scaling)	108	$1.504352198367087 \times 10^{-14}$
Colloc. with Legendre-Phi	76	$1.570965579844597 \times 10^{-14}$
Colloc. with Legendre-Phi(Scaling)	251	$1.654232306691483 \times 10^{-14}$
Guo-Wang	177	$1.521005543736465 \times 10^{-14}$

Table 6: Comparisons of the CPU times and the terminal errors among the spectral methods when $N = 15$ on $[0, 10000]$.

We end this example with the Tau method with Legendre-Phi together with Newton iteration. The error for this method is similar to the error of the Tau method without Newton iteration. We consider the number of iterations shown on Table 7 in order to see if the iterative process converges to the solution faster.

We compare the number of iterations and the CPU times for Tau with and without Newton iteration. The number of iterations is reduced by half.

Intervals/Method	N	time elapse	Iteration numbers
Coll w D matrix,$[0, 10]$	10	0.06s	16
Tau w Newton,$[0, 10]$	10	0.14s	6
Tau w/o Newton,$[0, 10]$	10	0.07s	14
Coll w Phi,$[0, 10]$	10	0.097s	18
Coll w Phi-Scaling,$[0, 10]$	10	0.21s	18
Guo-Wang,$[0, 10]$	10	0.07s	13
Guo-Wang,$[0, 10]$	20	0.115s	7
Tau w Newton,$[0, 10]$	20	0.45s	7
Tau w/o Newton,$[0, 10]$	20	0.110s	19
Coll w Phi,$[0, 10]$	20	1.104s	14
Coll w Phi-Scaling,$[0, 10]$	20	0.115s	7
Coll w D,$[0, 10]$	20	0.115s	7

Table 7: Comparisons of the iteration numbers and the CPU times by using the spectral methods.

Example 3: Consider a linear system of ordinary differential equations

$$\begin{aligned} p'(t) &= q(t) - \frac{8}{3}q^3(t) \\ q'(t) &= p(t) \end{aligned}$$

with initial condition $p(t_0) = \frac{1}{2}\cos(2t_0),\ q(t_0) = \frac{1}{4}\sin(2t_0)$.

The Hamiltonian for this system is given by $H(p,q) = \frac{1}{2}p^2 - \frac{1}{2}q^2(t) + \frac{2}{3}q^4(t)$. We choose $t_0 = 0$ so the initial conditions are $p(0) = 0.5$, $q(0) = 0$ and the initial energy $H(p_0, q_0) = H_0 = 0.125$.

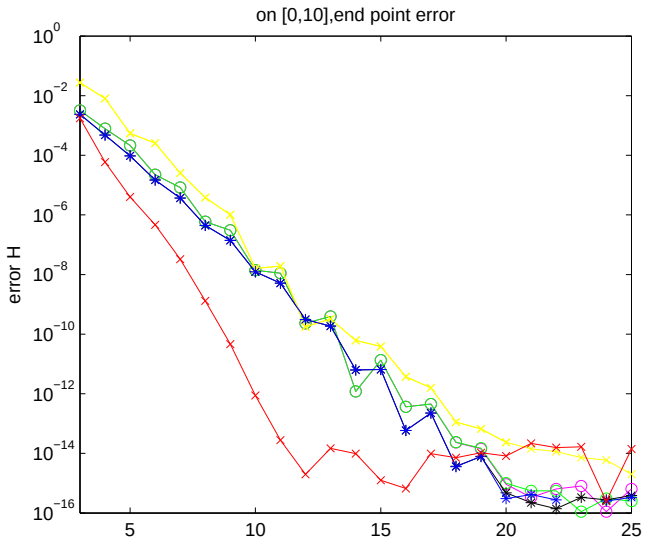

Figure 15: Errors of $|H_0 - H_N(T)|$ with respect to N on [0,10] by using 1) Guo-Wang(red-o) 2)Tau(black-*) with Phi 3) Tau(black-*) with Phi-Newton 4) collocation with Phi(x)(pink-o) 5) collocation with Phi(x)-Scaling(green-o) 6) collocation with differentiation matrix(yellow-o) matrix.

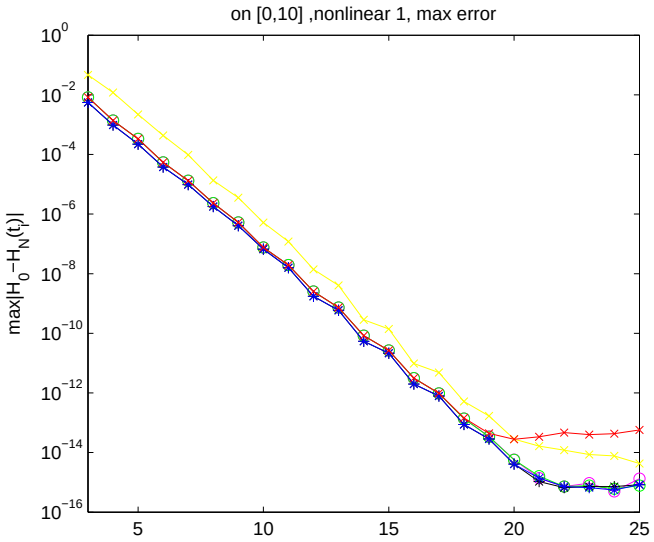

Figure 16: $\|\boldsymbol{H}(t_j) - \boldsymbol{H}_0\|_{L^\infty}$ with respect to N on [0,10] by using 1) Guo-Wang(red-o) 2) Tau(black-*) with Phi 3) Tau(black-*) with Phi-Newton 4) collocation with Phi(x)(pink-o) 5) collocation with Phi(x)-Scaling(green-o) 6) collocation with differentiation matrix(yellow-o) matrix.

Example 4: Threefold symmetry Hamiltonian system [22].

Consider a $k-$fold rotational symmetry system in phase plane with Hamiltonian

$$H_k(p,q) = \sum_{j=1}^{k} \cos(p\cos(\frac{2\pi j}{k}) + q\sin(\frac{2\pi j}{k})).$$

For $k = 3$, the three axis-symmetric Hamiltonian system is,

$$H(p,q) = \cos(p) + \cos(-\frac{1}{2}p + \frac{\sqrt{3}}{2}q) + \cos(\frac{1}{2}p + \frac{\sqrt{3}}{2}q).$$

The corresponding system of nonlinear ODE for this H is

$$\begin{aligned} p'(t) &= -\frac{\partial H}{\partial q} = \frac{\sqrt{3}}{2}\sin(-\frac{1}{2}p + \frac{\sqrt{3}}{2}q) + \frac{\sqrt{3}}{2}\sin(\frac{1}{2}p + \frac{\sqrt{3}}{2}q) \\ q'(t) &= \frac{\partial H}{\partial p} = -\sin(p) + \frac{1}{2}\sin(-\frac{1}{2}p + \frac{\sqrt{3}}{2}q) - \frac{1}{2}\sin(\frac{1}{2}p + \frac{\sqrt{3}}{2}q) \end{aligned}$$

with initial condition $p(0) = \pi,\ q(0) = 0$. In this case, $H_0 = -1$.

Figure 17 contains the graphs of p, q with respect to time t. The result from the symplectic method does not make a right corner like the one from the spectral collocation method with Chebyshev differentiation matrix. We can see it clearly if we consider the phase plot of the results. The phase plot from a sympletic method has fuzzy corners compared with sharp-corner hexagon from the spectral collocation as shown in Figure 18. The other spectral methods also give similar phase plots as in (a). Note that the possible solutions for threefold symmetry Hamiltonian system contain equilateral triangles and hexagons depending on the initial conditions. We consider only a hexagon case in this example. For the symplectic method, the smaller the h, the more horizontally stretched the graph is. The graph tends to have the same behavior as the collocation method when the size of h decreases.

From the observation on different spectral methods, the same N may give different results. For example, with $N = 20$, we have the collocation with D matrix and Tau with Legendre-Phi converge to a similar solution with number of iteration on the last interval less than 10 whereas the collocation method with Legendre-Phi and Guo-Wang converge to different solutions and reach the maximum iteration number(1000).

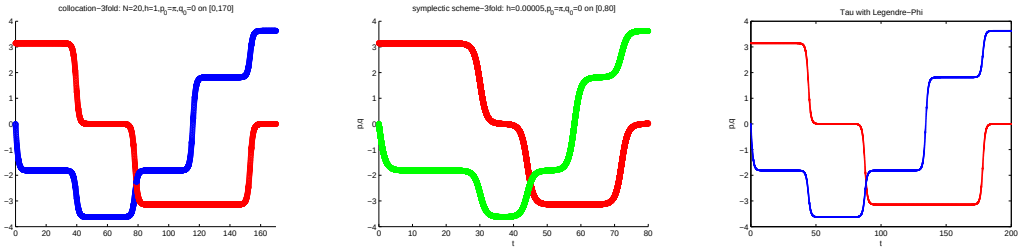

Figure 17: Graphs of p (upper) and q (lower) versus t by (a) collocation method with Chebyshev-D when N = 20 on [0,170]; (b) symplectic 3 $h = 0.00005$ on [0,80] (c) Tau with Legendre-Phi when N = 20 on [0,200].

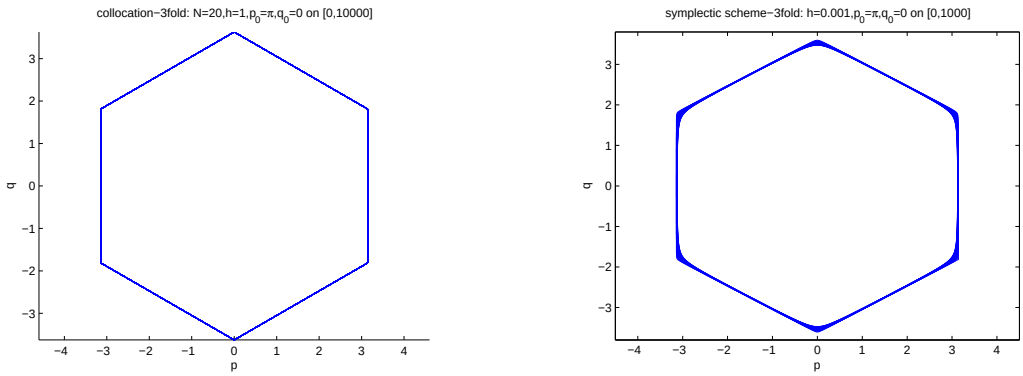

Figure 18: Phase plots q versus p by (a) spectral collocation with D matrix when $N = 20$ on $[0, 10000]$; (b) symplectic 3 when h=0.001 on [0,1000].

Figure 19, 20 and 21 show the error propagations of the spectral methods. The error from the collocation method with Chebyshev-Differentiation matrix increases

linearly as t increases. The other methods have a similar pattern but Tau method with Legendre-Phi gives the best error.

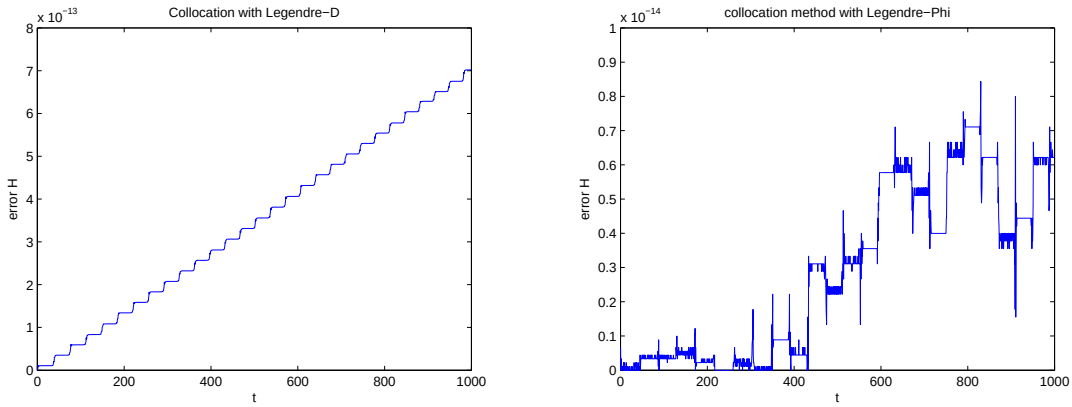

Figure 19: Patterns of errors $|H(t_i) - H_0|$ versus t on [0,1000] by (a) collocation method with Chebyshev-Differentiation matrix when $N = 15$ (b) collocation method with Legendre-Phi.

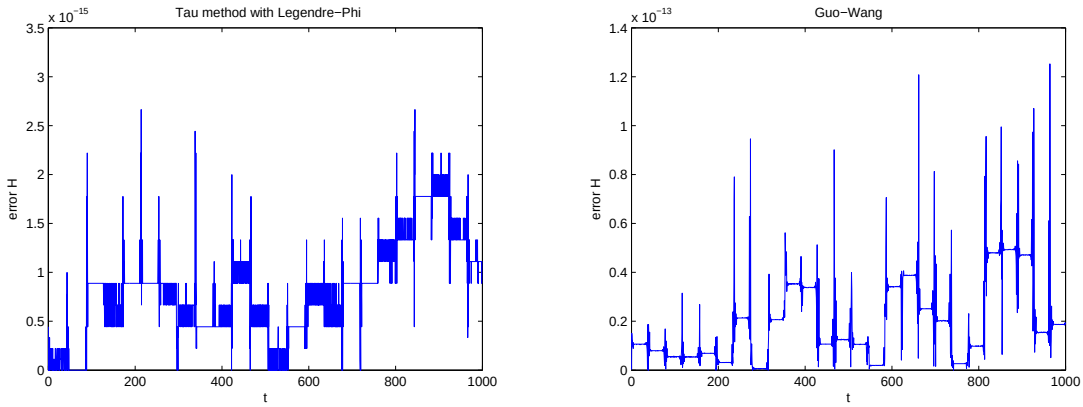

Figure 20: Patterns of errors $|H(t_i) - H_0|$ versus t on [0,1000] when $N = 15$ by (a) Tau method with Legendre-Phi (b) Guo-Wang.

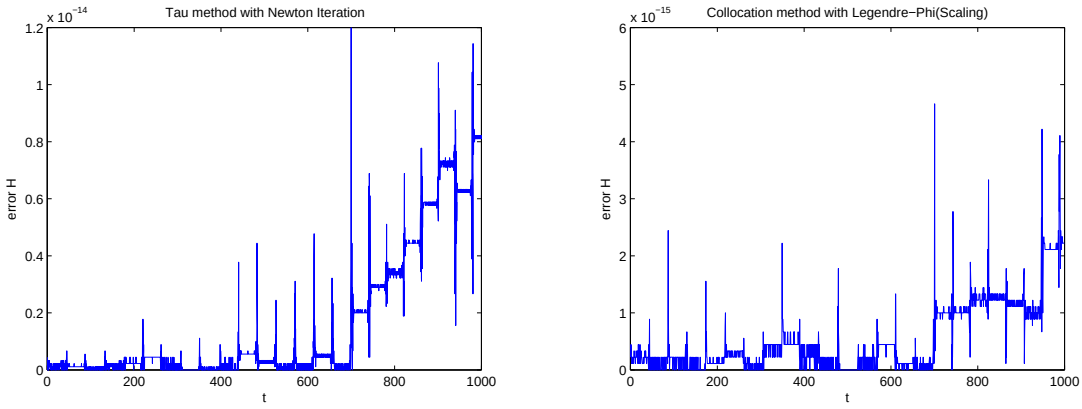

Figure 21: Patterns of errors $|H(t_i) - H_0|$ versus t on [0,1000] by (a) Tau method with Newton iteration when $N = 15$ (b) collocation method with Legendre-Phi(Scaling) when $N = 16$.

Figures 22 represents the errors from the spectral methods. We compare the errors by using the maximum norm in (b). The highest error is from Guo-wang and the next is the collocation with the differentiation matrix. The errors from the other methods drop down to the machine error right away.

The convergence rates for the symplectic and the collocation methods with the differentiation matrix are shown in Figure 23. For the spectral collocation method, the error drops down to machine error with relatively small N.

Table 8 shows convergent rates for the energy H and the CPU times. We use $h = 0.001$ for the symplectic schemes 3. The spectral collocation method with Chebyshev-Differentiation matrix used 45 minutes to obtain data in $[0, 10000]$ but with the same time used, the symplectic method produces data approximately on [0,450] with much lower accuracy.

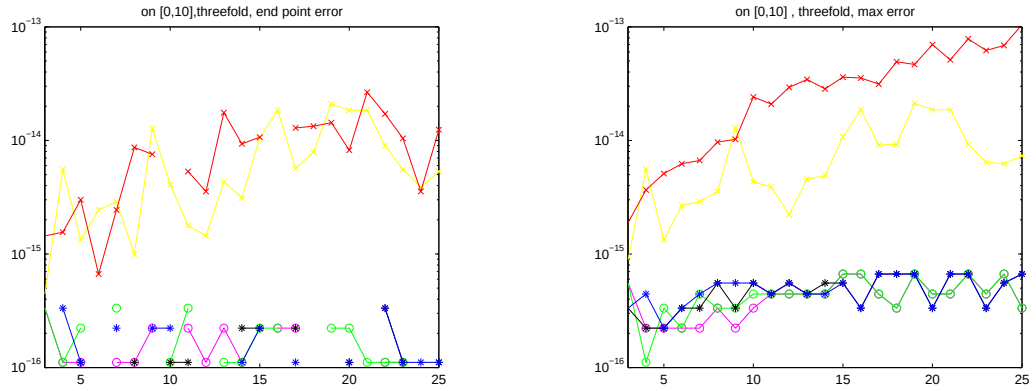

Figure 22: Errors of (a) $|H_0 - H_N(T)|$ (b) $\|\boldsymbol{H}(t_j) - \boldsymbol{H}_0\|_{L^\infty}$ with respect to N on [0,10] by using 1)Guo-Wang(red-o) 2)Tau(black-*) with Phi 3)Tau(black-*) with Phi-Newton 4)collocation with Phi(x)(pink-o) 5)collocation with Phi(x)-Scaling(green-o) 6) collocation with differentiation matrix(yellow-o) matrix.

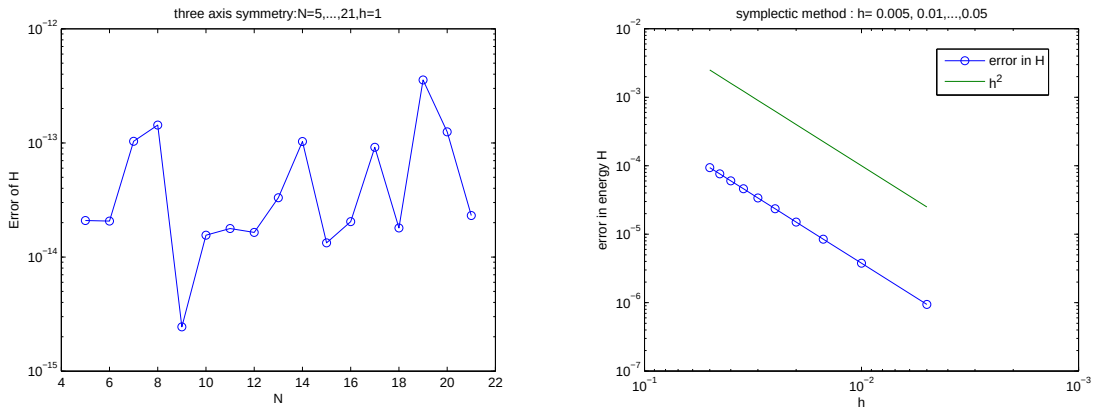

Figure 23: (a) Error in H versus N when $N = 5, 6, ..., 21$ by spectral collocation on $[0, 500]$; (b) Error in H versus h when $h = 0.005, 0.01, ..., 0.05$ by the symplectic scheme 3 on $[0, 10]$

.

	time(secs)	Error in Energy
Symplectic 3 on [0,400]	2190	$6.425967063916294 \times 10^{-3}$
Symplectic 3 on [0,600]	5360(89mins)	$1.0537382086 \times 10^{-2}$
Colloc. w Chebyshev-D, N=20 on [0,10000]	2725(45mins)	$2.7539082125 \times 10^{-12}$
Colloc. w Legendre-D, N=15 on [0,1000]	5	$7.022160630754115 \times 10^{-13}$
Tau w Legendre-Phi w/o Newton, N=15 on [0,1000]	6.59s	$4.218847493575595 \times 10^{-14}$
Tau w Legendre-Phi w Newton, N=15 on [0,1000]	118s	$1.565414464721471 \times 10^{-14}$
Coll w Legendre-Phi, N=15 on [0,1000]	93s	$1.132427485117660 \times 10^{-14}$
Coll w Legendre-Phi(Scaling), N=15 on [0,1000]	21s	$1.443289932012704 \times 10^{-15}$
Guo-Wang, N=15 on [0,1000]	69s	$3.811395643538162 \times 10^{-13}$

Table 8: Comparison of the CPU times between the spectral and symplectic methods.

This problem is a highly nonlinear problem with cosine and sine terms. The number of iterations is highly depending on N and the terminal value for t. Table 9 shows the comparisons of iteration numbers and the CPU times by using the spectral methods as we can see that Guo-wang's iteration number is larger than the other methods. It means the method doesn't converge as fast. It reaches the maximum number of iterations before reaching the tolerance. If the Newton method is applied, it reduces the number of iterations and the CPU times as shown in Table 9.

Intervals/Method	N	time elapse	Iteration numbers on the last interval
Tau w Newton,$[0, 10]$	10	0.136s	10
Tau w/o Newton,$[0, 10]$	10	0.09s	18
Coll w Phi,$[0, 10]$	10	0.103s	18
Coll w Phi-Scaling,$[0, 10]$	10	0.238s	18
Coll w D,$[0, 10]$	10	0.070s	15
Guo-Wang,$[0, 10]$	10	1.284s	1000

Table 9: Comparisons of iteration numbers and the CPU times by using the spectral methods.

Example 5: Consider a linear system of ordinary differential equations [31]

$$\begin{aligned} p'(t) &= q(t) \\ q'(t) &= p(t) - p^3(t) \end{aligned}$$

with the initial conditions $p(t_0) = \sqrt{2},\ q(t_0) = 0$.

The Hamiltonian for this system is given by $H(p,q) = -\frac{1}{2}q^2 + \frac{1}{2}p^2(t) - \frac{1}{4}p^4(t)$.The initial energy is $H(p_0, q_0) = H_0 = 0$.

Figure 24 shows the error propagations $|H(t_i) - H_0|$ versus t on [0,1000] when $N = 15$ by collocation method with Legendre-Differentiation matrix, collocation method with Legendre-Phi and Tau method with Legendre-Phi. The error propagations of the other spectral methods are similar to Figure 24 (b) and (c). In this case, for the spectral methods except the collocation method with Chebyshev-Differentiation matrix, the errors depend on the terminal point we chose. They fluctuate throughout the domain. Therefore the maximum norm is more reliable. Figure 25 shows the two different errors, the terminal errors and the maximum errors of the spectral methods. In part (b), all of the spectral methods are having the same convergence rate until $N = 17$ then the collocation method with Legendre-Phi and Tau method with Legendre-Phi and Guo-Wang errors stop decreasing even when N is smaller. The errors from the other methods still decrease until $N = 19$ and they maintain a stable tail.

The comparison of the CPU times between the spectral and symplectic methods is shown in Table 10 and the comparisons of the iteration numbers and the CPU times

by using the spectral methods are shown in Table 11.

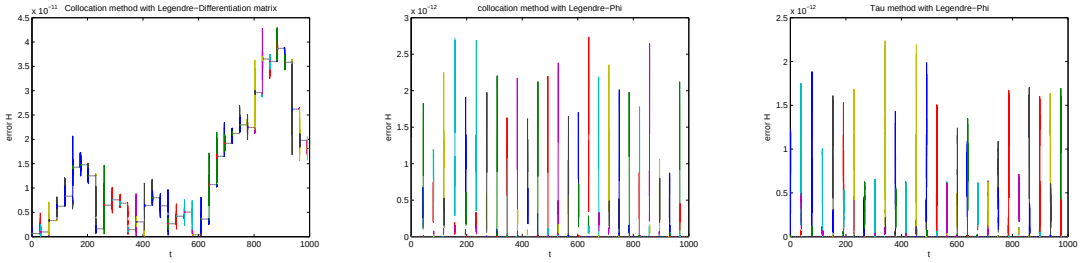

Figure 24: Patterns of errors $|H(t_i) - H_0|$ versus t on [0,1000] when $N = 15$ by (a) collocation method with Chebyshev-Differentiation matrix (b) collocation method with Legendre-Phi (c) Tau method with Legendre-Phi

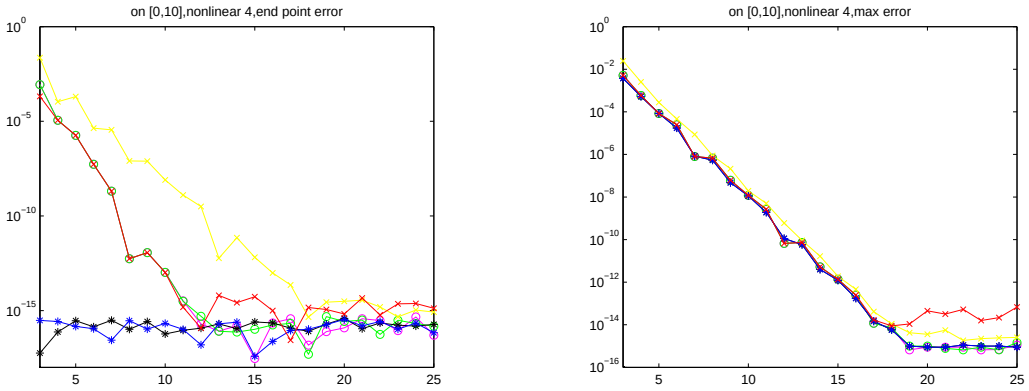

Figure 25: Errors of (a) $|H_0 - H_N(T)|$ (b) $\|\boldsymbol{H}(t_j) - \boldsymbol{H}_0\|_{L^\infty}$ with respect to N on [0,10] by using 1)Guo-Wang(red-o) 2) Tau(black-*) with Phi 3) Tau(black-*) with Phi-Newton 4) collocation with Phi(x)(pink-o) 5) collocation with Phi(x)-Scaling(green-o) 6) collocation with differentiation matrix(yellow-o) matrix.

	time(secs)	Error in Energy
Colloc. w Chebyshev-D, N=15 on [0,1000]	2.9	$4.293304600722081 \times 10^{-11}$
Tau w Legendre-Phi w/o Newton, N=15 on [0,1000]	5s	$2.234212814755665 \times 10^{-12}$
Tau w Legendre-Phi w Newton, N=15 on [0,1000]	6.6s	$2.261746345766369 \times 10^{-12}$
Coll w Legendre-Phi, N=15 on [0,1000]	4.9s	$2.731814774392660 \times 10^{-12}$
Coll w Legendre-Phi(Scaling), N=15 on [0,1000]	20s	$2.742139848521674 \times 10^{-12}$
Guo-Wang, N=15 on [0,1000]	4.5s	$2.732480908207435 \times 10^{-12}$

Table 10: Comparison of the CPU times between the spectral and the symplectic methods.

Intervals/Method	N	time elapse	Iteration numbers
Guo-Wang,$[0, 10]$	10	0.065s	9
Tau w Newton,$[0, 10]$	10	0.14s	3
Tau w/o Newton,$[0, 10]$	10	0.0707s	9
Coll w Phi,$[0, 10]$	10	0.089s	9
Coll w Phi-Scaling,$[0, 10]$	10	0.226s	9
Coll w D,$[0, 10]$	10	0.064s	9

Table 11: Comparisons of the iteration numbers and the CPU times by using the spectral methods.

Example 6: The Henon-Heiles(HH) system [23, 24].

The Henon-Heiles(HH) Hamiltonian was introduced in the study of galactic dynamics to describe the motion of stars around the galactic center.

$$H(p_1, p_2, q_1, q_2) = \frac{1}{2}(p_1^2 + p_2^2 + q_1^2 + q_2^2) + q_1^2 q_2 - \frac{1}{3}q_2^3.$$

The terms q_1^2 and q_2^2 form a potential well which is responsible for the oscillations of the particle (the first four terms are related to the Kinetic energy). The last two terms, $q_1^2 q_2$ and $\frac{1}{3}q_2^3$, are responsible for the existence of the exits from the orbit.

There are four equilibrium points for this system which are $E_1 = (\bar{p}_1, \bar{p}_2, \bar{q}_1, \bar{q}_1) = \mathbf{0}$, a center, $E_2 = (0, 0, 0, 1)$, $E_3 = (0, 0, \frac{\sqrt{3}}{2}, -\frac{1}{\sqrt{2}})$ and $E_4 = (0, 0, -\frac{\sqrt{3}}{2}, -\frac{1}{\sqrt{2}})$, saddle points. As a result, there are three exits for the energy to escape according to the three saddle points. The total energy $H_E = 0$ for E_1 and $H_E = \frac{1}{6}$ for E_2, E_3, and E_4. If the initial energy is far beyond this H_E, the particles wander inside the scattering region for a certain time until they cross one of the three energy line and escape to infinity. In other words, when the initial $H < \frac{1}{6}$, the solution is regular; when $H > \frac{1}{6}$, the solution is chaotic. Note that the time they spent in bounded region is called the "escape time". The higher the energy, the shorter the escape times are found.

Figure 26 shows the phase plots for potential energy H when $p_1 = 2, p_2 = 1$ are fixed, q_2 and q_1 vary. We can see that the three exits for the energy are at the three saddle points $E_2, E_3, \text{and} E_4$ located at three vertices of an equilateral triangle.

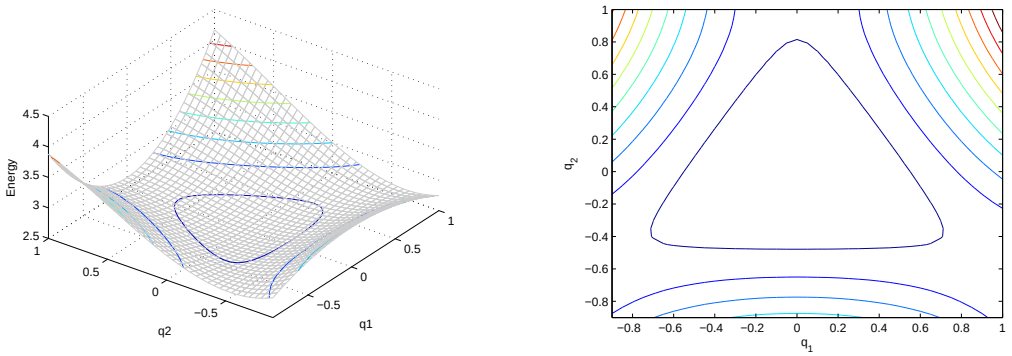

Figure 26: Graphs of contour plots of energy H when q_2 and q_1 vary and $p_1 = 2, p_2 = 1$ are fixed (a) 3-D (b) 2-D

The system of nonlinear ODE for this H is

$$\begin{aligned} p_1'(t) &= -\frac{\partial H}{\partial q_1} = -q_1 - 2q_1q_2 \\ p_2'(t) &= -\frac{\partial H}{\partial q_2} = -q_2 - q_1^2 + q_2^2 \\ q_1'(t) &= \frac{\partial H}{\partial p_1} = p_1 \\ q_2'(t) &= \frac{\partial H}{\partial p_2} = p_2 \end{aligned}$$

We select two different sets of the initial conditions. The first set represents a regular case with

$$p_1(0) = 0.011,\ p_2(0) = 0,\ q_1(0) = 0.013,\ q_2(0) = -0.4; \quad H_0 = 0.101410733 < 1/6.$$

The second set is a chaotic case with

$$p_1(0) = \sqrt{2 \times 0.15925},\ p_2(0) = q_1(0) = q_2(0) = 0.12; \quad H_0 = 0.18200200 > 1/6.$$

Figure 27 shows the chaotic solution and the phase plot when the particle wanders in the bounded region until it crosses the energy threshold line and escapes. Figure

28 represents phase plots of a regular solution from both methods. The trajectory from the symplectic method is denser than the one from the collocation method with the Chebyshev differentiation matrix. The plot of q_2 and p_2 from Tau method with Legendre-Phi is shown in part (c). The loop is very thin.

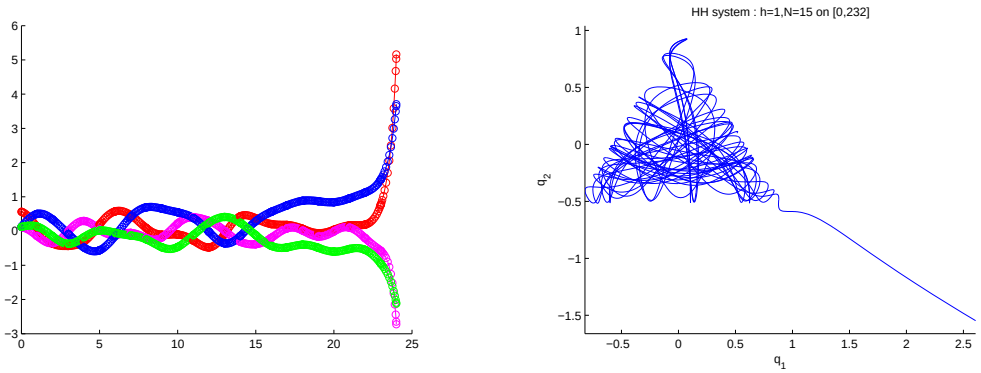

Figure 27: Chaotic solutions by the spectral collocation $N = 15$ (a) on $[0, 24]$; (b) phase plot q_2 versus q_1 on [0,232].

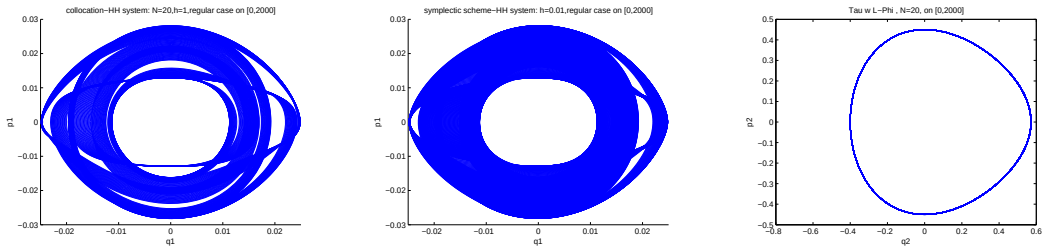

Figure 28: Phase plots of a regular case on [0,2000] by (a) the spectral collocation with Chebyshev D-matrix, $N = 20$; (b) symplectic 4 h=0.01. (b) Tau method with Legendre-Phi $N = 20$.

The errors in energy, H, and the CPU times are presented in Table 12. We choose the initial conditions from the regular case. We use $h = 0.001$ for the symplectic scheme 4. By comparing both times and errors, Tau method has the best error even

though it uses more CPU times than the collocation method with the differentiation matrix.

	time(secs)	Error in Energy
Collocation, N=20 on [0,10000]	2691	$1.9004658957 \times 10^{-12}$
Symplectic 4 on [0,65]	21	$6.0026862363 \times 10^{-5}$
Symplectic 4 on [0,200]	970(16mins)	$6.0026862363 \times 10^{-5}$
Symplectic 4 on [0,1000]	>2hrs	
Colloc. w Cheb-D, N=20 on [0,1000]	4s	$7.037426197342711 \times 10^{-13}$
Tau w Legendre-Phi, N=20 on [0,1000]	8s	$6.800116025829084 \times 10^{-16}$
Tau w Legendre-Phi(Scaling), N=20 on [0,1000]	8.5s	$1.415534356397075 \times 10^{-15}$
Coll w Legendre-Phi(Scaling), N=20 on [0,1000]	22s	$6.106226635438361 \times 10^{-16}$
Guo-Wang, N=20 on [0,1000]	6s	$3.122779812514409 \times 10^{-13}$

Table 12: Comparison of the CPU times of the spectral and the symplectic methods.

The rates of convergence in energy using the regular initial values are shown in Figure 29. Spectral collocation gives the rate in the order of $(\frac{1}{N})^{(0.85N)}$ and the symplectic scheme 4 is of the order one. The convergence rates of the other spectral methods versus N where $N = 3, ..., 20$ are demonstrated in Figure 30. Again, the errors from the collocation method with the differentiation matrix and Guo-Wang reach 10^{-14} then stay at that rate as N increases. Figure 30(b) shows that the rate of Tau method is about $(0.03\frac{1}{2.1N})^{(0.85N)}$ when $N = 3, ..., 14$.

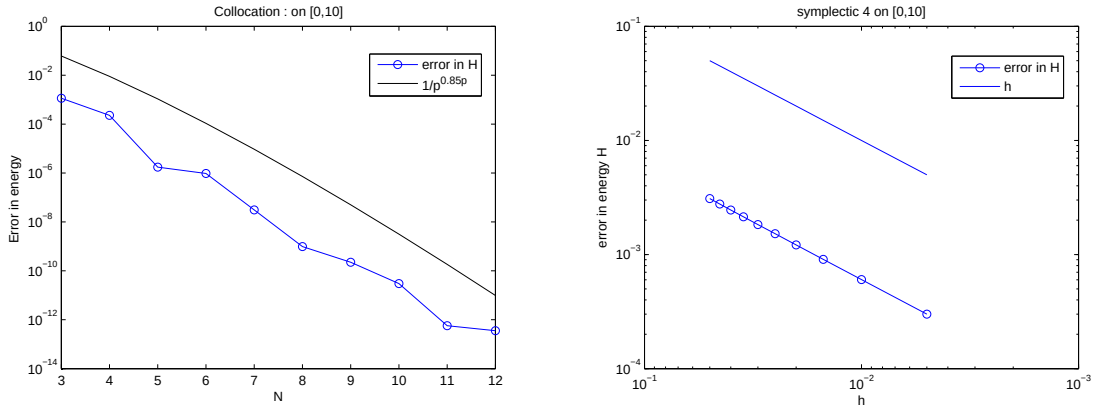

Figure 29: (a) Error in H and $(\frac{1}{N})^{(0.85N)}$ versus N when $N = 3, 4, ..., 12$ by spectral collocation on $[0, 10]$; (b) Error in H versus h when $h = 0.005, 0.01, ..., 0.05$ by symplectic 4 on $[0, 10]$.

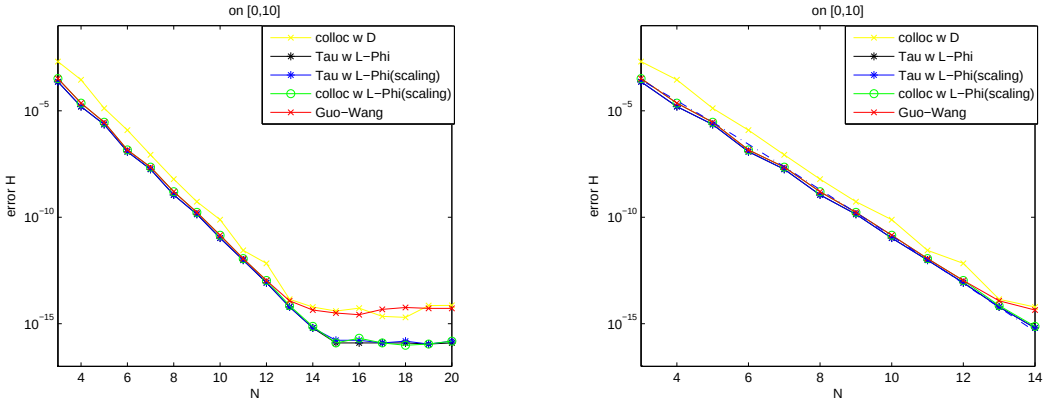

Figure 30: (a) $\|\boldsymbol{H}(t_j) - \boldsymbol{H}_0\|_{L^\infty}$ with respect to N on [0,10] by using 1) Guo-Wang(red-o) 2) Tau with Legendre-Phi(black-*) 3) Tau with Legendre-Phi-scaling(blue-*) 4) collocation with Legendre-Phi(scaling)(green-o) 5) collocation with differentiation matrix(yellow-o) (b) The convergence rates of the spectral methods and $(0.03\frac{1}{2.1N})^{(0.85N)}$ versus N (blue -.).

Example 7: A modified Two-body Problem [52].

The Hamiltonian for this system is $H = T + V$ where $T = \frac{1}{2}\|\boldsymbol{p}\|^2$ and $V = -\frac{1}{\|\boldsymbol{q}\|} - \frac{\epsilon}{2\|\boldsymbol{q}\|^3}$. Thus

$$H(\boldsymbol{p},\boldsymbol{q}) = \frac{1}{2}\|\boldsymbol{p}\|^2 - \frac{1}{\|\boldsymbol{q}\|} - \frac{\epsilon}{2\|\boldsymbol{q}\|^3}.$$

where ϵ is a small perturbation parameter.

The system of nonlinear ODEs for this energy is

$$\begin{aligned} p_1'(t) &= -\frac{q_1}{\sqrt{(q_1^2+q_2^2)^3}} - \frac{3\epsilon q_1}{2\sqrt{(q_1^2+q_2^2)^5}} \\ p_2'(t) &= -\frac{q_2}{\sqrt{(q_1^2+q_2^2)^3}} - \frac{3\epsilon q_2}{2\sqrt{(q_1^2+q_2^2)^5}} \\ q_1'(t) &= p_1 \\ q_2'(t) &= p_2 \end{aligned}$$

with the initial conditions $p_1(0) = p_{10}, p_2(0) = p_{20}, q_1(0) = q_{10}, q_2(0) = q_{20}$.

This is a modification of the two-body problem. It is about the system of two massive bodies that attract each other by the gravitational force. We are seeking for the positions and velocities of those two bodies. The first body is located at the origin. The second body is located where its coordinates are (q_1, q_2) and the corresponding velocity is $(q_1', q_2') = (p_1, p_2)$. This model describes the motion of a particle in a plane. A particle in this model is attracted gravitationally by a slightly oblate sphere instead of a point mass. The attracting body rotates symmetrically with respect to an axis perpendicular to the plane of the particle. If there is no perturbation (ϵ), the problem is just a regular two-body problem[24].

Besides the energy H, this system also preserves the angular momentum which is $p^T Bq$, where $B = J$ for this problem, i.e $\frac{d(p^T Jq)}{dt} = 0 \Rightarrow p^T Jq = p_0^T Jq_0$. We use the initial values $p_1(0) = 0, p_2(0) = \sqrt{\frac{1+e}{1-e}}, q_1(0) = 1 - e, q_2(0) = 0$, where e is the eccentricity of the orbit. Here if we choose e closer to one, the solution tends to diverge and does not conserve energy well for both spectral collocation and symplectic methods. We choose e small enough in order for the solution to converge to an equilibrium point.

We compare the spectral methods and a second order symplectic method. The eccentricity e is chosen to be 0.001 (almost a circle) for the numerical test. Both methods preserve the structure. Figures 31 represents the phase plots by the spectral collocation with the differentiation matrix and with a perturbation value $\epsilon = 0.005$. For all reasonable N and h, the solutions from all methods are almost the same, but with a slightly thicker orbit at the left and the right corners for the symplectic method scheme 1 (not shown). Note that with a larger perturbation ϵ, the body rotates in an oblique pattern. If we compare the times and errors, the spectral methods give a better result.

The convergence rates for both methods are shown in Figure 32. The convergence rate for the symplectic scheme is of order three and for the spectral collocation is of the order $(\frac{1}{N})^{(1.1N)}$. Figure 33 represents the convergence rates of the spectral methods when $N = 3, ...16$. The pattern is similar to the errors in the previous example. In part (b), we consider the rates when $N = 3, ...12$. Excluding the spectral collocation method, the other spectral methods have the errors of the order $(4\frac{1}{10})^{(1.28N)}$ which

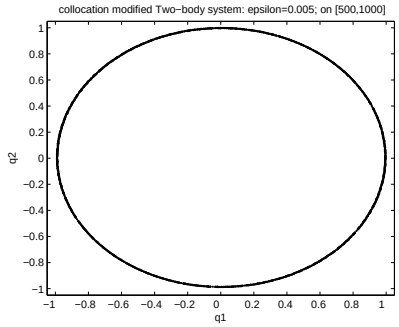

Figure 31: Phase plots of q_1 and q_2 when $\epsilon = 0.005$ by the collocation method with D matrix on [500,1000] when $N = 20$.

is the same as the convergence rate of the angular momentum by using the spectral methods shown in Figure 34.

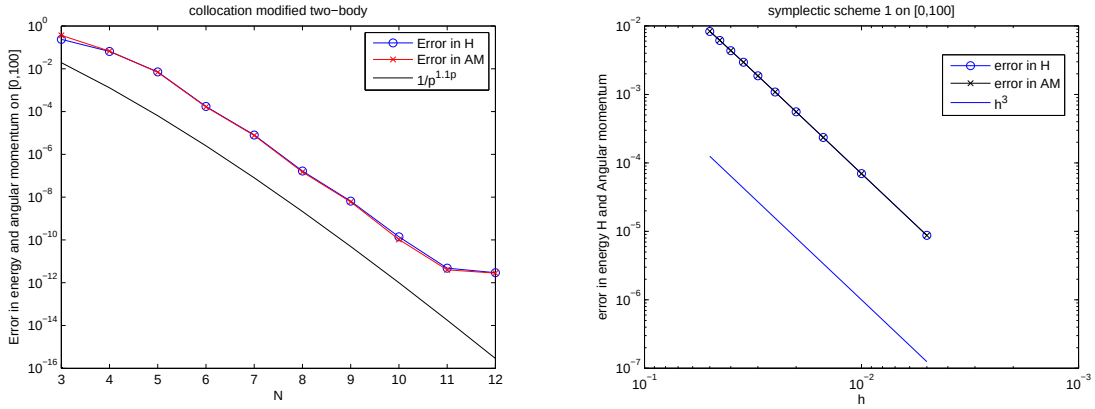

Figure 32: (a) Errors in H and in the angular momentum with $(\frac{1}{N})^{(1.1N)}$ versus $N = 3, 4, ..., 12$ by the spectral collocation with D on $[0, 100]$; (b) Errors in H and in the angular momentum versus h=0.005,0.01,0.015,...,0.05, on [0,100] by symplectic 1.

Table 13 represents the errors in energy H, the errors in the angular momentum, and the CPU times. For these initial conditions, both errors and the CPU times

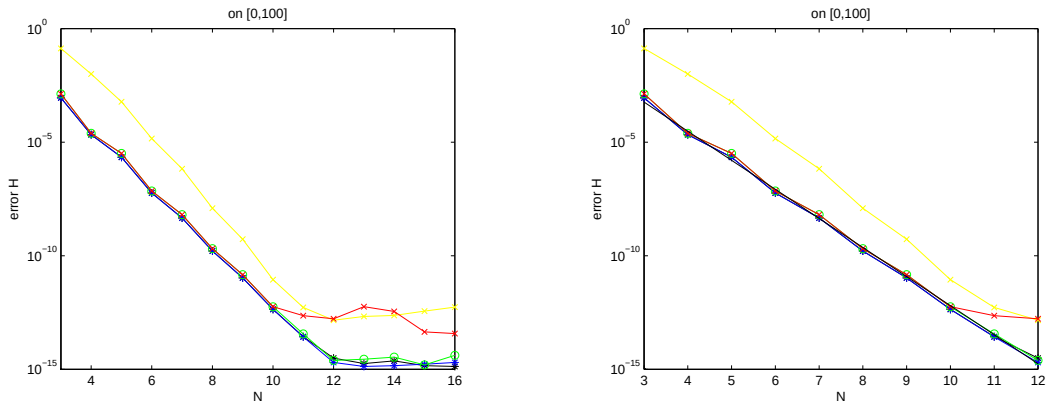

Figure 33: (a) Errors in H versus $N = 3, 4, ..., 16$ by using 1) Guo-Wang(red-o) 2) Tau with Legendre-Phi(black-*) 3) Tau with Legendre-Phi-scaling(blue-*) 4) collocation with Legendre-Phi(scaling)(green-o) 5) collocation with differentiation matrix(yellow-o) (b) Errors in part (a) and $4(\frac{1}{10})^{(1.28N)}$ versus $N = 3, 4, ..., 12$ (solid black).

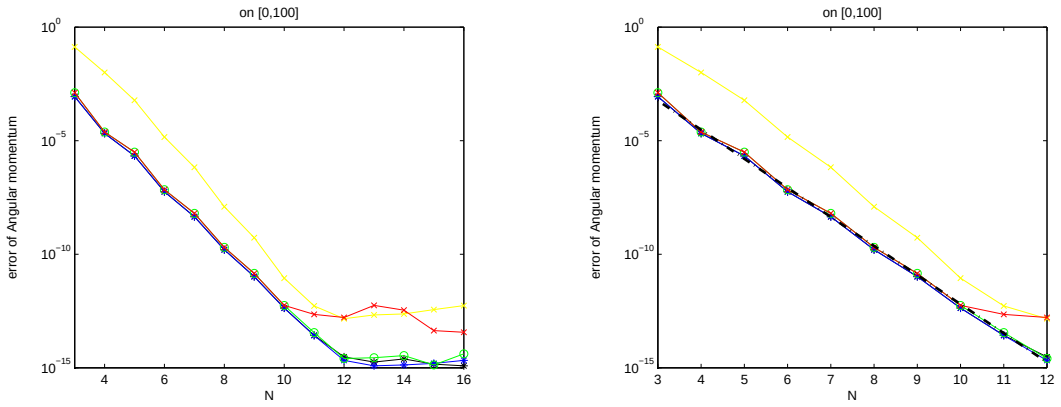

Figure 34: (a) Errors of the angular momentum versus $N = 3, 4, ..., 16$ by using 1) Guo-Wang(red-o) 2) Tau with Legendre-Phi(black-*) 3) Tau with Legendre-Phi-scaling(blue-*) 4) collocation with Legendre-Phi(scaling)(green-o) 5) collocation with differentiation matrix(yellow-o) (b) Errors in part (a) and $4(\frac{1}{10})^{(1.28N)}$ versus $N = 3, 4, ..., 12$ (solid black).

from the spectral collocation are better than any symplectic method. However, if we change the initial conditions to $p_{10} = 0.1$, $p_{20} = 0.9$, $q_{10} = q_{20} = 1$, the errors from both methods are almost in the same order but the spectral collocation is time efficient as we can see from Table 14 with the two-body case ($\epsilon = 0$).

	time(secs)	Error in Energy	Error in Angular Momentum
Colloc,N=20,$[0, 10^4]$	3230	$2.15614193 \times 10^{-11}$	$2.09121608 \times 10^{-11}$
Symp 1,h=0.001,[0,75]	53	$6.05561933 \times 10^{-8}$	$5.85881273 \times 10^{-8}$
Symp 1,h=0.001,[0,80]	72	$6.48879968 \times 10^{-8}$	$6.18349377 \times 10^{-8}$
Colloc,N=20,[0,1000]	4.6	$7.54918350 \times 10^{-12}$	$7.43594075 \times 10^{-12}$
Tau w Legendre-Phi	9.5s	$5.32907051 \times 10^{-15}$	$5.21804821 \times 10^{-15}$
Tau w Legendre-Phi(Scaling)	9.5s	$5.32907051 \times 10^{-15}$	$5.21804821 \times 10^{-15}$
Coll w Legendre-Phi(Scaling)	24s	$1.09912079 \times 10^{-14}$	$1.08801856 \times 10^{-14}$
Guo-Wang, N=20 on [0,1000]	32s	$3.19833048 \times 10^{-12}$	$3.15036885 \times 10^{-12}$

Table 13: Comparison of the CPU times of the spectral and the symplectic methods.

	time(secs)	Error in Energy	Error in Ang. Momentum
Colloc, N=20 on [0,100]	3	$4.28660520 \times 10^{-7}$	1.3618605×10^{-7}
Symp 1,h=0.001,[0,40]	75	$3.02104066 \times 10^{-7}$	$1.06633042 \times 10^{-6}$
Symp 1,h=0.001,[0,50]	166	$3.02104066 \times 10^{-7}$	$1.06633042 \times 10^{-7}$

Table 14: Comparisons of the CPU times between the two methods with the same order of errors when $\epsilon = 0$.

Example 8: The Three-body system [40].

Consider the Hamiltonian of the Earth-Moon-Satellite system given by

$$H(p_x, p_y, x, y) = \frac{p_x^2 + p_y^2}{2} + (yp_x - xp_y) - (\frac{(1-\mu)}{r_1} + \frac{\mu}{r_2}),$$

where $r_1^2 = (x+\mu)^2 + y^2,\ r_2^2 = (x+\mu-1)^2 + y^2$.

This model describes the motion of the satellite around the Earth and Moon. The Earth and Moon are located on the x-axis where their center of mass is placed at the origin. The coordinate of the satellite is (x, y). It rotates in the orbit around the Earth and Moon at the rate one moon month so the Earth and Moon are always on the x-axis. The mass of the Moon is $\mu = 0.01215$ (the length unit is 384400 km).

The corresponding system is given by

$$\begin{aligned}
p_x'(t) &= p_y - \frac{(1-\mu)}{r_1^3}(x+\mu) - \frac{\mu}{r_2^3}(x+\mu-1) \\
p_y'(t) &= -p_x - \frac{(1-\mu)}{r_1^3}y - \frac{\mu}{r_2^3}y \\
x'(t) &= p_x + y \\
y'(t) &= p_y - x
\end{aligned}$$

We compare the spectral collocation with a second order symplectic method under a transformation $q_1 = \frac{1}{2}(x+y)$, $q_2 = \frac{1}{2}(x-y)$, $p_1 = p_x + p_y$, $p_2 = p_x - p_y$. The initial conditions for Figure 35 are $p_1(0) = 1.259185, p_2(0) = -1.259185, q_1(0) = -0.25, q_2(0) = -0.25$ where we can see an orbit (the coordinate plot for this case is a circle (not shown)) and $p_1(0) = -0.16, p_2(0) = -0.7, q_1(0) = 1.3, q_2(0) = -0.31$ for Figure 36 to observe the orbit of the satellite. Solutions are plotted by using the

same frame sizes. In Figure 36, the orbit from a symplectic method is thicker than the collocation method especially at the left and right sides.

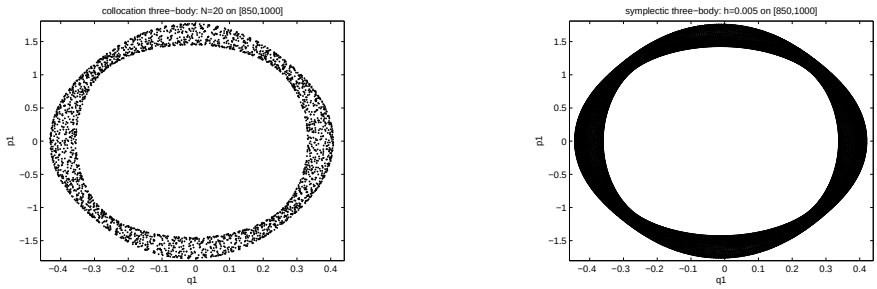

Figure 35: Phase plots p_1 versus q_1 of the orbit by (a) spectral collocation on $[850, 1000]$; (b) symplectic 1 h=0.005 on [850,1000].

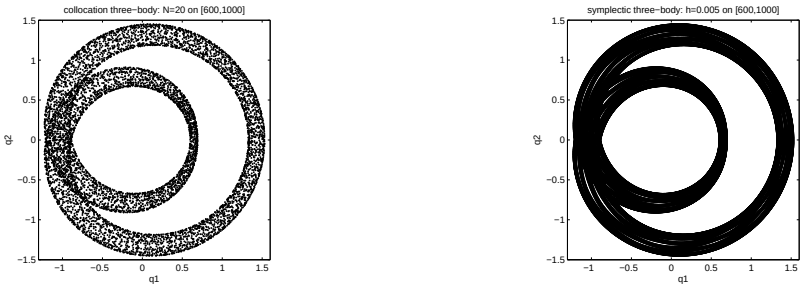

Figure 36: Phase plots of the coordinate of the satellite, q_2 versus q_1 by (a) spectral collocation on $[600, 1000]$; (b) symplectic 1 h=0.005 on [600,1000].

Table 15 compares the errors in energy H and the CPU times by using the first set of the initial conditions. We use $h = 0.005$ for the symplectic method. At $t = 300$, the spectral collocation method uses much less time (5.4 second vs. 18 second) and yet, offers much better accuracy in energy (2×10^{-7}) than the symplectic method (9×10^{-3}).

The convergence rates of each method are plotted in Figure 37. We use the first set of the initial conditions on $[0, 10]$ when $N = 11, ..., 21$. The rate of Tau method with

	time(secs)	Error in Energy
Symplectic 1 on [0,300]	18	$9.3757448742 \times 10^{-3}$
Symplectic 1 on [0,150]	4.6	$4.8046166186 \times 10^{-3}$
Collocation, N=20 on [0,300]	5.4	$1.6617218332 \times 10^{-6}$
Tau w Legendre-Phi, N=20 on [0,300]	120s	$1.9503096782 \times 10^{-7}$
Guo-Wang, N=20 on [0,1000]	121s	$2.9193665396 \times 10^{-7}$

Table 15: Comparison of the CPU times between the spectral and the symplectic methods.

Legendre-Phi is the best which is of the order $0.3(\frac{e}{N})^{(0.675N)}$ and for the symplectic scheme 1 is of order three. The collocation method with Legendre-Phi (with and without scaling) doesn't converge to the solution in this case.

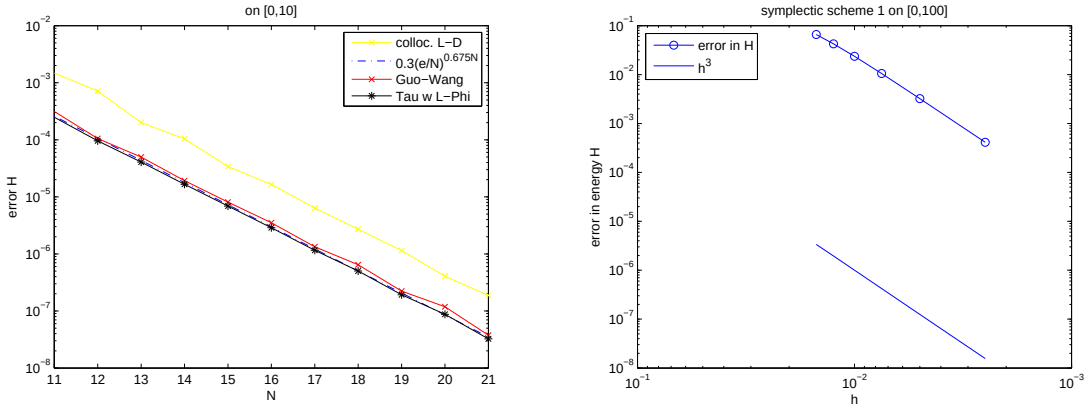

Figure 37: (a) Errors in H versus $N = 11, 12, ..., 21$ on $[0, 100]$ by (a) spectral collocation with Chebyshev D (yellow), Tau with Legendre-Phi(black), Guo-Wang (red) and the rate $(0.3\frac{e}{N})^{(0.675N)}$ (green)(b) Error in H versus h= 0.0025,0.005,....,0.015 by symplectic 1 on [0,100].

5 Discussion and Conclusion Remarks

We have compared numerical results of the spectral methods discussed in Chapter 2 and several symplectic methods in solving Hamiltonian dynamical systems. Our numerical evidences have demonstrated that the spectral methods have several advantages.

1) They require less CPU times in order to reach the same level of accuracy.

2) They preserve energy and symplectic structure better.

3) They predict more accurate trajectories for long time.

In addition, the proposed spectral methods are systematic and can be applied to any Hamiltonian system without changing the basic algorithm. On the other hand, one needs to design a different symplectic method for each different problem.

In comparison among the spectral methods, we shall discuss by cases. For a linear Hamiltonian system, the collocation method with Chebyshev differentiation matrix has the highest error. Tau method with Legendre-Phi and Guo-Wang have the best convergence rates. However, the rate from Guo-Wang oscillates at the tail when $N \geq 9$ while the Tau method has a stable tail.

For a nonlinear Hamiltonian system, based on the numerical results, if we compare the error

$$\max_{1 \leq j \leq N} \|H(t_j) - H_0\|_{L^\infty},$$

the convergence rates for the spectral methods are almost the same except for the collocation with differentiation matrix. However, the error from Guo-Wang method

reaches only around 10^{-14} but Tau and the collocation methods with Legendre-Phi could reach 10^{-15} or less and the tails are more stable.

If we consider the CPU times of each method in all the examples, we can see that Tau method with Legendre-Phi and the collocation method with Legendre-Phi used shortest times.

If we compare in the sense of iterative methods used in nonlinear problems, the method with Newton iteration reduces the number of iterations in each interval by half. The method converges to the solution faster for a highly nonlinear problem. However, it takes up more CPU times than the regular spectral methods due to matrix multiplications.

The condition numbers of matrices for each method on [0,1] are shown in the following table.

size	Guo-Wang(A)	Tau with L-Phi(L.H.S.)	Phi	derivative of Phi(Legendre)
5×5	28.3386	9	42.5607	3.4141
10×10	116.9317	19	143.4796	5.2792
11×11	142.5557	21	170.3999	5.5894
12×12	170.8949	23	199.7876	5.8853
20×20	498.1924	39	517.6680	7.9122
50×50	3420	99	3036.2	13.1456

The condition numbers of the left-hand-side matrix A [31] obtained from recursive

relation of Guo-Wang method are large($\sim O(n^2)$) while the Legendre has the smallest condition number due to the orthogonality property. This may give the advantage to Tau and the collocation methods with Legendre-Phi compared with the left hand side matrix A from Guo-Wang.

The theoretical investigations for the stability, convergence on any time interval and symplectic preserving properties of the spectral methods are underway.

5.1 Extension to the Integral Equations of the Second Kind

General form of Integral equation of the second kind is [9, 2]

$$\lambda x(t) - \int_D K(t,s)x(s)ds = y(t), \quad t \in D, \lambda \neq 0$$

where D is closed and bounded set in $\Re^m$ for some $m \geq 1$ where

$K(t,s)$ is a Kernel function which is assumed to be absolutely integrable.

- If $y \neq 0$ and the λ are given, then the equation is called "nonhomogeneous problem"

- If $y = 0$, then it is an "eigenvalue problem". In this case, we seek for the eigenvalue λ, and corresponding eigenfunction x.

5.2 Spectral Collocation Method for the Integral Equations

For collocation method, we seek for a solution of the form

$$x_n(t) = \sum_{j=0}^{n} c_j \phi_j(t).$$

where $x_n \in \mathrm{X}_n$,a finite space $\mathrm{X}_n \subset \mathrm{X} = C(D)$, where $\mathrm{X}_n = \{\phi_0, \phi_1, ..., \phi_n\}$. Then solve for c_j. The solution is unique if $[\det(\phi_j(t_i))] \neq 0$.

Approximate form:

$$\lambda x_n(t) - \int_D K(t,s)x_n(s)ds = y(t)$$

Define the residual

$$r_n(t) = \lambda x_n(t) - \int_D K(t,s)x_n(s)ds - y(t).$$

Then

$$r_n(t) = \lambda \sum_{j=0}^{n} c_j\phi_j(t) - \int_D K(t,s) \sum_{j=0}^{n} c_j\phi_j(s)ds - y(t).$$

$$r_n(t) = \sum_{j=0}^{n} c_j\{\lambda\phi_j(t) - \int_D K(t,s)\phi_j(s)ds\} - y(t).$$

We apply the spectral collocation method for the Integral equations. For the collocation method, we require $r_n(t_i) = 0$ for each $t_0, t_1, ..., t_N \in D$, i.e

$$\sum_{j=0}^{N} c_j\{\lambda\phi_j(t_i) - \int_D K(t_i,s)\phi_j(s)ds\} - y(t_i) = 0 \tag{5.1.1}$$

for each $i = 0, ..., n$.

This equation is equivalent to the system of equation $A\boldsymbol{c} = B$ then we solve for $\boldsymbol{c}$.

Define a projection P_n:X $\rightarrow$ X_n such that

$$P_n x(t) = \sum_{j=0}^{n} \alpha_j\phi_j(t)$$

with the coefficient $\{\alpha_j\}_{j=0}^{n}$ determined by solving

$$x(t_i) = \sum_{j=0}^{n} \alpha_j\phi_j(t_i), \quad i = 0, ..., n.$$

Then (5.1.1) becomes $P_n r_n = 0$.

Note that $P_n z = 0$ iff $z(t_i) = 0, \quad i = 0, ..., n.$

5.2.1 Example of a Smooth Kernel

Consider some examples on a smooth domain[3, 39] .

Example 1: $\lambda x(t) - \int_0^1 e^{st}x(s)ds = y(t)$, $t \in [0,1]$

where $y(t) = \lambda e^t - \frac{1}{t+1}(e^{t+1} - 1)$ and $K(t,s) = e^{st}$.

The exact solution for this example is $x(t) = e^t$.

In this problem, we seek the solution x_n which is a linear combination of Legendre polynomials

$$x(t) = \sum_{j=0}^{n} c_j L_j(t).$$

Then $r(t_i) = 0$ implies

$$\lambda x_n(t_i) - \int_0^1 e^{st_i}x(s)ds - [\lambda e^{t_i} - \frac{1}{t_i+1}(e^{t_i+1} - 1)] = 0$$

$$\lambda x_n(t_i) - \int_0^1 e^{st_i}x(s)ds = [\lambda e^{t_i} - \frac{1}{t_i+1}(e^{t_i+1} - 1)]$$

$$\lambda \sum_{j=0}^{n} c_j L_j(t_i) - \int_0^1 e^{st_i} \sum_{j=0}^{n} c_j L_j(s)ds = [\lambda e^{t_i} - \frac{1}{t_i+1}(e^{t_i+1} - 1)]$$

$$\sum_{j=0}^{n} c_j[\lambda L_j(t_i)] - \sum_{j=0}^{n} c_j[\int_0^1 e^{st_i} L_j(s)ds] = [\lambda e^{t_i} - \frac{1}{t_i+1}(e^{t_i+1} - 1)]$$

$$\sum_{j=0}^{n} c_j\{[\lambda L_j(t_i)] - [\int_0^1 e^{st_i} L_j(s)ds]\} = [\lambda e^{t_i} - \frac{1}{t_i+1}(e^{t_i+1} - 1)]$$

for each $i = 0, ..., n$ and $0 < t_0 < t_1 < ... < t_n < 1$(Use $n+1$ Gaussian points). The equation becomes the system

$$(\lambda L - A)c = B$$

where

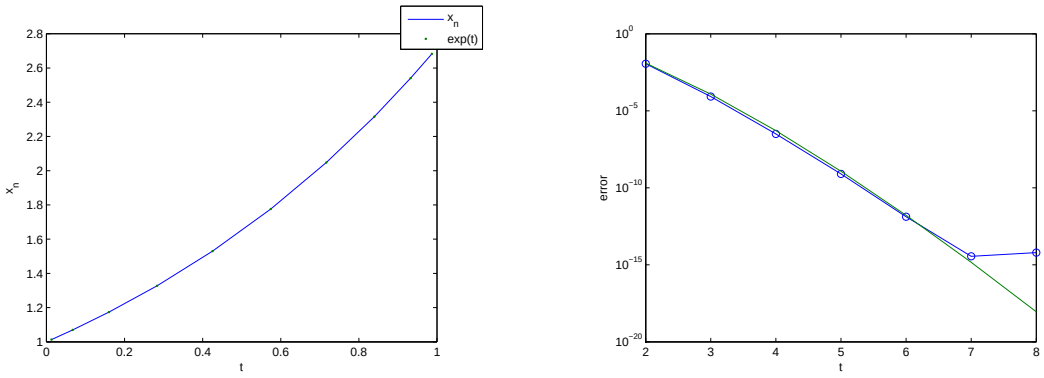

Figure 38: (a) Graph of the numerical solution x_n(dash line) compared with the exact solution e^t (b) Graph of p and $\max(|(x - x_n)(t_i)|)$ when $\lambda = 1$(blue with o-) and p and $\frac{2}{\sqrt{2(n+1)}}(\frac{e}{2(n+2)})^{2.7n}$.

$$L = \begin{pmatrix} L_0(t_0) & L_1(t_0) & \dots & L_n(t_0) \\ L_0(t_1) & L_1(t_1) & \dots & L_n(t_1) \\ \vdots & \vdots & \ddots & \vdots \\ L_0(t_n) & L_1(t_n) & \dots & L_n(t_n) \end{pmatrix}, A = \begin{pmatrix} A_{00} & A_{01} & \dots & A_{0n} \\ A_{10} & A_{11} & \dots & A_{1n} \\ \vdots & \vdots & \ddots & \vdots \\ A_{n0} & A_{n1} & \dots & A_{nn} \end{pmatrix}.$$

where $A_{ij} \approx \int_0^1 e^{st_i} L_j(s)ds$.

$$\int_0^1 e^{st_i} L_j(s)ds \approx \sum_{k=0}^{n} w_k e^{t_k t_i} L_j(t_k) = A_{ij}$$

$$A_{ij} = (w_0, w_1, ..., w_k) * \begin{pmatrix} e^{t_0 t_i} L_j(t_0) & \dots & e^{t_n t_i} L_j(t_n) \end{pmatrix}^T$$

Based on the theory, the error from the Nyström-Trapezoidal method [2] is of order $O(h^2)$. The spectral collocation method gives the error approximately of order $O(\frac{2}{\sqrt{2(n+1)}}(\frac{e}{2(n+2)})^{2.7n})$.

5.2.2 Examples of C^1-Kernels

Example 2:[3], Page 171,

$$\lambda x(t) - \int_0^1 K(t,s)x(s)ds = 0 \quad , \quad t \in [0,1]$$

where $K(t,s) = \begin{cases} \frac{1}{2}t(2-s), 0 \le t \le s \le 1 \\ \frac{1}{2}s(2-t), 0 \le s \le t \le 1 \end{cases}$.

This kernel is symmetric with $K(t,s) = K(s,t)$. Notice that it is a green function of the ODE:

$$\lambda x''(t) + 0.5x(t) = 0.$$

$$\int_0^1 K(t,s)x(s)ds = \lambda x(t)$$

$$\frac{d}{dt}\int_0^1 K(t,s)x(s)ds = \lambda x'(t)$$

$$\frac{d}{dt}[\int_0^t s(1-0.5t)x(s)ds + \int_t^1 s(1-0.5t)x(s)ds] = \lambda x'(t)$$

$$-0.5x(t) = \lambda x''(t), \quad t \in [0,1]$$

$$\lambda x''(t) + 0.5x(t) = 0, \quad t \in [0,1].$$

We know that the solution of this equation is analytic on the domain $[0,1]$. We can apply the collocation method to this problem i.e. the solution $x(t)$ can be expanded by using a family of orthogonal functions. Repeat the procedure as in Example 1 but with 2(n+1) nodes along integration line $t = t^*$, t^* is to be chosen on the line $s = t$. If we use only n+1 node across the line of discontinuity,$s = t$, we would get the error $|\lambda - \lambda_h| \sim O(\frac{1}{n^2})$ as shown in Figure 39.

The exact eigenvalues for this equation are the roots of the equation

$$\frac{1}{\lambda} + \tan(\frac{1}{\lambda}) = 0.$$

We can obtain this by Mathematica program (FindRoot command, approximate solutions which is exact up to 16 digits). The first largest three eigenvalues are

0.24296268509503405, 0.04142614984032116, and 0.01570867161341755.

The exact eigenfunctions are $\sin(\frac{t}{\lambda})$.

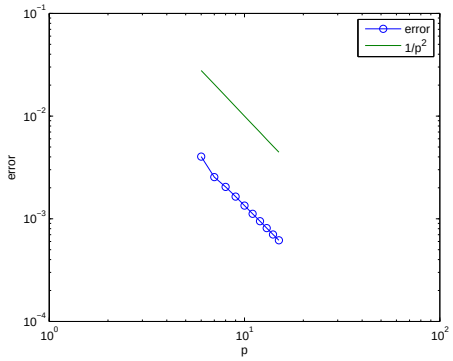

Figure 39: Graph of n and $|\lambda - \lambda_h|$ for the first eigenvalue(blue with o-) and n and $\frac{1}{n^2}$.

By using $n+1$ points for $s < t^*$ and $n+1$ pints for $s > t^*$, we got error $|\lambda - \lambda_h| \sim O(\frac{1}{\sqrt{n}}(\frac{eM}{2n+0.5})^{2.5n+3})$

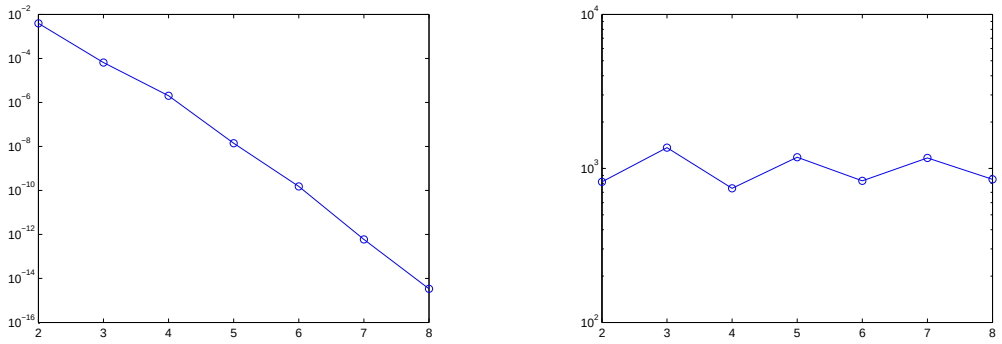

Figure 40: (a) Graph of p and $|\lambda - \lambda_h|$ for the first eigenvalue (b) Graph of $\frac{1}{\sqrt{n}}(\frac{eM}{2n+0.5})^{2.5n+3}$ over $|\lambda - \lambda_h|$ for the first eigenvalue.

5.2.3 Singular Equations

$$x(t) - \lambda \int_D K(t,s)x(s)ds = f(t), \quad t \in D$$

Singularities due to lack of analyticity in an integral equation.[2, 9]

There are 3 different types of singular integral equations.

1. Equations with semi-infinite or infinite ranges.

2. Equations with discontinuous derivative in either the kernel or the free term $K(t,s)$ or $f(t) \in C$ but does not belong to C^1.

3. Equations with either infinite or nonexisting derivative of some finite order.

Singular equations arise in areas of potential problems, Dirichlet problems, radiative equilibrium for example. We will consider singularities in Linear equations as follows:

I. The case of jump singularities

• The functions $K(t,s)$ and $f(t)$ are piecewise continuous with jump discontinuities only along the lines parallel to the coordinate axes as shown in Figure 41.

• In this case, the integral equations can be reformulated in a similar way as the original equation.

II. The case that $f(t)$ is badly behaved

In this case bad behavior will propagate from $f(t)$ to the solution $x(t)$. We remove the singularities by setting

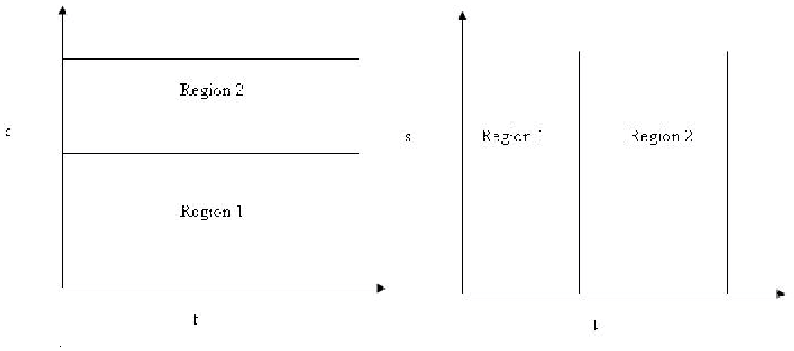

Figure 41: Sketches of the jump discontinuities along the lines parallel to the coordinate axes.

(a) $\quad x(t) = \psi(t) + f(t)$

Then the integral equation becomes

$$\psi(t) + f(t) - \lambda \int_D K(t,s)(\psi(s) + f(s))ds = f(t)$$

$$\psi(t) = \lambda \int_D K(t,s)\psi(s)ds + \lambda \int_D K(t,s)f(s)ds$$

and solve for $\psi(t)$

(b) $\quad x(t) = \psi(t) + \gamma(t)$

such that $f(t) - \gamma(t)$ is well-behaved and $\gamma(t)$ has the bad characteristics of $f(t)$ that are propagated to $x(t)$. Then the integral equation becomes

$$\psi(t) + \gamma(t) - \lambda \int_D K(t,s)(\psi(s) + \gamma(s))ds = f(t)$$

$$\psi(t) = [f(t) - \gamma(t)] + \lambda \int_D K(t,s)\psi(s)ds + \lambda \int_D K(t,s)\gamma(s)ds$$

and solve for $\psi(t)$(use quadrature rule).

Note that in both setting, we need $\int_D K(t,s)\psi(s)ds$ and $\int_D K(t,s)\gamma(s)ds$ to be smooth.

III. The case that $f(t)$ has discontinuous derivatives

In this case, a high-order accuracy from a quadrature rule may not generally be obtained since a bad behavior of $f(t)$ may affect $x(t)$.

IV. $K(t,s)$ is discontinuous along a line parallel to the s-axis pass onto the solution $x(t)$,

$$K(t,s) = \frac{g(t,s)}{|t-t_1|^\alpha}, \qquad 0 < \alpha < 1, t_1 \in D.$$

and g is a continuous function.

• We cannot use quadrature method or collocation (h-version) but might be able to use Galerkin method.

• We use product-integration or modification method since kernel is unbounded at $t = t_1$,

$$K(t,s) = \frac{g(t,s)}{|s-s_1|^\alpha}, \qquad 0 \leq \alpha < 1.$$

• Use product-integration or expansion method with orthogonal polynomial.

IV. $k(t,s)$ is weakly singular with the form

$$K(t,s) = \frac{g(t,s)}{|t-s|^\alpha}, \qquad 0 < \alpha < 1,$$

and g is continuous on D having singularity along $t = s$.

• It is sometimes possible to reformulate the equation so that $K(t,s)$ becomes at least continuous. • If $K(t,s)$ is of the form with $0 < \alpha < \frac{1}{2}$, $f \in C[a,b]$ then the second iterated kernel $K_2(t,s)$ is bounded and continuous.

Example 3:[39],Page 47, [3], Page 214.

$$\lambda x(t) - \int_0^1 K(t,s)x(s)ds = 0 \quad , \quad t \in [0,1]$$

where $K(t,s) = \begin{cases} t, 0 \le t \le s \le 1 \\ \\ s, 0 \le s \le t \le 1 \end{cases}$.

i.e., $K(t,s) = K(s,t)$.

Notice that this Kernel is a green function of the ODE: $\lambda x''(t) + x(t) = 0$.

$$\int_0^1 K(t,s)x(s)ds = \lambda x(t)$$

$$\frac{d}{dt}[\int_0^t sx(s)ds + \int_t^1 tx(s)ds] = \lambda x'(t)$$

$$-x(t) = \lambda x''(t), \quad t \in [0,1]$$

$$\lambda x''(t) + x(t) = 0, \quad t \in [0,1]$$

This equation has an analytic solution. We use the spectral method to approximate the numerical solution for this integral equation. The exact solution for the first eigenvalue is $\frac{4}{\pi^2}$ with the corresponding eigenfunction $\varphi(x) = \alpha \sin(\frac{1}{2}\pi x)$.

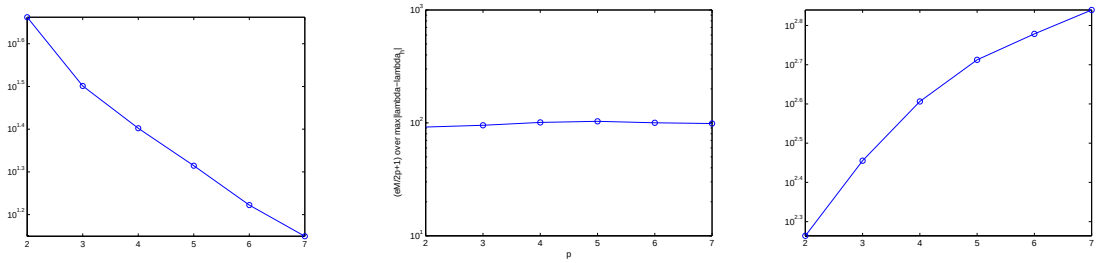

(a) (b) (c)

Figure 42: Graph of n versus $g = (\frac{1}{n})(\frac{eM}{2n+1})^{2.5n+1.8}$ over $\max(\lambda - \lambda_h)$ where $M = \frac{1}{2}$(a) $\frac{1}{n}g$ / $\max(\lambda - \lambda_h)$,(b) g / $\max(\lambda - \lambda_h)$ (c) $n \cdot g$ / $\max(\lambda - \lambda_h)$

From the Figure 42, we can conclude that the maximum error for the first eigenvalue is in the order $\sim O((\frac{1}{n})(\frac{eM}{2n+1})^{2.5n+1.8})$.

Example 4:

$$x(t) + \int_0^1 \sqrt{ts}x(s)ds = \sqrt{t}, \quad 0 \leq t \leq 1.$$

The exact solution is $x(t) = \frac{2\sqrt{t}}{3}$.

• Without knowing the exact solution, if we look at a kernel function for this problem $K(t,s) = \sqrt{ts}$, the first derivative of this kernel is unbounded at $t = 0$. Kernel has a discontinuous and unbounded first derivative on the domain.

• A solution for this problem is $x(t) = \frac{2\sqrt{t}}{3}$ which has a singularity at $t = 0$. This solution has an unbounded first derivative and so on. As a result, this solution is not analytic so the collocation would not give a good result.

• If we transform it into the ODE, we get the ODE as follows:

$$x(t) + \int_0^1 \sqrt{ts}x(s)ds = \sqrt{t}$$

$$x'(t) + \frac{d}{dt}[\int_0^1 \sqrt{ts}x(s)ds] = \frac{1}{2\sqrt{t}}$$

$$-\frac{1}{4}[\int_0^1 \frac{\sqrt{s}}{t^{\frac{3}{2}}}x(s)ds] = -\frac{1}{4t^{\frac{3}{2}}} - x''(t)$$

$$-\frac{1}{4t^2}[\sqrt{t} - x(t)] = -\frac{1}{4t^{\frac{3}{2}}} - x''(t)$$

$$x''(t) + \frac{x(t)}{4t^2} = 0$$

From here we can see clearly that there is a singularity at t=0 and a solution for this ODE is $x(t) = \frac{2\sqrt{t}}{3}$.

It turns out that the error is of order $O(\frac{1}{n^4})$.

We first try to obtain a numerical solution by using a regular spectral collocation. The result is shown in Figure 43 with the convergence rate of order $O(\frac{1}{n^{5/2}})$. Since the solution has a problem around $t = 0$ and the derivative is unbounded at $t = 0$, we increase the number of nodes near $t = 0$. We use $n + 1$ Gaussian nodes for the numerical integration and use $n + 1$ Gaussian nodes for the rest of the domain. The result is shown in Figure 5 with the convergence rate of order $O(\frac{1}{n^4})$. The last one is using both techniques. We rewrite equation and then rediscretize the quadrature nodes. The result is shown in Figure 6 with the convergence rate of order $O(\frac{1}{n^4})$.

This shows the rediscretization quadrature node technique is better than the other techniques used.

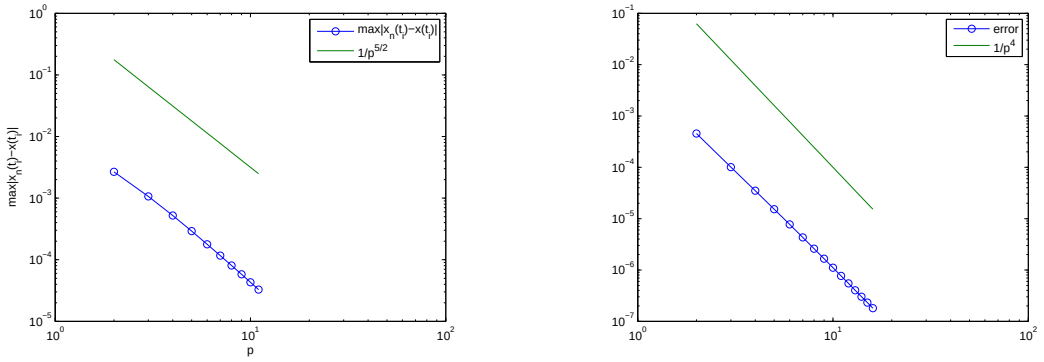

Figure 43: (a) Graph of n versus error $\max|x_n(t_i) - x(t_i)|$ for $i = 0, \ldots, p$ (in blue) and Graph of n versus $\frac{1}{n^{2.5}}$ (in green) and (b)Graph of n versus error $\max|x_n(t_i) - x(t_i)|$ for $i = 0, \ldots, n$ (in blue) and Graph of n versus $\frac{1}{n^4}$ (in green).

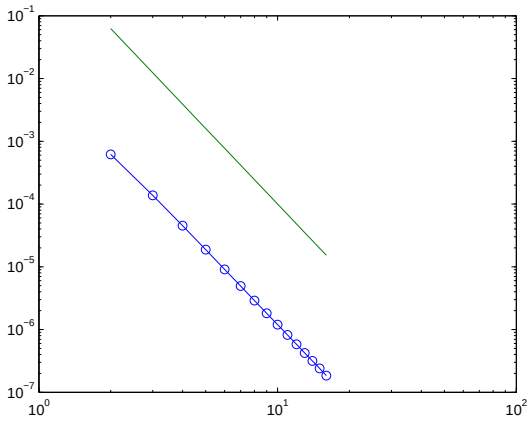

Figure 44: Graph of n versus error $\max|x_n(t_i) - x(t_i)|$ for $i = 0, \ldots, n$ (in blue) and Graph of n versus $\frac{1}{n^4}$ (in green).

Example 5:

$$\lambda x(t) - \int_0^1 K(t,s)x(s)ds = 0 \quad , \quad t \in [0,1]$$

where $K(t,s) = \begin{cases} -\sqrt{ts}\ln(s), t \leq s \\ -\sqrt{ts}\ln(t), s \leq t \end{cases}$.

The Kernel has unbounded first derivative and has discontinuity along line $s = t$ and the Kernel itself is unbounded at $t = 0$. Without using technique, we get the convergence rate of order $O(\frac{1}{n^4})$.

We tried the same method as mentioned previously by using $n+1$ Gaussian nodes when $s < t$ and $n+1$ Gaussian nodes when $s < t$ for the numerical integration. Then we reduce the effect of discontinuity on the solution $x(t)$ by setting

$$x(t)\left[\lambda - \int_a^b K(t,s)ds\right] - \int_a^b K(t,s)[x(s) - x(t)]ds = 0$$

$$x(t)\left[\int_a^b K(t,s)ds\right] + \int_a^b K(t,s)[x(s) - x(t)]ds = \lambda x(t)$$

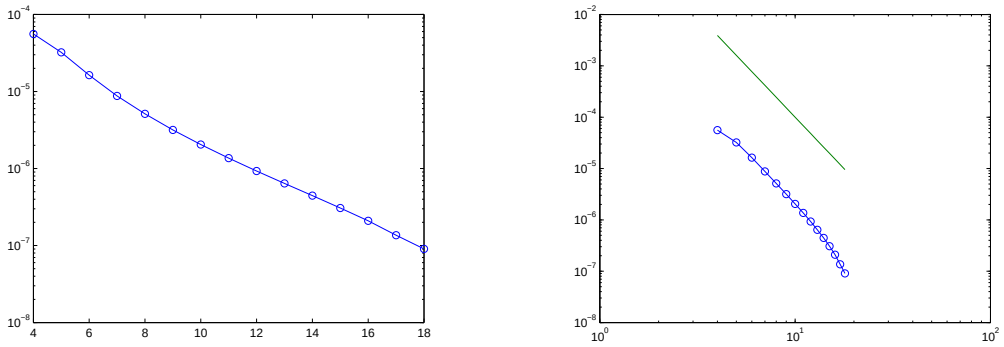

Figure 45: (a) Graph of p versus the error $|\lambda - \lambda_n|$ (b) Graph of n versus error $max|x_n(t_i) - x(t_i)|$ for $i = 0, \ldots, n$ (in blue) and Graph of n versus $\frac{1}{n^4}$ (in green).

$$x(t)[A(t) - \sum_{k=0}^{n} K(t, t_k)w_k] + \sum_{k=0}^{n} K(t, t_k)w_k x(t_k) = \lambda x(t).$$

$$A(t) = \int_0^1 K(t,s)ds = \int_0^t -\sqrt{ts}ln(t)ds + \int_t^1 -\sqrt{ts}ln(s)ds = \frac{4}{9}\sqrt{t} - \frac{4}{9}t^2$$

We seek for $x_n(t) = \sum_{j=0}^{n} c_j L_k(t)$ then the equation becomes

$$\sum_{j=0}^{n} c_j\{L_k(t_i)[A(t_i) - \sum_{k=0}^{n} K(t_i, t_k)w_k] + \sum_{k=0}^{n} K(t_i, t_k)w_k L_{k-1}(t_k)\} = \lambda \sum_{j=0}^{n} c_j L_k(t_i), i = 0, ..., n$$

In matrix notation,

$$Bc = \lambda Dc$$

where

$$B = [b_{ij}]_{(n+1)x(n+1)}, b_{ij} = L_j(t_i)[A(t_i) - \sum_{k=0}^{n} K(t_i, t_k)w_k] + \sum_{k=0}^{n} K(t_i, t_k)w_k L_k(t_k)$$

$$c = [c_0, c_1, c_2, ..., c_n]^T, D = [d_{ij}] = [L_j(t_i)].$$

We will solve for eigenvalue λ and corresponding eigenfunction. This is a general-

ized eigenvalue problem. From our numerical solution, the convergence rate of $|\lambda_n - \lambda|$ is of order $(e/n)^{ln(n)}$. Figure 46 shows n versus error $|\lambda_n - \lambda|$ when $n = 4, ..., 19$ (in blue) and p versus $(e/n)^{ln(n)}$ (in green) on the same graph. In this figure we can see that both graphs are of the same shape. This is slightly better than the rate shown in Figure 45, using only $n+1$ Gaussian nodes when $s < t$ and $n+1$ Gaussian nodes when $s > t$ for the numerical integration, and without reducing the effect of discontinuity of the kernel on the solution.

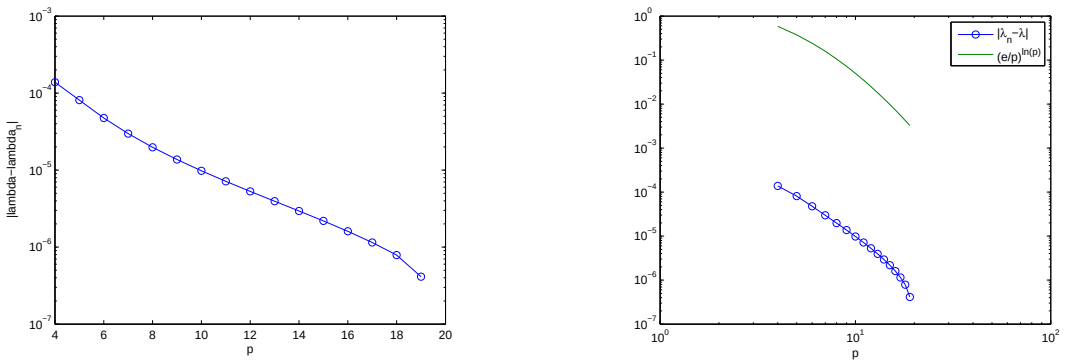

Figure 46: (a) Graph of n versus error $|\lambda_n - \lambda|$ when $n = 4, ..., 19$ (b) Graph of n versus error $|\lambda_n - \lambda|$ when $n = 4, ..., 19$ (in blue) and Graph of n versus $(e/n)^{ln(n)}$ (in green).

Example 6: Love's Equation $(d = -1, \lambda = 1)$

$$x(t) - \frac{1}{\pi}\int_{-1}^{1} \frac{1}{1+(t-s)^2} x(s)ds = f(t)$$

In this case, $K(t,s) = \frac{1}{\pi}\frac{1}{1+(t-s)^2}$. We apply the same technique as in Example 5 together with the collocation method. The general form of the integral equation

can be rewritten as

$$x(t)\left[1-\lambda\int_a^b K(t,s)ds\right]-\lambda\int_a^b K(t,s)[x(s)-x(t)]ds=f(t)$$

$$x(t)\left[1-\lambda\sum_{k=0}^{n}K(t,t_k)w_k\right]-\lambda\sum_{k=0}^{n}K(t,t_k)w_k[x(t_k)-x(t)]=f(t),$$

where $t_0 \leq t_1 \leq t_2 \leq, ..., t_k$ are quadrature nodes, to reduce the effect of the singularity of $K(t,s)$ (along $t=s$) on $x(t)$. The first sum and first term of the second sum cancel out. The remaining integrand is still $K(t,s)x(s)$.

However, this technique works well only in the case that $\int_a^b K(t,s)ds$ can be obtained analytically. It does not make much difference in the case that $\int_a^b K(t,s)ds$ is computed numerically because the first integration term cancel out with the second integration term(they both use the same quadrature rule).

But if $\int_a^b K(t,s)ds = A(t)$(can be obtain analytically), then the equation becomes

$$x(t)[1-\lambda A(t)+\lambda\sum_{k=0}^{n}K(t,t_k)w_k]-\lambda\sum_{k=0}^{n}K(t,t_k)w_kx(t_k)=f(t).$$

Apply the collocation method with the Legendre expansion and Gaussian nodes $-1<t_0<t_1<t_2<...<t_n<1$ and $x_n(t)=\sum_{j=0}^{n}c_jL_k(t)$. Equation becomes

$$\sum_{j=0}^{n}c_j\{L_k(t_i)[1-\lambda A(t_i)+\lambda\sum_{k=0}^{n}K(t_i,t_k)w_k]-\lambda\sum_{k=0}^{n}K(t_i,t_k)w_kL_k(t_k)\}=f(t_i)$$

In matrix notation,

$$Bc=F$$

where

$$B=[b_{ij}]_{(n+1)x(n+1)}, b_{ij}=L_j(t_i)[1-\lambda A(t_i)+\lambda\sum_{k=0}^{n}K(t_i,t_k)w_k]-\lambda\sum_{k=0}^{n}K(t_i,t_k)w_kL_k(t_k)$$

$$c = (c_0, c_1, c_2, ..., c_n)^T, F = (f(t_0), f(t_1), f(t_2), ..., f(t_n))^T.$$

For this example, $K(t,s) = \frac{1}{\pi}\frac{1}{1+(t-s)^2}, f(t) = 1, \lambda = 1.$

It follows that

$$\begin{aligned} A(t) = \int_{-1}^{1} K(t,s)ds &= \int_{-1}^{1} \frac{1}{\pi}\frac{1}{1+(t-s)^2}ds = -\frac{1}{\pi}\int_{t+1}^{t-1} \frac{1}{1+u^2}du \\ A(t) &= \frac{1}{\pi}[\text{Arctan}(t+1) - \text{Arctan}(t-1)] \\ F = (1,1,...,1)^T \quad , \quad K(t_i,t_k) &= \frac{1}{\pi}\frac{1}{1+(t_i-t_k)^2} \end{aligned}$$

The numerical result shown below is the numerical value of x(t) when $t = 0$ and $n = 3, 5, ..., 19$(odd). The maximum pointwise error $\max|x_n(0) - x(0)|$ was computed with x(0) = 1.919031993126952 obtained from MATLAB when $n = 25$(i.e. $x_25(0)$). Figure 47 shows that the convergence rate is of order $(\frac{e}{n})^{0.8n}$ or closer. Note that we don't have the exact solution to compare with our numerical result but what we use is the numerical value when n is high.

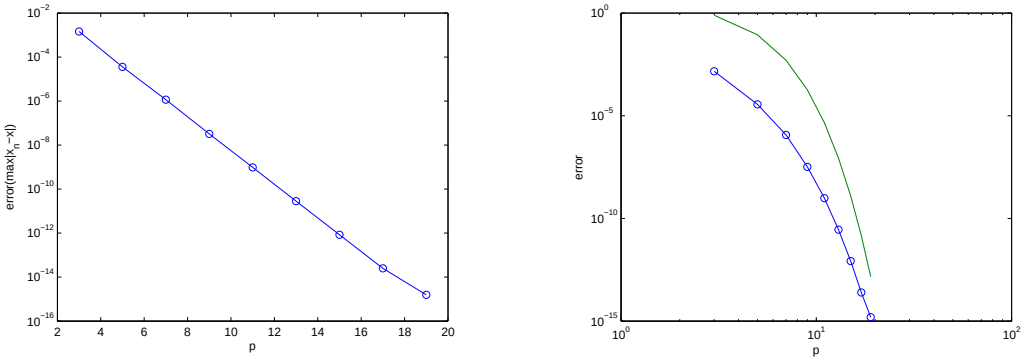

Figure 47: (a)Graph of n versus error $|x_n(0) - x(0)|$ when $n = 3, ..., 19$ (b) Graph of n versus error $|x_n(0) - x(0)|$ for $n = 3, \ldots, 19$ (in blue) and Graph of n versus $(e/n)^{0.8n}$ (in green).

Appendices

A Basic Theorems and Analysis

A1. The Fundamental Theorem of Calculus

From the Fundamental Theorem of Calculus

$$\int_t^T \frac{d}{dy}(E_N(y))^2 dy = E_N^2(T) - E_N^2(t)$$

$$\text{so} \quad 2\int_0^T E_N \cdot \frac{d}{dt} E_N dt = [E_N(T)]^2 - [E_N(0)]^2$$

$$(\frac{d}{dt}E_N, E_N) = \frac{1}{2}[E_N(T)]^2 - \frac{1}{2}[E_N(0)]^2$$

A2.Gronswall's Inequality[36], Page 36

If φ, α are real-valued functions and continuous on [a,b] , $t \in [a,b]$ with $\beta(t) \geq 0$ integrable on [a,b] and

$$\varphi(t) \leq \alpha(t) + \int_a^t \beta(s)\varphi(s)ds.$$

Then

$$\varphi(t) \leq \alpha(t) + \int_a^t \beta(s)\alpha(s)e^{\int_s^t \beta(u)du} ds.$$

In particular, if r_0 and k are constant and

$$\varphi(t) \leq r_0 + \int_a^t k\varphi(s)ds.$$

Then

$$\varphi(t) \leq r_0 e^{k(t-a)} \quad , \quad \forall t \in [a,b]$$

A3. Upper bound for maximum norm [17], Page 301

If $u : [0,T] \to X$ then

$$\max_{t\in[0,T]}\|u(t)\| \le C\|u\|_{W^{1,p}(0,T,X)},$$

For $p = 2$,$u \in W^{1,2}_{(0,T,X)} \Rightarrow u \in H^1_{(0,T)}$,

$$\begin{aligned}
\max_{t\in[0,T]}\|u(t)\| &\le C\|u\|_{W^{1,2}(0,T,X)} \\
\max_{t\in[0,T]}\|u(t)\| &\le C(\|u\|^2_{L^2(0,T)} + \|Du\|^2_{L^2(0,T)})^{\frac{1}{2}} \\
(\max_{t\in[0,T]}\|u(t)\|)^2 &\le C(\|u\|^2_{L^2(0,T)} + \|Du\|^2_{L^2(0,T)}) \\
\max_{t\in[0,T]}|u(t)|^2 &\le C(\|u\|^2_{L^2(0,T)} + \|\frac{du}{dt}\|^2_{L^2(0,T)})
\end{aligned}$$

A4.Shifted Chebyshev Polynomials on [0,T] [43, 44]

$$[a,b] \to [-1,1] \quad , \quad x = \frac{2t-a-b}{b-a}$$
$$[-1,1] \to [a,b] \quad , \quad t = \frac{(b-a)x+a+b}{2}$$

Chebyshev polynomials of the first kind: $\hat{T}_n$ on [0,T] and T_n on [-1,1]

$$\hat{T}_n(t) = T_n(\frac{2t-T}{T}) = T_n(x) \ , \ T_n(\theta) = \cos(n\theta), x = \cos(\theta).$$

$$\begin{aligned}
(\hat{T}_i, \hat{T}_j)_{\hat{\omega}} &= \int_0^T \hat{T}_i(t)\hat{T}_j(t)\frac{1}{\sqrt{tT-t^2}}dt \\
&= \int_0^T \hat{T}_i(t)\hat{T}_j(t)\frac{T}{\sqrt{T^2-4t^2+4tT-T^2}}\frac{2}{T}dt \\
&= \int_0^T \hat{T}_i(t)\hat{T}_j(t)\frac{1}{\sqrt{1-(\frac{2t-T}{T})^2}}\frac{2}{T}dt \\
&= \int_{-1}^1 T_i(x)T_j(x)\frac{1}{\sqrt{1-x^2}}dx
\end{aligned}$$

$$
\begin{aligned}
(\hat{T}_i, \hat{T}_j)_{\hat{\omega}} &= (T_i, T_j)_{\omega} \\
&= \begin{cases} \pi \ , \ n = 0 \\ \\ \frac{\pi}{2} \ , \ n \geq 1 \end{cases}
\end{aligned}
$$

where $\hat{\omega} = \frac{1}{\sqrt{tT - t^2}}$ is the weight corresponding to $\hat{T}_n$ on $[0, T]$

$$
\begin{aligned}
(\hat{T}_i', \hat{T}_j')_{\hat{\omega}} &= \int_0^T \hat{T}_i'(t)\hat{T}_j'(t)\frac{1}{\sqrt{tT - t^2}}dt \\
&= \frac{4}{T^2}\int_{-1}^{1} T_i'(x)T_j'(x)\frac{1}{\sqrt{1 - x^2}}dx \\
&= \frac{4}{T^2}\int_{\pi}^{0} \frac{\frac{-i\sin(i\theta)}{-\sin(\theta)}\frac{-j\sin(j\theta)}{-\sin(\theta)}}{\sin(\theta)} - \sin(\theta)d\theta \\
&= \frac{4}{T^2}ij\int_0^{\pi} \frac{\sin(i\theta)\sin(j\theta)}{\sin^2(\theta)}d\theta \\
&= \begin{cases} \frac{4}{T^2}\pi j^3 \ , \ i = j \geq 1 \\ \\ 0 \ , \ i \neq j \end{cases}
\end{aligned}
$$

Chebyshev polynomials of the second kind: $\hat{U}_n$ on [0,T] and U_n on [-1,1]

$$
\hat{U}_n(t) = U_n(\frac{2t - T}{T}) = U_n(x) \ , \ U_n(\theta) = \frac{\sin((n+1)\theta)}{\sin(\theta)}, x = \cos(\theta).
$$

$$
\begin{aligned}
(\hat{U}_i, \hat{U}_j)_{\tilde{\omega}} &= \int_0^T \hat{U}_i(t)\hat{U}_j(t)\frac{4}{T^2}\sqrt{tT - t^2}dt \\
&= \int_0^T \hat{U}_i(t)\hat{U}_j(t)\frac{\sqrt{T^2 - 4t^2 + 4tT - T^2}}{T}\frac{2}{T}dt \\
&= \int_0^T \hat{U}_i(t)\hat{U}_j(t)\sqrt{1 - (\frac{2t - T}{T})^2}\frac{2}{T}dt \\
&= \int_{-1}^{1} U_i(x)U_j(x)\sqrt{1 - x^2}dx
\end{aligned}
$$

where $\tilde{\omega} = \frac{4}{T^2}\sqrt{tT - t^2}$ is the weight corresponding to $\hat{T}_n$ on $[0, T]$

A5. Projection Error [54, 55, 37, 43]

A5.1 Projection Error on [0,T]

Consider the expansion

$$p(t) = \sum_{k=0}^{\infty} p_k \hat{T}_k(t) \quad , \quad q(t) = \sum_{k=0}^{\infty} q_k \hat{T}_k(t)$$

We design $\Pi_N p(t) = \sum_{k=0}^{N} p_k \hat{T}_k(t)$ so that $(p - \Pi_N p, \hat{T}_m) = 0 \quad , \quad m = 0, ..., N.$

$$p - \Pi_N p = \sum_{k=N+1}^{\infty} p_k \hat{T}_k(t) \quad , \quad q - \Pi_N q = \sum_{k=N+1}^{\infty} q_k \hat{T}_k(t).$$

With this projection we have

$$(p - \Pi_N p, \hat{T}_m)_{\hat{\omega},T} = 0 \quad \text{for} \quad m = 0, ..., N$$

$$\|p - \Pi_N p\|^2_{\hat{\omega},T} = \sum_{k=N+1}^{\infty} p_k^2 \frac{\pi}{2} \ , \ \|q - \Pi_N p\|^2_{\hat{\omega},T} = \sum_{k=N+1}^{\infty} q_k^2 \frac{\pi}{2}$$

Consider the coefficient for $k \geq 1$, [44] page 71.

$$\begin{aligned} p_k &= \frac{2}{\pi} \int_0^T p(t) \hat{T}_k(t) \frac{1}{\sqrt{tT - t^2}} dt = \frac{2}{\pi} \int_{-1}^{1} \hat{p}(x) T_k(x) \frac{1}{\sqrt{1 - x^2}} dx \\ &= \frac{2^{k+1} k!}{\pi (2k)!} \int_{-1}^{1} \hat{p}^{(k)}(x) (1 - x^2)^{k - \frac{1}{2}} dx \\ &= \frac{2^{k+1} k!}{\pi (2k)!} \left(\frac{T}{2}\right)^k p^{(k)}(\xi_k) \frac{\pi (2k)!}{2^{2k} (k!)^2} \quad , \quad \xi_k \in (0, T) \\ p_k &= \frac{1}{2^{2k-1} (k!)} \left(\frac{T}{2}\right)^k p^{(k)}(\xi_k) \end{aligned}$$

$$\begin{aligned} \|p - \Pi_N p\|^2_{\hat{\omega},T} &= \frac{\pi}{2} \sum_{k=N+1}^{\infty} \left(\frac{1}{2^{2k-1} k!} \left(\frac{T}{2}\right)^k p^{(k)}(\xi_k) \right)^2 \\ &\leq \frac{\pi}{2} \sum_{k=N+1}^{\infty} \left(\frac{1}{2^{2k-1} k!} \left(\frac{T}{2}\right)^k c M^k \right)^2 \\ &\leq 4\pi c^2 \sum_{k=N+1}^{\infty} \left(\frac{1}{2^{3k} k!} T^k M^k \right)^2 \end{aligned}$$

$$\begin{aligned}\|p-\Pi_N p\|^2_{\hat{\omega},T} &= 4\pi c^2\Big[\frac{T^{2(N+1)}M^{2(N+1)}}{2^{6(N+1)}(N+1)!^2}+\frac{T^{2(N+2)}M^{2(N+2)}}{2^{6(N+2)}(N+2)!^2}+\dots\Big]\\ &= 4\pi c^2\Big(\frac{T^{N+1}M^{N+1}}{2^{3(N+1)}(N+1)!}\Big)^2\Big[1+\frac{T^2M^2}{2^4(N+2)^2}+\frac{T^4M^4}{2^8(N+3)^2(N+2)^2}+\dots\Big]\end{aligned}$$

Choose N such that $\frac{T^2M^2}{2^3(N+2)^2}<1$. Then

$$\begin{aligned}\|p-\Pi_N p\|^2_{\hat{\omega},T} &\le 4\pi c^2\Big(\frac{T^{N+1}M^{N+1}}{2^{3(N+1)}(N+1)!}\Big)^2\Big[1+\frac{1}{2}+\frac{1}{2^2}+\dots\Big]\\ &= 8\pi c^2\Big(\frac{T^{N+1}M^{N+1}}{2^{3(N+1)}(N+1)!}\Big)^2\end{aligned}$$

Use Stirling's formula: $n!\approx\left(\frac{n}{e}\right)^n\sqrt{2\pi n}$. In fact, $\frac{1}{n!}<\left(\frac{e}{n}\right)^n\frac{1}{\sqrt{2\pi n}}$

$$\begin{aligned}\|p-\Pi_N p\|^2_{\hat{\omega},T} &\le 8\pi c^2\Big(\frac{T^{N+1}M^{N+1}}{2^{3(N+1)}}\Big)^2\Big(\frac{e}{N+1}\Big)^{2(N+1)}\Big(\frac{1}{\sqrt{2\pi(N+1)}}\Big)^2\\ &= \frac{2c^2}{N+1}\Big(\frac{TMe}{8(N+1)}\Big)^{2(N+1)}\\ \|p-\Pi_N p\| &\le \frac{\sqrt{2}c}{\sqrt{N+1}}\Big(\frac{eTM}{8(N+1)}\Big)^{(N+1)}\end{aligned}$$

Similarly,

$$\|q-\Pi_N q\|\le\frac{\sqrt{2}c}{\sqrt{N+1}}\Big(\frac{eTR}{8(N+1)}\Big)^{(N+1)}$$

A5.2 Projection Error on [0,T]

$$p-\Pi_N p=\sum_{k=N+1}^{\infty}p_k\hat{T}_k(t)\quad,\quad q-\Pi_N q=\sum_{k=N+1}^{\infty}q_k\hat{T}_k(t).$$

$$\frac{d}{dt}(p-\Pi_N p)=\sum_{k=N+1}^{\infty}p_k\hat{T}_k'(t)\quad,\quad\frac{d}{dt}(q-\Pi_N q)=\sum_{k=N+1}^{\infty}q_k\hat{T}_k'(t).$$

Then

$$\begin{aligned}\|\frac{d}{dt}(p-\Pi_N p)\|^2_{\hat{\omega},T} &= (\sum_{k=N+1}^{\infty}p_k\hat{T}_k',\sum_{j=N+1}^{\infty}p_j\hat{T}_j')_{\hat{\omega}}\\ &= \sum_{k=N+1}^{\infty}p_k^2\frac{4}{T^2}\pi k^3\\ &= \frac{4}{T^2}\pi\sum_{k=N+1}^{\infty}k^3\Big(\frac{1}{2^{2k-1}k!}\Big(\frac{T}{2}\Big)^k p^{(k)}(\xi_k)\Big)^2\quad,\quad\xi_k\in(0,T)\end{aligned}$$

$$\begin{aligned}\|\frac{d}{dt}(p-\Pi_N p)\|^2_{\hat{\omega},T} &\leq \frac{4\pi c^2}{T^2}\sum_{k=N+1}^{\infty} k^3\Big(\frac{1}{2^{2k-1}k!}\Big(\frac{T}{2}\Big)^k M^k\Big)^2 \\ &= \frac{16\pi c^2}{T^2}\sum_{k=N+1}^{\infty}\Big(\frac{\sqrt{k}T^kM^k}{2^{3k}(k-1)!}\Big)^2\end{aligned}$$

By Stirling's formula, $\frac{1}{n!} < \Big(\frac{e}{n}\Big)^n \frac{1}{\sqrt{2\pi n}}$ so $\frac{\sqrt{n}}{(n-1)!} < \frac{n}{\sqrt{2\pi}}\Big(\frac{e}{n}\Big)^n$.

$$\begin{aligned}\|\frac{d}{dt}(p-\Pi_N p)\|^2_{\hat{\omega},T} &\leq \frac{16\pi c^2}{T^2}\sum_{k=N+1}^{\infty}\Big(\frac{kT^kM^k}{\sqrt{2\pi}2^{3k}}\Big(\frac{e}{k}\Big)^k\Big)^2 \\ &= \frac{8c^2e^2}{T^2}\sum_{k=N+1}^{\infty}\Big(\frac{T^kM^k}{2^{3k}}\Big(\frac{e}{k}\Big)^{k-1}\Big)^2 \\ &= \frac{8c^2e^2}{T^2}\Big(\frac{T^{N+1}M^{N+1}}{2^{3(N+1)}}\Big(\frac{e}{N+1}\Big)^N\Big)^2\Big[1+\frac{T^2M^2e^2}{2^4(N+2)^2}\Big(\frac{N+1}{N+2}\Big)^{2N} \\ &\quad +\frac{T^4M^4e^4}{2^8(N+3)^4}\Big(\frac{N+1}{N+3}\Big)^{2N}+\dots\Big]\end{aligned}$$

Choose N such that $\frac{T^2M^2e^2}{2^3(N+2)^2} < 1$. Then

$$\begin{aligned}\|\frac{d}{dt}(p-\Pi_N p)\|^2_{\hat{\omega},T} &\leq \frac{8c^2e^2}{T^2}\Big(\frac{T^{N+1}M^{N+1}}{8^{(N+1)}}\Big(\frac{e}{N+1}\Big)^N\Big)^2\Big[1+\frac{1}{2}+\frac{1}{2^2}+\dots\Big] \\ &= \frac{16c^2e^2}{T^2}\frac{T^2M^2}{4^2}\Big(\frac{TMe}{8(N+1)}\Big)^{2N} \\ \|\frac{d}{dt}(p-\Pi_N p)\|_{\hat{\omega},T} &\leq ceM\Big(\frac{TMe}{8(N+1)}\Big)^N\end{aligned}$$

Similarly,

$$\|\frac{d}{dt}(q-\Pi_N p)\|_{\hat{\omega},T} \leq ceM\Big(\frac{TRe}{8(N+1)}\Big)^N$$

A5.3 Projection Error on [0,T]

Consider the expansion

$$p(t)=\sum_{k=0}^{\infty}p_k\hat{T}_k(t) \quad , \quad \frac{d}{dt}p(t)=\sum_{k=1}^{\infty}p_k\hat{T}'_k(t)$$

By using the identity of the Jabobi polynomials [12]

$$\frac{dP_k^{(\alpha,\beta)}}{dx}=\frac{1}{2}(k+1+\alpha+\beta)P_{k-1}^{(\alpha+1,\beta+1)}$$

The relationship for the derivative of the Chebyshev polynomials of the first kind ($\alpha = \beta = -\frac{1}{2}$) and the Chebyshev polynomials of the second kind ($\alpha = \beta = \frac{1}{2}$) becomes

$$T'_{k+1}(x) = (k+1)U_k(x) \quad ; \quad \hat{T}'_{k+1}(t) = \frac{T}{2}(k+1)\hat{U}_k$$

$$p'(t) \;=\; \sum_{k=1}^{\infty} p_k \frac{T}{2} k \hat{U}_{k-1} = \sum_{k=0}^{\infty} \tilde{p}_k \hat{U}_k$$

where $\tilde{p}_k = p_{k+1}\frac{2}{T}(k+1) \quad , \quad k \geq 0.$

We define

$$\Pi_N p' = \sum_{k=0}^{N} \tilde{p}_k \hat{U}_k \quad \text{so} \qquad (p' - \Pi_N p', \hat{U}_m)_{\hat{\omega},T} = 0 \quad \text{for} \quad m = 0, ..., N.$$

$$p' - \Pi_N p' = \sum_{k=N+1}^{\infty} \tilde{p}_k \hat{U}_k \quad , \quad q' - \Pi_N q' = \sum_{k=N+1}^{\infty} \tilde{q}_k \hat{U}_k.$$

Then

$$\begin{aligned} \|p' - \Pi_N p'\|^2_{\hat{\omega},T} &= (\sum_{k=N+1}^{\infty} \tilde{p}_k \hat{U}_k, \sum_{k=N+1}^{\infty} \tilde{p}_k \hat{U}_k)_{\hat{\omega}} \\ &= \sum_{k=N+1}^{\infty} \tilde{p}_k^2 \frac{\pi}{2} \end{aligned}$$

We have from **A5.1** that

$$\begin{aligned} p_k &= \frac{1}{2^{2k-1}(k!)} \Big(\frac{T}{2}\Big)^k p^{(k)}(\xi_k) \;\; \text{so} \\ \|p' - \Pi_N p'\|^2_{\hat{\omega},T} &= \frac{\pi}{2} \sum_{k=N+1}^{\infty} \Big(\frac{2(k+1)}{T} \frac{1}{2^{2k+1}(k+1)!} \Big(\frac{T}{2}\Big)^{k+1} p^{(k+1)}(\xi_k) \Big)^2 \quad , \quad \xi_k \in (0,T) \\ &\leq \frac{\pi c^2 M}{8} \sum_{k=N+1}^{\infty} \Big(\frac{1}{2^{2k}k!} \Big(\frac{T}{2}\Big)^k M^k \Big)^2 \\ &= \frac{\pi c^2 M}{8} \sum_{k=N+1}^{\infty} \Big(\frac{TM}{8}\Big)^{2k} \frac{1}{k!^2} \|p' - \Pi_N p'\|^2_{\hat{\omega},T} \\ &= \frac{\pi c^2 M}{8} \Big(\frac{TM}{8}\Big)^{2(N+1)} \frac{1}{(N+1)!^2} [1 + \Big(\frac{TMe}{8(N+2)}\Big)^2 \\ &\quad + \Big(\frac{(TMe)^4}{8^4(N+2)^2(N+3)^2}\Big) + \dots \Big] \end{aligned}$$

Choose N such that $\frac{TMe}{8(N+2)} < \frac{1}{\sqrt{2}}$. Then

$$\begin{aligned} \|p' - \Pi_N p'\|^2_{\hat{\omega},T} &\leq \frac{\pi c^2 M}{8}\Big(\frac{TM}{8}\Big)^{2(N+1)} \frac{1}{(N+1)!^2}\Big[1+\frac{1}{2}+\frac{1}{2^2}+\dots\Big] \\ &= \frac{\pi c^2 M}{4}\Big(\frac{TM}{8}\Big)^{2(N+1)} \frac{1}{(N+1)!^2} \end{aligned}$$

By Stirling's formula, $\frac{1}{n!} < \Big(\frac{e}{n}\Big)^n \frac{1}{\sqrt{2\pi n}}$

$$\begin{aligned} \|p' - \Pi_N p'\|^2_{\hat{\omega},T} &\leq \frac{\pi c^2 M}{4}\Big(\frac{TM}{8}\Big)^{2(N+1)} \frac{1}{(N+1)!^2}\Big[1+\frac{1}{2}+\frac{1}{2^2}+\dots\Big] \\ &= \frac{\pi c^2 M}{4}\Big(\frac{TMe}{8(N+1)}\Big)^{2(N+1)} \frac{1}{(\sqrt{2\pi(N+1)})^2} \\ \|p' - \Pi_N p'\|_{\hat{\omega},T} &\leq \frac{cM}{2\sqrt{2}}\frac{1}{\sqrt{N+1}}\Big(\frac{TMe}{8(N+1)}\Big)^{(N+1)} \end{aligned}$$

Similarly,

$$\|q' - \Pi_N q'\|_{\hat{\omega},T} \leq \frac{cR}{2\sqrt{2}}\frac{1}{\sqrt{N+1}}\Big(\frac{TRe}{8(N+1)}\Big)^{(N+1)}$$

A6. Interpolation Error on [0,T]

Newton Divided Difference [15]: an interpolation at points $x_0, x_1, .., x_n$,i.e.

$p_n(x_0) = f(x_0), ..., p_n(x_n) = f(x_n)$,

$$p_n(x) = f(x_0) + \psi_0(x) f[x_0, x_1] + ... + \psi_{n-1}(x) f[x_0, x_1, ..., x_n]$$

where $\psi_n(x) = (x - x_0)...(x - x_n)$ (degree n+1) and

$f[x_0, x_1, ..., x_n] = a_n = \dfrac{f(x_n) - p_{n-1}(x_n)}{(x - x_0)...(x - x_{n-1})}$.

For any interpolation at $x_0, x_1, .., x_n, t$,i.e. $p_{n+1}(x_0) = f(x_0), ..., p_{n+1}(x_n) = f(x_n), p_{n+1}(t) = f(t)$,

$$p_{n+1}(t) - p_n(t) = f(t) - p_n(t) = (t - x_0)...(t - x_n) f[x_0, x_1, ..., x_n, t]$$

and we have

$$f[x_0, x_1, ..., x_n, t] = \frac{f^{(n+1)}(\xi)}{(n+1)!} \quad , \ \xi \in \mathcal{H}\{x_0, x_1, ..., x_n, t\}$$

(smallest interval containing $x_0, x_1, ..., x_n, t$).

On any interval $[a, b]$, the linear mapping from $[-1, 1] \rightarrow [a, b]$ resulting $C(\frac{h}{2})^{n+1}$ as an extra term for the transformation involving ψ_n.

A6.1 Interpolation Error of Legendre-Gauss-Lobatto points on [-1,1]

These are the points $-1 = \xi_0 < \xi_1 < ... < \xi_n = 1$ where ξ_i's , i=1,...,n-1 are zeros of Legendre polynomial $L'_n(x)$.

It follows that $(x - \xi_1)...(x - \xi_{n-1})$ are factors of $L'_n(x)$ and it is a polynomial of degree $n - 1$ so

$$L'_n(x) = a(x - \xi_1)...(x - \xi_{n-1}).$$

Note that the expanded form for Legendre polynomial is given by

$$\begin{aligned} L_n(x) &= \frac{1}{2^n} \sum_{l=0}^{[n/2]} (-1)^l \binom{n}{l} \binom{2n-2l}{n} x^{n-2l} \\ L'_n(x) &= \frac{1}{2^n} \sum_{l=0}^{[n/2]} (-1)^l \binom{n}{l} \binom{2n-2l}{n} (n-2l) x^{n-2l-1} \end{aligned}$$

Therefore we can fine the leading coefficient a (when the degree of x is $n-1$) which is when $l = 0$

$$a = \frac{n}{2^n} \binom{2n}{n}.$$

Then

$$(x - \xi_1)...(x - \xi_{n-1}) = \frac{L'_n(x)}{a} = \frac{2^n}{n\binom{2n}{n}} L'_n(x)$$

Thus the interpolation error

$$\begin{aligned} f(x)-p_n(x) &= (x-\xi_0)(x-\xi_1)...(x-\xi_{n-1})(x-\xi_n)f[\xi_0,\xi_1,...,\xi_n,x] \\ &= (x^2-1)\frac{2^n}{n\binom{2n}{n}}L_n'(x)f[\xi_0,\xi_1,...,\xi_n,x] \\ &= \frac{2^n}{n\binom{2n}{n}}\frac{n(n+1)}{2n+1}(L_{n+1}(x)-L_{n-1}(x))f[\xi_0,\xi_1,...,\xi_n,x] \\ f(x)-p_n(x) &= c_1(n)(L_{n+1}(x)-L_{n-1}(x))\frac{f^{(n+1)}(\xi)}{(n+1)!} \end{aligned}$$

where $c_1(n)=\frac{2^n}{\binom{2n+1}{n}}=\frac{2^{n+1}}{\binom{2n+2}{n+1}}$. By Stirling's formula, we obtain the upper bound for the interpolation error

$$\begin{aligned} f(x)-p_n(x) &\le \sqrt{\pi}\frac{\sqrt{n+1}}{2^n}\frac{\|f^{(n+1)}(\xi)\|_\infty}{(n+1)!} \\ &\le C(\frac{eM}{2(n+1)})^{n+1} \end{aligned}$$

Note that on any interval $[0,T]$,

$$\begin{aligned} f(x)-p_n(x) &\le C(\frac{eM}{2(n+1)})^{n+1}(\frac{T}{2})^{n+1} \\ f(x)-p_n(x) &\le C(\frac{eMT}{4(n+1)})^{n+1} \end{aligned}$$

Next, consider the remainder of the derivative [54]

$$\begin{aligned} f'(x)-p_n'(x) &= c_1(n)(L_{n+1}'(x)-L_{n-1}'(x))f[\xi_0,\xi_1,...,\xi_n,x]+c_1(n)(L_{n+1}(x)-L_{n-1}(x))f'[\xi_0,\xi_1,...,\xi_n,x] \\ &= c_1(n)(2n+1)L_n(x)f[\xi_0,\xi_1,...,\xi_n,x]+c_1(n)(L_{n+1}(x)-L_{n-1}(x))f[\xi_0,\xi_1,...,\xi_n,x,x] \\ &\le c_1(n)\frac{2cM^{n+2}}{(n+2)!}+c_1(n)(2n+1)\frac{cM^{n+1}}{(n+1)!} \\ &\le C(\frac{eM}{2(n+1)})^n \end{aligned}$$

On an interval $[0,T]$,

$$f'(x)-p_n'(x) \le C(\frac{eM}{2(n+1)})^n(\frac{T}{2})^n \le C(\frac{eMT}{4(n+1)})^n$$

A6.2 Interpolation Error of Legendre-Gaussian points

These are the points $-1 < z_0 < z_1 < ... < z_n < 1$ where z_i's are zeros of Legendre polynomial $L_{n+1}(x)$.

It follows that $(x - z_0)...(x - z_n)$ are factors of $L_{n+1}(x)$ so

$$L_{n+1}(x) = a(x - z_0)...(x - z_n).$$

Note that the expanded form for Legendre polynomial is given by

$$L_{n+1}(x) = \frac{1}{2^{n+1}} \sum_{l=0}^{[(n+1)/2]} (-1)^l \binom{n+1}{l} \binom{2(n+1)-2l}{n+1} x^{n+1-2l}$$

Therefore the leading coefficient a is

$$a = \frac{1}{2^{n+1}} \binom{2n+2}{n+1}.$$

Then

$$(x - z_0)...(x - z_n) = \frac{L_{n+1}(x)}{a} = \frac{2^{n+1}}{\binom{2n+2}{n+1}} L_{n+1}(x)$$

Thus the interpolation error

$$\begin{aligned} f(x) - p_n(x) &= (x - z_0)...(x - z_n) f[z_0, z_1, ..., z_n, x] \\ &= \frac{2^{n+1}}{\binom{2n+2}{n+1}} L_{n+1}(x) f[z_0, z_1, ..., z_n, x] \\ &= \frac{2^{n+1}(n+1)!^2}{(2n+2)!} L_{n+1}(x) \frac{\|f^{(n+1)}(\xi)\|_\infty}{(n+1)!} \end{aligned}$$

By Stirling's formula and the smoothness of the function, we obtain the upper

bound for the interpolation error

$$\begin{aligned} f(x)-p_n(x) &\leq cM^{n+1}\frac{2^{n+1}\sqrt{2\pi}(n+1)^{n+3/2}}{e^{n+1}}(1+\frac{1}{4(n+1)})\frac{e^{2(n+1)}}{\sqrt{2\pi}(2n+2)^{2n+5/2}} \\ &= C\frac{1}{\sqrt{2}}(\frac{eM}{2(n+1)})^{n+1}(1+\frac{1}{4(n+1)}) \\ &\leq \sqrt{2}c(\frac{eM}{2(n+1)})^{n+1} \quad , \quad (1+\frac{1}{4(n+1)})<2 \end{aligned}$$

Note that on any interval $[0,T]$,

$$\begin{aligned} f(x)-p_n(x) &\leq \sqrt{2}C(\frac{eM}{2(n+1)})^{n+1}(\frac{T}{2})^{n+1} \\ f(x)-p_n(x) &\leq \sqrt{2}C(\frac{eMT}{4(n+1)})^{n+1} \end{aligned}$$

A7.Difference of Projection and Interpolation Errors on [0,T]

$$\|\Pi_N p'-(\mathcal{I}_N p)'\| \leq \|\Pi_N p'-p'\|+\|p'-(\mathcal{I}_N p)'\|$$

From **A5.3** and **A6.1**

$$\begin{aligned} \|\Pi_N p'-(\mathcal{I}_N p)'\| &\leq \frac{cM}{2\sqrt{2}}\frac{1}{\sqrt{N+1}}\Big(\frac{TMe}{8(N+1)}\Big)^{(N+1)}+C(\frac{TMe}{8(N+1)})^N \\ &\leq C(\frac{TMe}{8(N+1)})^N \end{aligned}$$

and

$$\begin{aligned} \|\Pi_N q'-(\mathcal{I}_N q)'\| &\leq \frac{cR}{2\sqrt{2}}\frac{1}{\sqrt{N+1}}\Big(\frac{TRe}{8(N+1)}\Big)^{(N+1)}+C(\frac{TRe}{8(N+1)})^N \\ &\leq C(\frac{TRe}{8(N+1)})^N \end{aligned}$$

B Symplectic Algorithms

Scheme 1: Second order midpoint Euler Scheme [19].

This is an implicit method. Let $z = (p_1, p_2, ..., p_n, q_1, ..., q_n)$,

$$J = \begin{pmatrix} 0 & I_n \\ -I_n & 0 \end{pmatrix} \text{ so } J^{-1} = \begin{pmatrix} 0 & -I_n \\ I_n & 0 \end{pmatrix} = -J \ , \ H_z = [H_{p_1}, ..., H_{p_n}, H_{q_1}, ..., H_{q_n}]^T$$

$$\frac{1}{h}(z^{k+1} - z^k) = J^{-1} H_z(\frac{1}{2}z^{k+1} + \frac{1}{2}z^k).$$

Simply written as

$$\begin{aligned} p_i^{k+1} &= p_i^k - hH_{q_i}(\frac{1}{2}(p^{k+1} + p^k), \frac{1}{2}(q^{k+1} + q^k)) \\ q_i^{k+1} &= q_i^k + hH_{p_i}(\frac{1}{2}(p^{k+1} + p^k), \frac{1}{2}(q^{k+1} + q^k)), \quad i = 1, ..., n. \end{aligned}$$

For a linear system, we can replace the right hand side as

$$\begin{aligned} \frac{1}{h}(z^{k+1} - z^k) &= J^{-1}[\frac{1}{2}H_z(z^{k+1}) + \frac{1}{2}H_z(z^k)] \\ \text{or} \quad p_i^{k+1} &= p_i^k - h\frac{1}{2}[H_{q_i}(p^{k+1}, q^{k+1}) + H_{q_i}(p^k, q^k)] \\ q_i^{k+1} &= q_i^k + h\frac{1}{2}[H_{p_i}(p^{k+1}, q^{k+1}) + H_{p_i}(p^k, q^k)]. \end{aligned}$$

The equivalent scheme is symplectic for the linear system only. It is not symplectic for nonlinear system.

Scheme 2: Second order scheme [26].

$$\begin{aligned} p_i^{k+1} &= p_i^k - hH_{q_i}(p^{k+1}, q^k) - \frac{h^2}{2}\sum_{j=1}^{n}(H_{q_j}H_{p_j})_{q_i}(p^{k+1}, q^k) \\ q_i^{k+1} &= q_i^k + hH_{p_i}(p^{k+1}, q^k) + \frac{h^2}{2}\sum_{j=1}^{n}(H_{q_j}H_{p_j})_{p_i}(p^{k+1}, q^k) \quad , i = 1, ..., n. \end{aligned}$$

Note: $\sum_{j=1}^{n}(H_{q_j}H_{p_j})_{q_i}(p^{k+1},q^k)=\sum_{j=1}^{n}(H_{q_j}H_{p_j})_{q_i}(p_1^{k+1},...,p_n^{k+1},q_1^k,...,q_n^k)^T$.

For n=1,

$$\begin{aligned} p^{k+1} &= p^k - hH_q(p^{k+1},q^k) - \frac{h^2}{2}(H_{qq}H_p + H_{pq}H_q)(p^{k+1},q^k) \\ q^{k+1} &= q^k + hH_p(p^{k+1},q^k) + \frac{h^2}{2}(H_{qp}H_p + H_{pp}H_q)(p^{k+1},q^k). \end{aligned}$$

Scheme 3: Second order scheme for the three axis-symmetric Hamiltonian system [25].

$$\begin{aligned} P_1 &= p + \frac{\sqrt{3}}{4}h\sin(\frac{1}{2}p + \frac{\sqrt{3}}{2}q) \\ Q_1 &= q - \frac{1}{4}h\sin(\frac{1}{2}p + \frac{\sqrt{3}}{2}q) \\ P_2 &= P_1 - \frac{\sqrt{3}}{4}h\sin(\frac{1}{2}P_1 - \frac{\sqrt{3}}{2}Q_1) \\ Q_2 &= Q_1 - \frac{1}{4}h\sin(\frac{1}{2}P_1 - \frac{\sqrt{3}}{2}Q_1) \\ P_3 &= P_2 - \frac{\sqrt{3}}{4}h\sin(\frac{1}{2}P_2 - \frac{\sqrt{3}}{2}Q_2) \\ Q_3 &= Q_2 - h\sin(P_2) \\ Q_4 &= Q_3 - \frac{1}{4}h\sin(\frac{1}{2}P_3 - \frac{\sqrt{3}}{2}Q_3) \\ \hat{p} &= P_3 + \frac{\sqrt{3}}{4}h\sin(\frac{1}{2}P_3 + \frac{\sqrt{3}}{2}Q_4) \\ \hat{q} &= Q_4 - \frac{1}{4}h\sin(\frac{1}{2}P_3 + \frac{\sqrt{3}}{2}Q_4) \end{aligned}$$

Scheme 4: Second order scheme for the Henon-Heiles(HH) system [24].

$$\begin{aligned} p_1^{k+1} &= p_1^k - h(q_1^k + 2q_1^k q_2^k) \\ p_2^{k+1} &= p_2^k - h(q_2^k + (q_1^2)^k - (q_2^2)^k) \\ q_1^{k+1} &= q_1^k + hp_1^{k+1} \\ q_2^{k+1} &= q_2^k + hp_2^{k+1} \end{aligned}$$

REFERENCES

[1] V.I. Arnold, *Mathematical Methods of Classical Mechanics*, Springer, New York, 1978.

[2] K.E. Atkinson, *The Numerical Solution of Integral Equations of the Second Kind*, Campridge University Press, New York, 1997.

[3] T.H. Baker, *Numerical Treatment of Integral Equations*, Clarendon Press, Oxford, 1978.

[4] C. Bernardi and Y. Maday, Spectral Methods. In *Handbook of Numerical Analysis*, Vol. V, P.G. Ciarlet and J.-L. Lions eds., North-Holland (1997), 209-485.

[5] J.P. Boyd, *Chebyshev and Fourier Spectral Methods*, 2nd edition, Dover, New York, 2001.

[6] C.J. Budd , M.D. Piggott, Geometric Integration and its Applications, *Handbook of Numerical Analysis* 11(2003) 35-139.

[7] J.C. Butcher , Implicit Runge-Kutta processes, *J. Math. Comp.* 18 (1964) 50-64.

[8] J.C. Butcher , *The Numerical Analysis of Ordinary Differential Equations, Runge-Kutta and General Linear methods*, John Wiley & Sons, Chichester, 1987.

[9] H. Brunner, *Collocation Methods for Volterra Integral and Related Functional Differential Equations*, Cambridge University Press, 2004.

[10] M.P. Calvo and J.M. Sanz-Serna, Instabilities and inaccuracies in the integration of highly oscillatory problems, *SIAM J. Sci. Comput.* (to appear).

[11] C. Canuto, M.Y. Hussaini, A. Quarteroni, and T.A. Zang, *Spectral Methods in Fluid Dynamics*, Springer-Verlag, New York, 1988.

[12] C. Canuto, M.Y. Hussaini, A. Quarteroni, and T.A. Zang, *Spectral Methods: Fundamentals in Single Domains*, Springer Series: Scientific Computation, Berlin, 2006.

[13] D. Cohen, E. Hairer and C. Lubich, Numerical energy conservation for multi-frequency oscillatory differential equations, *BIT* 45 (2005) 287-305.

[14] D. Cohen, E. Hairer, and C. Lubich, Conservation of energy, momentum and actions in numerical discretizations of nonlinear wave equations, *Numerische Mathematik* 110 (2008) 113-143.

[15] P.J. Davis and P. Rabinowitz, *Methods of Numerical Integration*, 2nd ed., Academic Press, Boston, 1984.

[16] B. Engquist, A. Fokas, E. Hairer and A. Iserles, *Highly Oscillatory Problems*, Cambridge University Press, New York, 2009.

[17] L.C. Evans, *Partial Differential Equations* , 2nd ed., AMS, 2010.

[18] E. Faou, E. Hairer and, T.-L. Pham, Energy conservation with non-symplectic methods: examples and counter-examples, *BIT* 44 (2004) 699-709.

[19] K. Feng, On difference schemes and symplectic geometry. In: *Proceedings of the 1984 Beijing Symposium on Differential Geometry and Differential Equations* (K. Feng editor), pp.42-58, Science Press, Beijing, 1985.

[20] K. Feng, Difference schemes for Hamiltonian formalism and symplectic geometry, *J. Comput. Maths.*, 4 (1986), 279-289.

[21] K. Feng, How to compute properly Newton's equation of motion?. In: *Proceedings of 2nd Conf on Numerical Methods for Partial Differential Equations* (L.A. Ying, B.Y. Guo editors), Singapore, pp.15-22, World Scientific, 1992.

[22] K. Feng, The Hamiltonian way for computing Hamiltonian dynamics. In: *Applied and Industrial Mathematics. Netherlands: Kluwer* (R. Spigler editor), pp.17-35, Kluwer Acadamic, 1991.

[23] K. Feng, M.Z. Qin, *Sympletic Geometric Algorithms for Hamiltonian Systems*, Zhejiang Science and Technology Press, Hangzhou, 2003.

[24] K. Feng, M.Z. Qin, The symplectic methods for the computation of Hamiltonian equations, *Lect. Notes in Math.*, 1297 (1987), 1-37.

[25] K. Feng, D.L. Wang, Variations on a theme by Euler, *J. Comput. Maths.*, 12 (1998), 97-106.

[26] K. Feng, H.M. Wu, M.Z. Qin, D.L. Wang, Construction of canonical difference schemes for Hamiltonian formalism via generating functions, *J. Comput. Maths.*, 7 (1989), 71-96.

[27] B. Garia-Archilla, J.M. Sanz-Serna, and R.D. Skeel, Long-Time-Step Methods for Oscillatory Differential Equations, *SIAM J. Sci. Comput.* 20-3 (1999).

[28] G. Zhong and J.E. Marsden, Lie-Piosson Himilton-Jacobi theory and Lie-Poisson integrators, *Phys. Lett. A* 133-3 (1988), 134-139.

[29] D. Gottlieb and T.A. Orszag, *Numerical Analysis of Spectral Methods: Theory and Applications*, SIAM, Philadelphia, 1977.

[30] B.-Y. Guo, *Spectral Methods and their Applications*, World Scietific, Singapore (1998).

[31] B.-Y. Guo and Z.-Q. Wang, Legendre-Gauss collocation methods for ordinary differential equations, *Adv. Comput. Math.* 30 (2009), 249-280.

[32] E. Hairer, Long-time energy conservation of numerical integrators, *Foundations of Computational Mathematics*, Santander 2005, London Math. Soc. Lecture Notes Ser. 331, Cambridge University Press (2006), 162-180.

[33] E. Hairer and C. Lubich, Symmetric multistep methods over long times, *Numer. Math.* 97 (2004), 699-723.

[34] E. Hairer and C. Lubich, Spectral semi-discretisations of weakly nonlinear wave equations over long times, *Found. Comput. Math.* 8 (2008), 319-334.

[35] E. Hairer, C. Lubich, and G. Wanner, *Geometric Numerical Integration: Structure-Preserving Algorithms for Ordinary Differential Equations*, Springer Series in Comput. Mathematics, vol. 31. Springer-Verlag, Berlin (2002).

[36] J. Hale, *Ordinary Differential Equations* , Wiley-Interscience, New York, 1969.

[37] J.S. Hestheven, S. Gottlieb and D. Gottlieb, *Spectral Methods for Time-Dependent Problems*, Cambridge University Press, 2007.

[38] G.E. Karniadakis and S.J. Sherwin, *Spectral/hp Element Methods for CFD*, Oxford University Press, New York, 1999.

[39] P.K. Kythe and P. Puri, *Computational Methods for Linear Integral Equations*, Birkhäuser, Boston, 2002.

[40] W. Lu, H. Zhang and S. Wang, Application of Symplectic Algebraic Dynamics Algorithm to Circular Restricted Three-Body Problem, *Chin. Phys. Lett.* 25 (2008) 2342-2345.

[41] J.E. Marsden, G. Misiolek, J.-P. Ortega, M. Perlmutter, and T.S. Ratiu, Hamiltonian Reduction by Stages, Lecture Notes in Mathematics, Springer Berlin, 2007.

[42] J.E. Marsden and M. West, Discrete mechanics and variational integrators, in: Acta Numerica 2001, 357-514.

[43] J.C. Mason and D.C. Handscomb *Chebyshev Polynomials*, Chapman ans Hall/CRC, New York, 2002.

[44] G.M. Phillips, *Interpolation and Approximation by Polynomials*, Springer, New York, 2003.

[45] R. Peyret, *Specrtral Methods for Incompressible Viscous Flow*, Springer, New York, 2002.

[46] J.M. Sanz-Serna, Symplectic integrators for Hamiltonian problems: an overview, in: Acta Nemerica 1992, 243-286.

[47] J.M. Sanz-Serna and M.P. Calvo, *Numerical Hamiltonian Problems*, Chapman & Hall, 1994.

[48] J. Shen and T. Tang, *Spectral and High-Order Methods with Applications*, Science Press, Beijing, 2006.

[49] J. Shen and L.-L. Wang, Fourierization of the Legendre-Galerkin method and a new space-time spectral method, *Applied Numerical Mathematics*, 57 (2007), 710-720.

[50] A.M. Stuart and A.R. Humphries, *Dynamical Systems and Numerical Analysis*, Cambridge University Press, 1996.

[51] L.N. Trefethen, *Spectral Methods in Matlab*, SIAM, 2000.

[52] H. Van de Vyver, A fourth-order symplectic exponentially fitted integrator, *Computer Phys. Comm.*, 174 (2006), 255-262.

[53] T. Wu, C. Shen, G. Ju, N. Ju, Application of symplectic algorithm to QCT calculation: $H + H_2$ system, *Science in China(Series B)*, 45 (2002), 15-20.

[54] Z. Zhang, Superconvergence of Spectral collocation and p-version methods in one dimensional problems, *Math. Comp.*, 74 (2005), 1621-1636.

[55] Z. Zhang, Superconvergence of a Chebyshev spectral collocation method, *Journal of Scientific Computing* 34 (2008) 237-246.

[56] Z. Zhang, On the hp finite element method for the one dimensional singularly perturbed convection-diffusion problems, *Journal of Computational Mathematics* 20 (2002) 599-610.

ABSTRACT

SPECTRAL METHODS FOR THE HAMILTONIAN SYSTEMS

by

NAIRAT KANYAMEE

December 2010

Advisor: Prof. Zhimin Zhang

Major: Mathematics (Applied)

Degree: Doctor of Philosophy

We conduct a systematic comparison of spectral methods with some symplectic methods in solving Hamiltonian dynamical systems. Our main emphasis is on the nonlinear problems. Numerical evidences have demonstrated that the proposed spectral methods preserve both energy and symplectic structure up to the machine error in each time (large) step, and therefore have a better long time behavior.

AUTOBIOGRAPHICAL STATEMENT

NAIRAT KANYAMEE

Education

- Ph.D. in Mathematics, December 2010 (expected)
  Wayne State University, Detroit, Michigan
- M.A. in Mathematical Statistics, May 2010
  Wayne State University, Detroit, Michigan
- M.S. in Mathematics, May 2005
  Washington State University, Pullman, Washington
- M.S. in Applied Mathematics, December 2002
  Mahidol University, Bangkok, Thailand
- B.S. in Mathematics (1st Honor), March 2000
  Chiang Mai University, Chaing Mai, Thailand

Selected List of Awards and Scholarships

- The Alfred Nelson Award, Wayne State University,
- The Royal Thai government scholarship, Washington State University and Wayne State University, 2003-2007.
- The young scientist scholarship, Mahidol University, Bangkok, Thailand, 2000-2002.
- Scholarship from the Royal Thai Government, Chiang Mai University, Chiang Mai, Thailand, 1996-1999.

Selected List of Publications

1. N. Kanyamee and Z. Zhang, Comparison of A Spectral Collocation Method and Symplectic Methods for Hamiltonian Systems, *ijnam*, (to appear).
2. A. Kammanee, N. Kanyamee and I.M. Tang, Reproduction number for the transmission of Plasmodium vivax malaria, *SEA J Trop Med Pub Health*, **32(4)**,2001.
3. N. Kanyamee and I.M. Tang, The Effect of Migrant Workers on the Transmission of Malaria, *SEA J Trop Med Pub Health*, **. Special Volume** ,(2002) 297-308.